A STUDY ON THE SHEAR STRENGTH AND COLLAPSIBILITY OF DADAŞ CLAY IN ERZURUM

A MASTER'S THESIS

IN

CIVIL ENGINEERING

Middle East Technical University

By

Oğuz ÇALIŞAN

February, 1987

results of the double oedometer test was also used to investigate the collapse properties of the soil.

Furthermore the effect of consolidation pressure on collapse was examined by running one dimensional consolidation tests in which the specimens were flooded at different pressures.

Key words: triaxial test, pore pressure parameters, double oedometer test, collapsibility.

ÖZET

ERZURUM'DAKİ DADAŞ KİLİNİN KAYMA DAYANIMI VE ÇÖKEBİLİRLİĞİ ÜZERİNE BİR ÇALIŞMA

ÇALIŞAN , Oğuz
Yüksek Lisans Tezi, İnş. Müh Bölümü
Tez Yöneticisi : Doç. Dr. M. Yener Özkan
Şubat 1987, 101 sayfa

Bu çalışmada Erzurum cıvarından alınan killi, yarı doygun bir zeminin kayma dayanımı ve hacim değişimi özellikleri araştırılmıştır. Yapılan konsolidasyonsuz-drenajsız (U-U),konsolidasyonlu-drenajsız (C-U) ve konsolidasyonlu-drenajlı (C-D) tipi üç eksenli deneyleri sonucunda kayma dayanımı parametreleri toplam ve efektif gerilmeler cinsinden bulunmuştur. U-U tipi deneylerde, eksenel yüklemeye geçilmeden önce, boşluk suyu basınçları ölçülüp boşluk suyu parametresi, B, saptanmıştır. C-U tipi deneylerde de boşluk suyu basınçları, kırılma sırasında boşluk suyu parametresi, A'nın değişimini görmek için ölçülmüştür.

Bir adet çift odometre deneyi yapılmış ve ön

konsolidasyon basıncı ile konsolidasyon katsayısı hesaplanmıştır. Bu deneyin sonucu ayrıca zeminin çökebilirlik özelliğini araştırmak için de kullanılmıştır.

Bundan başka konsolidasyon basıncının çökebilirlik üzerindeki etkisi, numunelerin değişik basınçlarda suya boğulduğu odometre deneyleri yapılarak araştırılmıştır.

Anahtar Kelimeler: üç eksenli deneyleri, boşluk suyu basıncı parametreleri, çift konsolidasyon deneyi, çökebilirlik.

ACKNOWLEDGEMENT

The author wishes to express sincere gratitude to Assoc. Prof. Dr. M. Yener Özkan for his guidance and valuable suggestions throughout the research.

Very special thanks are extended to Assoc. Prof. Dr. Türker Mirata both for his valuable help during the laboratory study and his valuable suggestions and corrections in the text.

The author wishes to thank to Soil Mechanics laboratory staff for their help during the experimental study.

Thanks are also extended to Y. Müh Cengiz Al, Director of 12 th. Division of State Highways Department and technical personnel who helped during the field work in Erzurum.

TO MY MOTHER

AND

MY FATHER

TABLE OF CONTENTS

Page

Page

LIST OF TABLES

LIST OF FIGURES

Page

Page

NOMENCLATURE

A	pore pressure parameter
A_c	area of a consolidation test specimen
A_f	value of A at failure
A_o	area of a triaxial test specimen before shearing
A_s	area of a triaxial test specimen during shearing
a	cohesion obtained from modified failure envelopes (total stresses)
a'	cohesion obtained from modified failure envelopes (effective stresses)
a_r	area of ram
B	pore pressure parameter
C	coefficient of collapsibility
C_p	collapse potential
c'	cohesion (effective stresses)
c	cohesion (total stresses)
c_v	coefficient of consolidation
D_r	dial reading
e	void ratio
G_s	specific gravity
H	Henry's coefficient of solubility
H_s	equivalent thickness of solids

H_1 thickness of an oedometer test sample at the end of a load increment

h half the mean height of a triaxial test specimen

h' half the height of a triaxial test specimen after consolidation

L_o initial height of a triaxial sample

LL liquid limit

p_a initial pore air pressure

p_{cn} collapse pressure for soil at natural moisture content

p_{cs} collapse pressure for soaked soil

p_o vertical pressure due to overburden stress

p_s back pressure to be applied for full saturation

R_i transducer reading taken at an arbitrary pressure

R_o initial transducer reading

S initial degree of saturation

t_f duration of shearing

t_{100} time required for 100 % consolidation

U_w pore water pressure

U_f pore water pressure at failure

V_o initial volume of triaxial samples

V_o' volume of the triaxial samples at the start of shearing

V_r volume change registered by volume change apparatus

V_r' volume of water which enters the triaxial cell after the start of shearing

ΔL axial shortening during shearing

ΔU change in pore water pressure

ΔV volume change due to the application of cell pressure

ΔV_e volume of water entering the triaxial cell as a result of expansion of the cell

$\Delta V'$ volume change after the start of shearing at strain

ΔV_o volume of water entering the cell due to the leakage of castor oil

ΔV_r volume of water displaced by ram

$(\Delta\sigma_1 - \Delta\sigma_3)$ deviatoric stress increase

$\Delta\sigma_3$ all-around pressure increment

σ_3 chamber pressure

σ_c consolidation pressure

η a factor depending on drainage conditions

ϵ axial strain

ϵ_f axial strain at failure

ϕ angle of internal friction (total stresses)

ϕ' angle of internal friction (effective stresses)

α angle of internal friction obtained from modified failure envelopes (total stresses)

α' angle of internal friction obtained from modified failure envelopes (effective stresses)

γ_d natural dry unit weight

γ_w unit weight of water

1. INTRODUCTION

In most foundation engineering and soil mechanics problems the knowledge of shear strength of soils is essential. Also for partly saturated soils, especially for soils at low degrees of saturation, the behaviour after introducing water to the soil mass is very important as far as the safety and serviceability of the overlying structures are concerned.

There are various laboratory and in situ testing methods for the determination of the shear strength properties of soils. In order for a laboratory testing method to be adequate, the actual field conditions should be represented as much as possible. Among the various laboratory testing methods, triaxial test is a well developed one in which most of the field conditions can be duplicated. The main advantages of this test are that it is suitable for all types of soils and drainage conditions can be controlled.

During this study, triaxial tests were performed on undisturbed samples to examine shear strength properties. For the investigation of volume change behaviour due to wetting, one dimensional consolidation tests and a double oedometer test were carried out.

In chapter two of this thesis some theoretical considerations about collapse and pore pressure

parameters are given. Chapter three is related to the method of sampling and a brief survey of the geological formations in the vicinity of Erzurum. In chapter four, the procedures for the performed tests and the test results are given. Finally the tests results are discussed in chapter five.

2. THEORETICAL CONSIDERATIONS

2.1 Change in Volume as a Result of Wetting

When water is introduced to an initially unsaturated soil mass, generally there is a change in volume. Depending on conditions such as dry density, degree of saturation, applied pressure, clay content and type of clay mineral present, this volume change is either collapse or swell.

Especially in cohesionless or slightly cohesive soils with high void ratios and low unit weights, large settlements due to collapse may be experienced upon wetting (Das, 1984).

2.2 Estimation of Collapse Potential

1. In order to describe the collapse potential of a soil qualitatively Jennings and Knight (1975) defined the collapse potential, C_p , as ;

$$C_p = \frac{e_1 - e_2}{1 + e_o} \qquad \text{Equation 1.}$$

To determine the values of e_o, e_1 and e_2 , a consolidation test is carried out on an undisturbed soil specimen at its natural water content. The specimen is subjected to vertical pressures of 25, 50,

100, 200 kN/m^2 and flooded at 200 kN/m^2 . After 24 hours the change in void ratio, from e_1 to e_2 is determined. The value of e_0 to be substituted in equation (1) is the natural void ratio of the soil, that is the void ratio at the start of the test (Das, 1984).

In table 1, the relationship between the severity of foundation problem and collapse potential is given as summarized by Clemence and Finbarr (1981) (quoted by Das, 1984).

TABLE 1. Relationship Between the Severity of Foundation Problem and Collapse Potential (after Das, 1984)

C_p (%)	Severity of problem
0-1	No Problem
1-5	Moderate Trouble
5-10	Trouble
10-20	Severe Trouble
20	Very Severe Trouble

2. Collapse susceptibility of a soil deposit is related to a parameter called coefficient of collapsibility, determined from a double oedometer test as described by Reginatto and Ferraro (1975). In this test, two specimens one at its natural water content,

the other soaked are subjected to routine consolidation tests. From the test results expressed in terms of e-log p curves, (Figure 1), the coefficient of collapsibility, C, can be determined as;

$$C = \frac{p_{cs} - p_o}{p_{cn} - p_o} \qquad \text{Equation 2.}$$

where: p_o : vertical pressure due to overburden stress,

p_{cn} : collapse pressure for soil at natural moisture content,

p_{cs} : collapse pressure for soaked soil.

When $C < 0$ the soil is said to be "truly collapsible" indicating that it experiences large settlements even in the absence of external loading.

When $0 < C < 1$ the soil is called "conditionally collapsible". Collapse will not occur if collapse pressure for soaked condition is higher than the total vertical pressure acting on the soil.

When $C = 1$ the soil will behave in the same manner for any degree of saturation (Reginatto and Ferraro, 1973).

3. It was suggested by Holtz and Hilf (1961) that, for a soil to collapse, the void ratio should be large enough to allow its moisture content to exceed

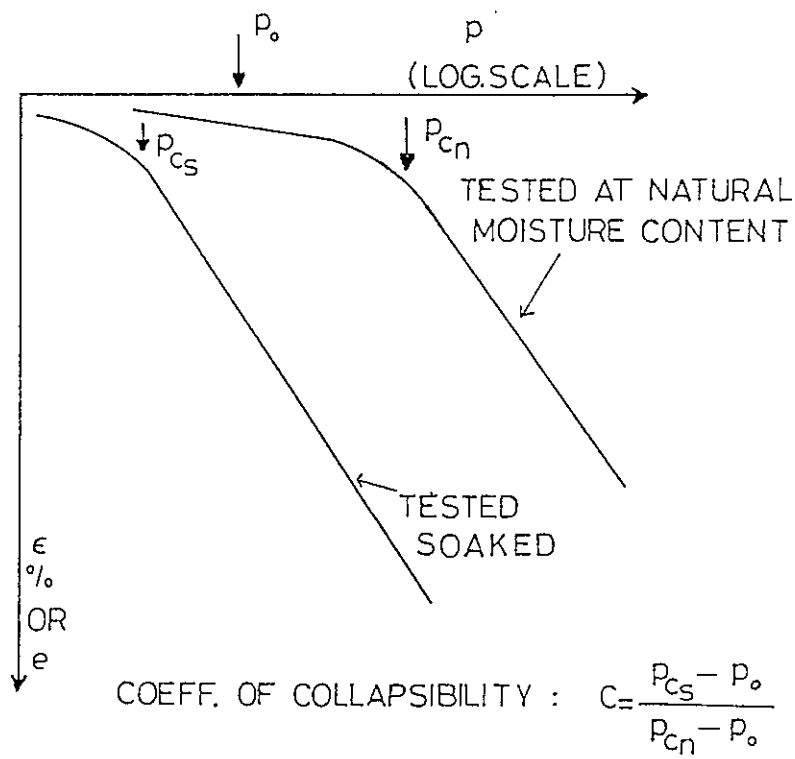

Figure 1. Determination of 'C' from the Results of Double Oedometer Test (after Reginatto and Ferraro, 1973)

its liquid limit upon soaking (Das, 1984). Then a collapsing soil should satisfy equation 3.

$$\gamma_d \leq \frac{G_s \cdot \gamma_w}{1 + (LL).G_s} \qquad \text{Equation 3.}$$

If natural dry unit weight γ_d , is evaluated for various values of liquid limit, (LL), a typical curve as shown in figure 2 is obtained. If the natural dry unit weight of a soil falls below the limiting line shown in figure 2 the soil is likely to collapse (Das, 1984).

2.3 Pore Pressure Parameters 'A' and 'B'

When there is a change in total stress in undrained conditions, the portion of it which is carried by the water in the pores can be determined by means of pore pressure parameters. When a soil element is subjected to an all-around pressure increment, $\Delta\sigma_3$, and a deviator stress increment , $(\Delta\sigma_1 - \Delta\sigma_3)$, under undrained conditions, the change in pore water pressure in the soil element, ΔU , is given as (Skempton 1954, quoted by Craig, 1984) ;

$$\Delta U = B.(\Delta\sigma_3 + A.(\Delta\sigma_1 - \Delta\sigma_3)) \qquad \text{Equation 4.}$$

where A and B are the pore pressure parameters.

The value of A depends on various factors such as strain to which the soil element has been subjected, initial stress system, stress history, type of stress change (Lambe and Whitman, 1969).

The value of B depends on the compressibility of the pore fluid and compressibility of the soil skeleton. The compressibility of pore fluid is very much affected by the amount of air present in the pores, therefore B depends largely on degree of saturation (Figure 3). For this reason, for a partially saturated soil the value of B which applies during the application of deviatoric stress is entirely different from that which applies during the increase in all-around stress. From the above discussion it is clear that the value of B which is determined before shearing can not be used for calculating the values of A during the shearing stage of a C-U test.

2.4 Use of Back Pressure in Triaxial Testing

Application of back pressure in the triaxial testing apparatus is a method of obtaining fully saturated samples of cohesive soils. This method is also used to apply the in situ value of pore pressure, in samples taken below the water table (Lowe and Johnson, 1960).

The magnitude of back pressure to be applied to

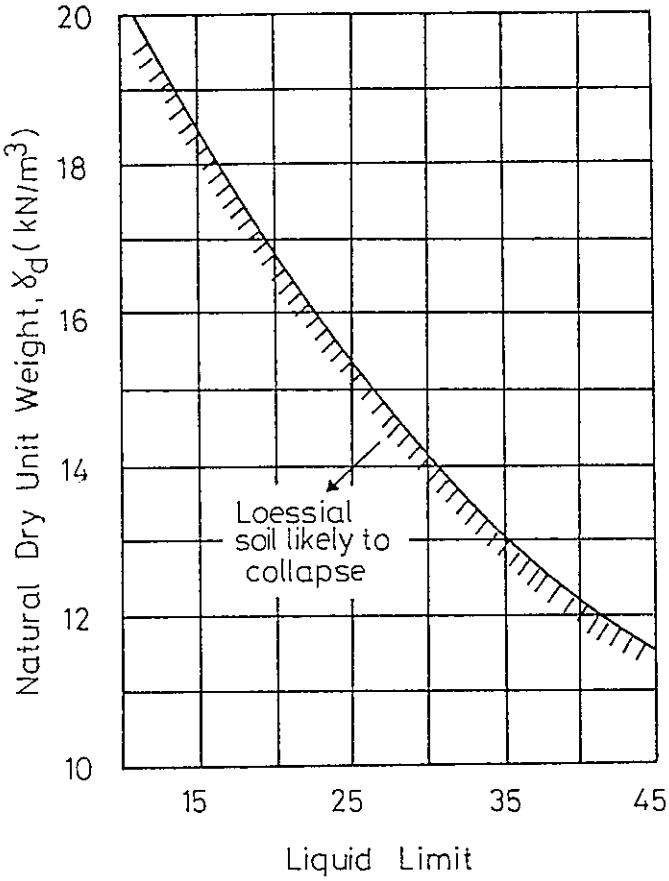

Figure 2. Loessial Soil Likely to Collapse
(after Das, 1984)

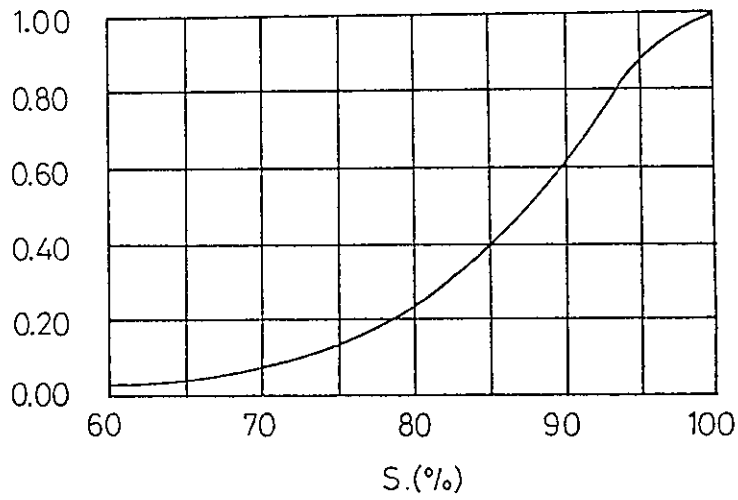

Figure 3. Typical Variation between B and S
(after R.F. Craig, 1984)

reach full saturation is a function of initial degree of saturation and initial absolute pressure of the air in the voids when the sample is unconfined. "For the case of an increase in pore pressure caused by the entry of additional water free from dissolved air with no change in overall volume of the sample" the value of back pressure to cause full saturation is given by equation 5 (Bishop and Henkel, 1962).

$$p_s = p_a \frac{(1 - H)}{H} (1 - S) \qquad \text{Equation 5}$$

where: p_s: back pressure to be applied for full saturation,

p_a: initial pore air pressure (absolute),

H : Henry's coefficient of solubility,

S : initial degree of saturation.

By using equation 5 and assuming p_a to be atmospheric with H = 0.02, for various degrees of saturation the values in table 2 are obtained.

TABLE 2. Values of Back Pressure for Different Initial Degrees of Saturation

S (%)	p_s (kN/m^2)
90	496
80	993
70	1489

From table 2 it is seen that back pressure values are considerably high especially for low degrees of saturation. However in many cases and especially for freshly compacted soils lower back pressures are sufficient to achieve full saturation. This is because the initial air pressure is generally less than atmospheric in sealed samples of freshly compacted soils and considerable loss of air occurs through the rubber membrane into a water filled triaxial cell (Bishop and Henkel, 1962).

Throughout the C-U and C-D tests in this study a back pressure of approximately 196 kN/m^2 was applied. The main reason for this was that if a high back pressure was used, the tests with high consolidation pressures could not be conducted, because the necessary chamber pressure could not be supplied due to the limited capacity of the pressure supply system.

3. INVESTIGATION OF THE SAMPLING AREA

3.1 Geology of Erzurum and its Vicinity

The Erzurum basin whose geology will be described is bounded by Palandöken Range on the south, the Dumlu Range on the north and the Kargapazarı Mountains on the east and northeast. The northwest and southeast boundaries of the basin are the Daphan Plain and Sakalikesık-Derebogazı plain respectively.

On the northwest part of the area shown in figure 4 upper miocene sediments occur. Upper miocene formation, in general, is composed of alternating layers of clayey, marly limestone and lenses of volcanic conglomerate. Around Gelinkaya Village which is on the northwest part of the basin , plio-quaternary sediments are entirely accumulated. Layers of marl, clay, limestone and the deposits of sand and gravel are the components of this formation .

The plio-quaternary formations containing clay, marl, limestone, silt, gravel and sand exist in the basin except the southeast part.

" The volcanic-sedimentary plio-quaternary deposits occur in the southwest of the area especially between the west of Palandöken Range and Çayırtepe village. In this area plio-quaternary deposits are covered by young basalt lavas which have flowed from

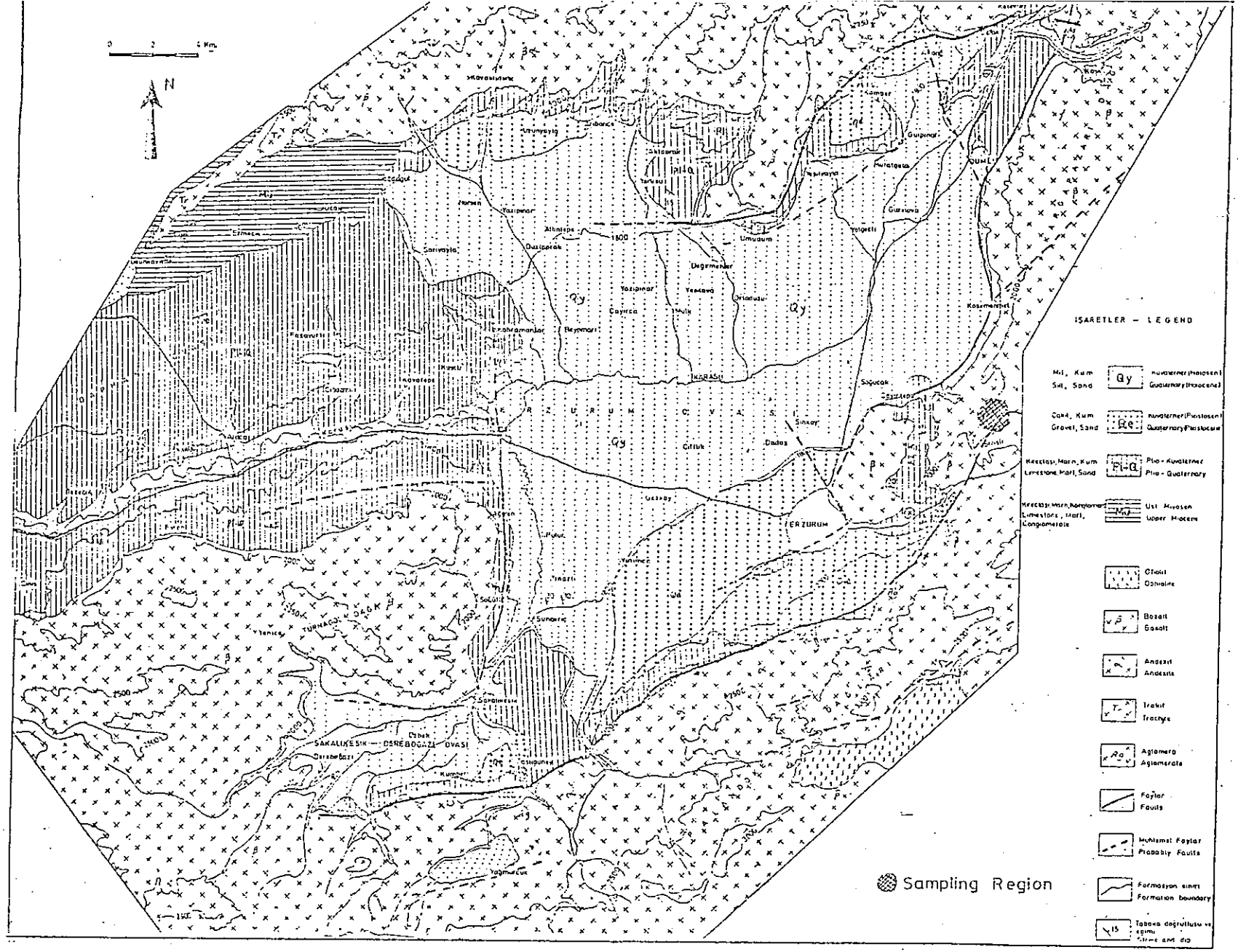

Figure 4. Geologic Map of Erzurum Plain and its Surroundings (after Atalay, 1978)

the Palandöken Mountains in some places" .

The mountains surrounding Erzurum basin are entirely volcanic. The foundations of these mountains are composed of trachytes and andesite which belong to the upper Eocene-oliogocene. The basalts which lie on the foundation in Dumlu-Kargapazarı and Palandöken took place in the Early Quaternary (the above text is summarized from Atalay, 1978).

The samples were taken from a place which was 11 km northeast of Erzurum. The location of sampling place is shown in figure 4. The sampling region is generally characterized by volcanic formations such as, basalt, trachyte and andesite.

3.2 In-situ Sampling Procedure

Block samples were taken from the pits excavated in the field. Old metal containers with 21.5*21.5 cm cross sectional area and 29 cm height were used to take the block samples.

In order to minimize the disturbance, the procedure outlined below was followed while sampling.

Firstly an area slightly larger than the cross sectional area of the metal container was marked. The soil surrounding this area was excavated by means of a pick-axe and a pit was formed around the soil column in order to provide a working space. When the depth of

this pit reached approximately twice the height of the container the digging operation was stopped. Then approximately 30 cm of soil was taken out from the top of the soil column in order to remove the top soil. The open side of the metal container was put on top of the soil column and by trimming the sides of the soil column the container was gently pushed down. After the container was completely filled with soil, the soil column was cut (Figure 5). The excess soil on top of the container was trimmed with a knife and a piece of moist cloth which was also covered by a piece of nylon was placed on the container to protect the specimen from the effect of wind during transportation to the laboratory in Erzurum.

In the laboratory the moist cloth and nylon cover were removed together with about the upper 2 cm of the sample in the container. Following this the remaining part of the container was covered with paraffin.

The samples were brought to Ankara by bus. In order to prevent the samples from being disturbed by the effect of suitcases the containers were inserted in a wooden cage which was specially constructed in Erzurum.

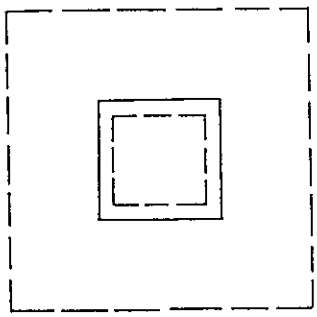

1 - An area slightly larger than the area of the container is marked.

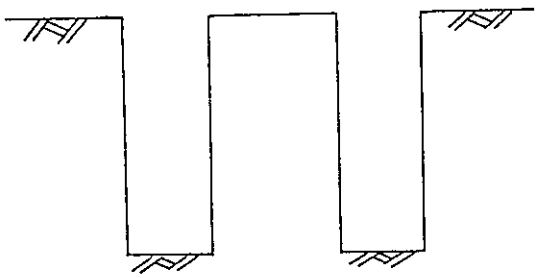

2 - The soil surrounding the marked area is removed.

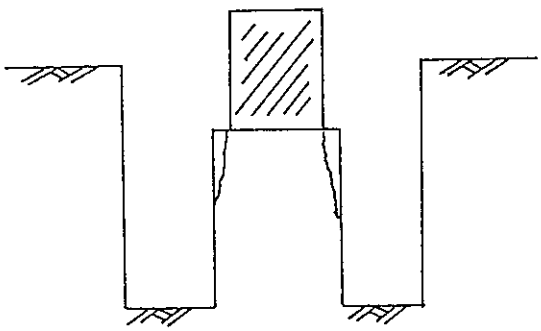

3 - Approximately 30 cm of soil is removed from the top and container is forced into the soil by trimming the sides of the soil column.

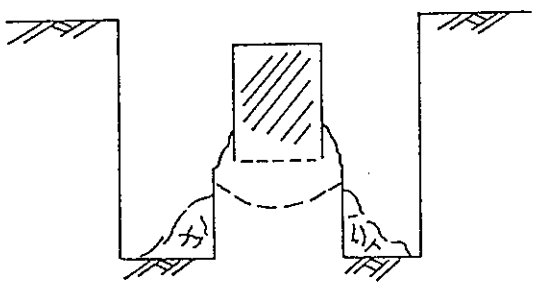

4 - When the container is completely filled with soil the soil column is cut.

Figure 5. Block Sampling Technique Used

4. LABORATORY TESTING

4.1 Determination of Basic Characteristics

Before running the triaxial and consolidation tests, grain size distribution, specific gravity and atterberg limits of the soil were determined by using disturbed samples. Grain size distribution of the soil tested is presented in figure 6. Specific gravity of the solid particles, G_s, as obtained from the avarage of two tests is 2.55. Two atterberg limits tests were performed and as a result liquid limit and plastic limit of the soil were determined as 47% and 27% respectively.

4.2 Triaxial Testing

4.2.1 Apparatus Used for Triaxial Testing

4.2.1.1 Loading Apparatus

Triaxial tests were carried out by the 1-ton capacity Wykeham Farrance testing machine. This machine is strain controlled and it can be operated at 25 different deformation rates, maximum and minimum being 1.52 mm/min and 0.0006 mm/min respectively. Out of these 25 rates of shearing, the rate closest to the desired value is selected and the loads that are

MIDDLE EAST TECHNICAL UNIVERSITY
DEPARTMANT OF CIVIL ENGINEERING
SOIL MECHANICS LABORATORY

GRAIN SIZE DISTRIBUTION CURVE

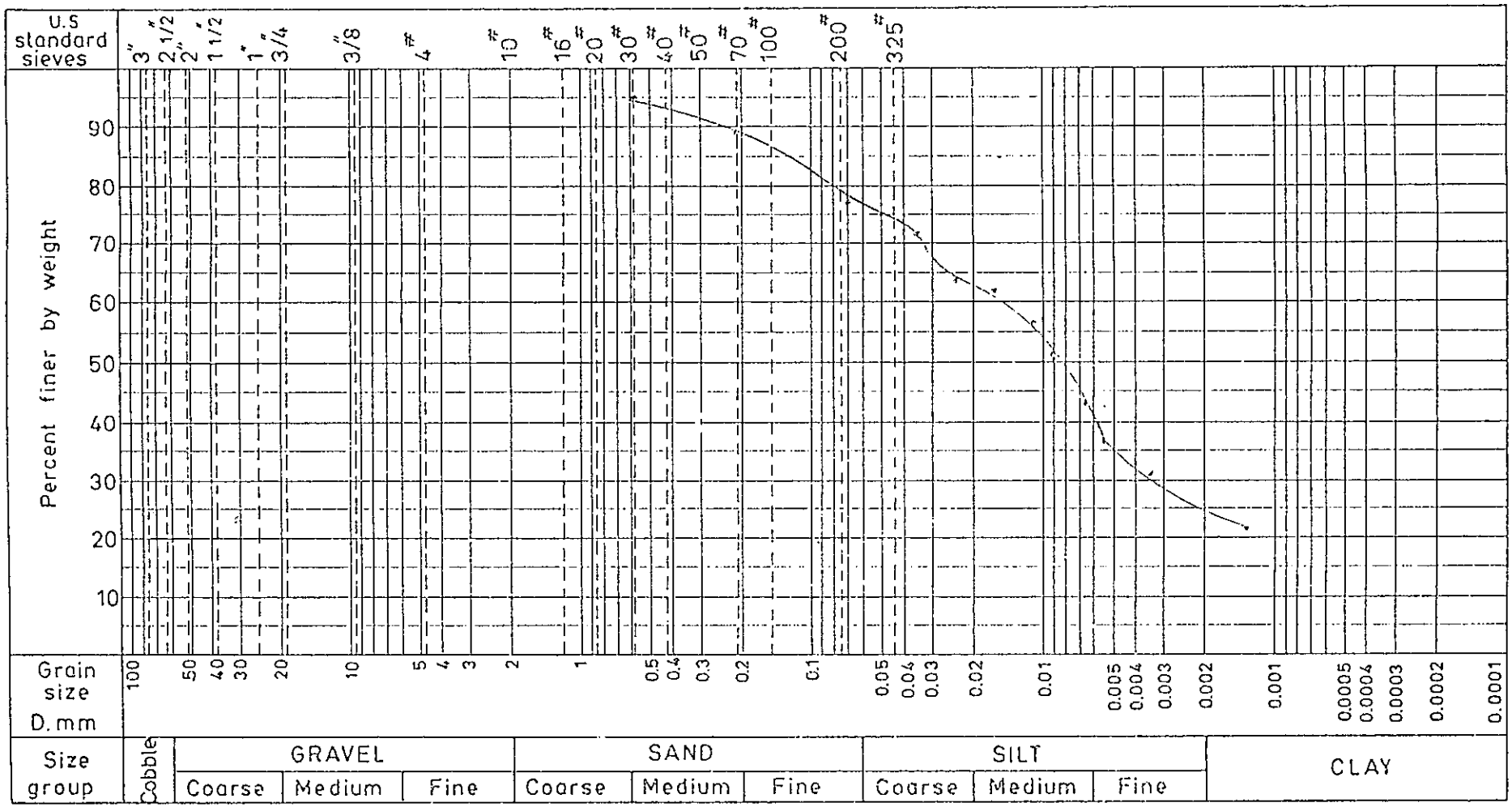

Figure 6. Grain Size Distribution Curve

applied on a triaxial specimen are measured by means of a previously calibrated proving ring.

4.2.1.2 Triaxial Cells

Wykeham-Farrance triaxial cells were used during the tests. The main parts of a triaxial cell are;base, perspex cylinder, loading ram, loading caps and rubber membrane (Bishop and Henkel, 1962).

Triaxial cell base has four valves connected to it. One of these is for filling, emptying and chamber pressure application; one is for being connected to the top of the specimen for drainage from the top. Other connections serve for back pressure application and pore pressure measurement at the bottom.

4.2.1.3 Cell Pressure Control

Cell pressure and back pressure were provided by means of a self compensating mercury control apparatus. In this apparatus, the pressure is supplied by the difference in the mercury surface levels in two cylindrical pots one being located on the floor and the other hung on a spring. The main advantage of this system is that if there is a loss of water by any means in the system, the resulting drop in the level of mercury is compensated by a simultaneous retraction

of the spring.

4.2.1.4 Volume Change Apparatus

Volume change measurements during the tests were made by instruments of Leonard Farnell and Wykeham Farrance Eng. Ltd. Both of these instruments are twin burette type and they are similarly operated. These instruments have two main advantages: i)Burettes are inserted in tubes from which water has to circulate through before leaving or entering into the triaxial cell. For that reason there is no difference in pressure of water inside and outside the burette, so an error which may result from the expansion of the burette is eliminated; ii)the system can be operated in two directions. When the amount of water entering or leaving the instrument is too much, the direction of flow in the system is reversed. This prevents the loss of cerosene in the pressure lines.

4.2.1.5 Pore Pressure Measuring Device

In this study pore pressure measurements were made before shearing and both before and during shearing stages of U-U and C-U tests respectively. These measurements were carried out by electronic

transducers connected to a strain gauge instrument. Main advantage of these transducers are: i)They have a very short response time, ii)they are very simple to operate, i.e, proving ring and transducer readings can be taken by one person at the same time without difficulty.

Calibration of the pore pressure measuring device was made in the following way. Transducer was connected to the cell base and saturated by circulating water through it while opening and closing the two valves one located at the base and the other at the tip of the transducer repeatedly. This operation is necessary for removing the air. After this the strain gauge reading, R_0, was recorded. Then the cell was subjected to a pressure of known magnitude and corresponding reading, R_1, was registered. The same procedure was followed by increasing the cell pressure and the readings, R_i, were obtained. The difference between the various readings and initial reading, i.e, $R_i - R_0$ was plotted against the values of pressure corresponding to R_i and calibration curve was obtained. The above procedure was repeated for two different transducers , and the calibration curves are given in appendix 1.

In calibration, a triaxial cell without a porous stone was used. The use of high air entry value ceramic

discs lengthens the duration of calibration process because of the reduced permeability due to the lime accumulated in the pores.

4.2.1.6 Porous Stones

In this study two types of porous stones were used. In all of the U-U tests high air entry value ceramic discs were used to prevent the sample from drawing in water from the saturated disc when placed in contact with it. However all C-U and C-D tests were conducted with coarse porous stones. As all these tests were performed under a back pressure, the air in the pressure lines and porous stone was dissolved in the water. Therefore the danger of air remaining in the pore pressure lines was automatically eliminated.

The advantage of using a coarse porous stone is that it shortens the duration of testing.

4.2.2 Sample Preparation

Triaxial specimens were extracted from the sample in the metal container by thin-walled core cutters which had an area ratio of 12% . After removing the paraffin wax at the surface of the metal container, ten core cutters were jacked into the soil. When the cutters were wholly embedded in the soil, they were

taken out by cutting the sides of the container and releasing the confinement. A total number of twenty samples were obtained in this way.

Before starting a triaxial test, the specimen to be tested was transferred to a former of 37 mm internal diameter and 74.5 mm height. Then the sample was trimmed at the ends and weighed with the former, moved from the former and placed in the triaxial cell. The rubber membrane which was already tested for leakage was placed around the sample. The top cap and the rubber O-rings were fitted and the ram was brought in contact with the top cap. Then the cell was filled with distilled and de-aired water. In order to reduce the leakage and decrease the friction on the loading ram the upper part of the cell was filled with castor oil.

4.2.3 Unconsolidated Undrained (U-U) Tests

4.2.3.1 Procedure Followed

In this study U-U tests on undisturbed samples have been performed. The test procedure followed after the application of cell pressure is outlined below.

Triaxial specimens were left for equalization of pore pressures under the applied cell pressure; during this equalization stage, pore water pressure

measurements were made. When two succesive readings taken from the strain gauge instrument at several hours intervals were nearly equal, equalization stage was terminated. This stage generally lasted about two days. After equalization, triaxial samples were sheared by the application of deviatoric stress. No drainage in and out of the specimen was permitted at either stage of the test.

4.2.3.2 Calculation of Corrected Area

Since the soil samples tested were partly saturated, after the application of cell pressure, sample area and volume was changed. This was caused by the compression of air in the voids of the sample. Therefore the area before shearing was not equal to the initial area at the beginning of the test, and a correction was to be made.

Assuming that the strains in radial and axial directions due to the application of cell pressure are equal, the area A_o which applies before shearing can be calculated by using equation 6.

$$A_o = \frac{V_o - \Delta V}{(1 - \Delta V/3.V_o).L_o} \qquad \text{Equation 6.}$$

where: V_o : initial volume of the sample,

ΔV : volume change in the sample due to the application of cell pressure,

L_0 : initial height of the sample.

The area calculated by using equation 6 is used as the initial area in calculating the corrected area during shearing. For the determination of the area, A_s, during shearing, equation 7 can be used (Bishop and Henkel, 1962).

$$A_s = A_0 \frac{1 - \Delta V'/V_0'}{1 - \epsilon} \qquad \text{Equation 7.}$$

where: V_0' : volume of the sample at the start of shearing ($V_0 - \Delta V$),

$\Delta V'$: volume change after the start of shearing at axial strain, ϵ,

ϵ : axial strain.

Axial strain, ϵ, can be calculated from equation 8

$$\epsilon = \frac{\Delta L}{(1 - \Delta V / 3.V_0).L_0} \qquad \text{Equation 8.}$$

where ΔL is the axial shortening during shearing.

4.2.3.3 Measurement of Volume Change in the Sample

In order to use equations 6,7 and 8 the changes in the volume of the sample during various stages of the testing has to be measured. For this purpose, cell pressure, σ_3 , is applied through the volume change apparatus and the amount of water entering the cell is calculated from the burette readings. As some amount of water enters into the cell because of the expansion of the cell under the applied cell pressure, in order to determine the volume change in the specimen this amount has to be subtracted from the amount of water entering the cell. Therefore volume change in the sample due to application of cell pressure, ΔV, is calculated from equation 9.

$$\Delta V = V_r - \Delta V_e - \Delta V_o \qquad \text{Equation 9.}$$

where: V_r : volume of water entering the cell as measured by volume change apparatus,

ΔV_e : volume of water entering the cell as a result of expansion of cell (Section 4.2.3.4),

ΔV_o : volume of water entering the cell due to the leakage of castor oil.

In order to calculate ΔV_0, the castor oil that leaked was wiped by a piece of cloth and its weight was determined. Then ΔV_0 was calculated by taking the specific gravity of castor oil as 0.965 (Mirata, 1976).

To determine the volume change during shearing equation 10 was used ;

$$\Delta V' = V_r' + \Delta V_r \qquad \text{Equation 10.}$$

where: V_r' : volume of water which entered the cell after the start of shear,

ΔV_r is the volume of water displaced by ram and was calculated by using equation 11,

$$\Delta V_r = 0.0254 \cdot a_r \cdot D_r \qquad \text{Equation 11.}$$

where: a_r : area of the ram in cm^2 (1.99),

D_r : dial reading (10^{-3} in.).

This way of volume change measurement has various disadvantages, the main one being that while filling the triaxial cell some air bubbles remain trapped. These bubbles dissolve after the application of cell pressure and this causes an additional amount of water to enter the cell, leading to an overestimate of the volume change in the specimen (Mirata 1976).

4.2.3.4 Expansion of Triaxial Cells

In order to determine the volume change characteristics, triaxial cells were calibrated by applying different cell pressures and measuring the change in volume. These volume changes were plotted against the applied cell pressure values and calibration curves were obtained. During calibration, the volume change values recorded at approximately ten minutes after the application of cell pressure were used because creep characteristics are not important for small cells (Mirata 1976). Calibration curves for three cells are given in appendix 2.

4.2.3.5 Time Rate of Shearing

In all U-U tests a shearing rate of 0.5 mm/min was used.

4.2.4 Consolidated Undrained (C-U) Tests

4.2.4.1 Procedure Followed

After performing the necessary operations described in section 4.2.2, cell pressure and back pressure were applied simultaneously so that saturation and consolidation of the specimens were completed at the same time. During consolidation of the specimens,

continuous volume change observations were made by the apparatus described in section 4.2.1.4. The volume change values were used to estimate the value of coefficient of consolidation and area of the specimen after consolidation.

In order to have an idea about the degree of saturation after consolidation, pore pressure parameter B was found after the consolidation was completed. When there was no further significant change in the volume of the specimen (i.e consolidation is completed), the drainage valve was closed and cell pressure was increased by a small amount. From the the increment in the pore pressure, the pore pressure parameter, B, was determined. Then the specimen was allowed to reconsolidate by opening the drainage valve. Then the sample was sheared.

4.2.4.2 Calculation of Coefficient of Consolidation

In order to estimate the rate of shearing, the value of coefficient of consolidation is needed. Coefficient of consolidation is calculated by using t_{100} , which is determined from the relationship between volume change and time that was recorded during the consolidation stage. This relationship is expressed in terms of a volume change versus square root of time

graph which has the typical shape shown in figure 7. The initial straight line portion of this graph is extended to intersect the horizantal line representing 100% consolidation. Square root of t_{100} is taken to be the ordinate of this intersection point (Bishop and Henkel, 1962).

For the condition of one end drainage, c_v is given by equation 12

$$c_v = \frac{\pi h^2}{t_{100}} \qquad \text{Equation 12.}$$

where: c_v : coefficient of consolidation,

t_{100} : time required for 100% consolidation,

h : half the mean height of specimen.

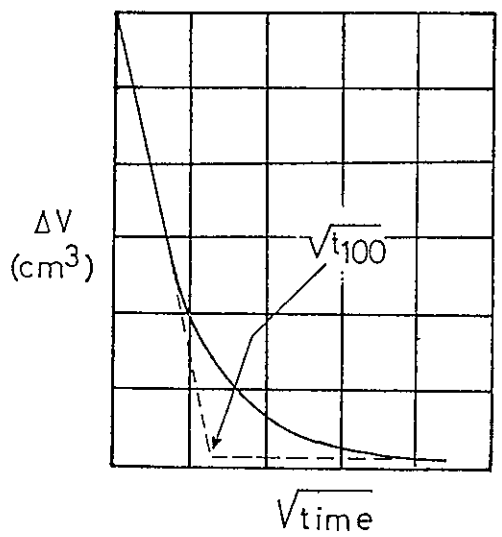

Figure 7. Volume Change versus $\sqrt{t}$ Graph

The outlined procedure of c_v determination is for fully saturated soils. However it may also be used for partly saturated soils to obtain a rough astimate of c_v (Bishop and Henkel, 1962).

4.2.4.3 Estimation of Time Rate of Shearing

The duration of shearing in C-U tests corresponding to 95% equalization of pore pressures for tests without side drains was given by Blight G.E (1963) as;

$$t_f = 1.6 \frac{h'^2}{c_v} \qquad \text{Equation 13.}$$

where: t_f : duration of shearing,

c_v : coefficient of consolidation as determined by equation 12,

h' : half the height of specimen after consolidation.

Rate of shearing was estimated by using equation 14.

$$\text{Rate of shearing} = \frac{\epsilon . h'}{t_f} \qquad \text{Equation 14.}$$

where ϵ is the approximate expected axial strain at failure (estimated in U-U tests).

4.2.4.4 Shearing of the Specimen

In the shearing stage no drainage in or out of the specimens was allowed. In all C-U tests continuous pore pressure measurements were made during shearing.

4.2.4.5 Calculation of Area at the End of Consolidation and During Shearing

The area at the end of consolidation, A_0 , in triaxial specimens subjected to C-U test was calculated from equation 6 given in section 4.2.3.2.

The area that applies during shearing was estimated by using equation 15. This equation is based on the assumption that the specimen reaches full saturation after consolidation.

$$A_s = \frac{A_0}{1 - \epsilon} \qquad \text{Equation 15.}$$

where ϵ is calculated by using equation 8 (section 4.2.3.2).

4.2.5 Consolidated Drained (C-D) Tests

4.2.5.1 Procedure Followed

The procedure followed in C-D tests was similar to the one applied in C-U tests up to the end of

consolidation stage. After consolidation the samples were sheared allowing drainage.

4.2.5.2 Calculation of Rate of Shearing

In C-D tests such a shearing rate should be applied that the excess pore pressure which develops during the shearing process can dissipate. In order to estimate the time to failure, the following equation which was based on the assumption of 95% dissipation of excess pore pressure was used (Bishop and Henkel, 1962)

$$t_f = \frac{20 \cdot h'^2}{\eta \cdot c_v} \qquad \text{Equation 16.}$$

where η is a factor depending on drainage conditions (η = 0.75 for drainage from one end only).

The rate of shearing to be applied was estimated by using equation 14 given in section 4.2.4.3.

4.2.5.3. Calculation of the Area at the End of Consolidation and During Shearing

Area after consolidation in C-D tests was calculated by using equation 6.

In the shearing stage a volume change occurs due to drainage of water out of the sample, therefore the

corrected area during shearing was calculated from equation 7.

The volume changes that were used in preceding two equations were also determined as explained in section 4.2.3.3.

4.2.6 Errors in Triaxial Testing and Their Corrections

4.2.6.1 Effect of Ram Friction

During a triaxial test if there is any friction on the loading ram which may arise mainly due to external causes or non-uniform deformation of the test specimen, there will be an error in the calculated stresses in the specimen. This error for a 1.905 cm diameter ram is between 1% and 3% of the axial load for most of the loading range. The best way to overcome this error is to use triaxial cells with rotating bushes (Bishop and Henkel, 1962).

In this study triaxial tests were carried with the cells without rotating bushes. Some castor oil was introduced for reducing the friction and no correction due to ram friction was applied to the test results.

4.2.6.2 Correction Due to Membrane Restraint

Rubber membranes cause an increase of the resistance of triaxial specimens during the testing due to their confining effect. The increase in strength becomes important especially in soft clays.

As most of the specimens failed by symmetrical bulging, the correction given by Henkel and Gilbert (1952) was used in this study. The amount of correction for a standard membrane (0.20 mm thick) is about 4.14 kN/m^2. However this value is for 15% failure strain and for strains other than 15% this correction (4.14 kN/m^2) is multiplied by a correction factor taken from figure 8.

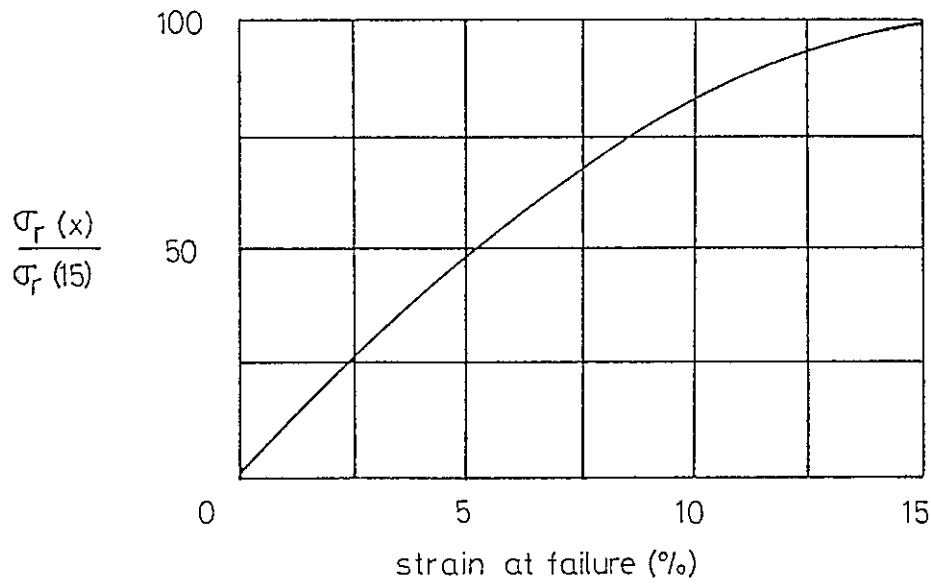

Figure 8. Experimental Relation between Rubber Correction and Failure Strain (after Henkel and Gilbert, 1952)

4.2.6.3 Seating Correction

Before the application of cell pressure in a triaxial test, the ram was brought in contact with the top cap as mentioned in section 4.2.2. However upon application of the cell pressure a volume change occurred, which caused a clearance between the top cap and the ram. Because of this effect some of the samples were tilted due to non-uniform deformation.

The top cap and the ram were brought in contact again, before starting to shear the specimens. However for tilted specimens the top cap and ram were not coaxial when proving ring started to deflect. In order to seat the top cap in the ram an initial loading which was followed by unloading to the same proving ring reading was applied to the specimen. Furthermore the effect of seating on stress-strain curves was corrected as described by Mirata(1976). (See, for example, Fig. 10.)

4.2.7 Calculation of Pore Pressure Parameters

The value of pore pressure parameter, B, was determined by using equation 17 in U-U tests.

$$B = \frac{\Delta U}{\sigma_3} \qquad \text{Equation 17.}$$

where: σ_3: applied all around pressure,

ΔU : increase in pore water pressure due to the application of σ_3 (ΔU is taken as the recorded value of pore pressure after equalization).

In C-U and C-D tests, B values were calculated from equation 18

$$B = \frac{\Delta U}{\Delta \sigma_3} \qquad \text{Equation 18.}$$

in which, $\Delta \sigma_3$ is the increase in all around-pressure under undrained condition and ΔU is the increase in pore water pressure due to the application of $\Delta \sigma_3$.

The pore pressure parameter A, at any instant of the shearing stage in C-U test corresponding to an axial strain ϵ(%) was calculated from equation 19 which, in fact, is a special form of equation 4, where $\Delta \sigma = 0$ and $B = 1$.

$$A = \frac{\Delta U}{(\Delta \sigma_1 - \Delta \sigma_3)} \qquad \text{Equation 19.}$$

in which: ΔU : increase in pore pressure after the start of shearing at the strain ϵ(%),

$(\Delta \sigma_1 - \Delta \sigma_3)$: deviatoric stress measured at axial strain ϵ(%).

4.3 Consolidation Tests

4.3.1 Double Oedometer Test

A double oedometer test was carried out on two undisturbed samples. Two specimens one at natural moisture content and the other flooded were loaded using the loading sequence of 25, 50, 100, 200, 400, 800, 1600, 3200 kN/m^2. Then the specimens were unloaded to 1600, 400, 100 and 25 kN/m^2. e-log p values were plotted and c_v values for the soaked specimen were calculated by using square root of time method.

4.3.2 One Dimensional Consolidation Tests

In order to understand the collapse potential of the soil, consolidation tests were performed by flooding the samples under pressure. Specimens were loaded by the same loading sequence given in section 4.3.1 and were flooded at different pressures. After 24 hours, the change in dial reading was recorded and the remaining part of the test was conducted as a normal consolidation test.

During the tests, each load was kept on for 24 hours.

4.3.3 Method of Calculation of Void Ratio

The void ratio at the end of any load increment, e, was calculated by

$$e = \frac{H_1 - H_s}{H_s} \qquad \text{Equation 20.}$$

where: H_s : equivalent thickness of solids

: $M_s / A_c . G_s . \rho_w$

A_c : area of the specimen,

M_s : dry mass of the specimen,

H_1 : thickness at the end of related load increment.

Table 3. Summary of Triaxial Test Results

TEST NO	TEST TYPE	σ_3 (kN/m^2)	BACK. PRESS. (kN/m^2)	W_n (%)	W_{final} TOP (%)	W_{final} MIDD. (%)	W_{final} BOTT. (%)	WT. OF SPEC. (gr)	VOL. OF SPEC. (cm^3)	γ (kN/m^3)	ΔV (cm^3)	$\Delta V'$ (cm^3)	$(\sigma_1-\sigma_3)$ (kN/m^2)	U_f (kN/m^2)	ϵ_f (%)	B	A
1	U-U	49	---	36.93	42.89	43.41	--	105.6	80.10	12.93	2.45	2.89	150	--	9.64	0.042	--
2	U-U	98	---	---	41.46	40.15	41.36	110.8	80.10	13.57	4.12	1.36	211	--	7.93	0.304	--
3	U-U	196	---	---	45.54	45.89	45.97	101.4	80.10	12.42	5.27	2.18	264	--	10.15	0.366	--
4	U-U	294	---	---	58.75	60.33	57.96	106.6	73.65	14.20	3.95	1.62	140	--	6.42	0.838	--
5	U-U	294	---	38.44	40.61	41.48	41.46	100.9	80.10	12.36	8.38	3.95	346	--	15.19	0.216	--
6	U-U	392	---	35.92	40.55	39.29	35.64	105.1	80.10	12.87	6.37	2.68	510	--	11.95	0.448	--
7	C-U	255	196	37.66	44.06	44.79	--	113.4	80.10	13.87	3.92	--	156	194	3.81	0.903	-0.004
8	C-U	304	196	38.90	49.80	44.98	--	115.0	80.10	14.07	5.90	--	111	256	3.50	0.874	0.515
9	C-U	402	196	36.54	57.23	51.92	51.19	99.8	80.10	12.21	8.00	--	225	312	4.23	0.807	0.540
10	C-U	490	196	33.14	47.48	49.29	49.45	107.7	80.10	13.18	11.56	--	282	366	2.51	0.874	0.593
11	C-U	294	196	--	52.79	--	53.15	102.7	80.10	12.57	7.90	--	85	259	3.88	---	0.610
12	C-D	255	196	39.41	--	--	--	99.7	80.10	12.21	7.99	2.74	135	--	8.46	0.732	--
13	C-D	314	196	38.14	45.22	48.33	50.19	100.5	80.10	12.30	6.02	2.10	160	--	2.90	0.831	--
14	C-D	412	196	37.53	42.73	45.70	47.96	100.2	80.10	12.27	11.97	4.40	426	--	11.12	0.846	--
15	C-D	490	196	35.74	40.93	43.68	46.06	103.1	80.10	12.63	15.81	5.30	558	--	14.96	0.864	--

Table 4 Data for Plotting Failure Envelopes

TEST NO	$(\sigma_1 - \sigma_3)_f$	$(\sigma_3)_f$	$(\sigma_1)_f$	U_f	q_f	p_f	p'_f	σ_c
1	150	49	199	--	75	124	--	49
2	211	98	309	--	106	204	--	98
3	264	196	460	--	132	328	--	196
4	140	294	434	--	70	364	--	294
5	346	294	640	--	173	467	--	294
6	510	392	902	--	255	647	--	392
7	156	255	411	194	78	333	139	59
8	111	304	415	256	56	360	104	108
9	225	402	627	312	113	515	203	206
10	282	490	772	366	141	631	265	294
11	85	294	379	259	43	337	78	98
12	135	255	---	---	68	---	127	59
13	160	314	---	---	80	---	198	118
14	426	412	---	---	213	---	429	216
15	558	490	---	---	279	---	573	294

All units are in kN/m^2

Subscript f denotes the failure condition

Table 5. Data for Plotting Failure Envelopes for C-U Tests

TEST	σ_3	(1) σ_1'	(1) σ_3'	(1) $(\sigma_d)_f$	(1) U_f	(1) ϵ_f	(2) σ_1'	(2) σ_3'	(2) $(\sigma_d)_f$	(2) U_f	(2) ϵ_f
7	255	204	56	148	199	1.73	217	59	156	194	3.81
8	304	142	40	102	264	5.59	159	48	111	256	3.50
9	402	288	72	206	330	5.64	315	90	225	312	4.23
10	490	374	95	279	395	6.08	406	124	282	366	2.51
11	294	120	35	85	259	3.88	120	35	85	259	3.88

Units of Stresses are in kN/m^2

Subscript f denotes the failure condition

1. Maximum Principal Stress Ratio Failure Criterion

2. Maximum Deviatoric Stress Failure Criterion

TABLE 6. Shear Strength Parameters Obtained from U-U Tests.

σ (kN/m^2)	c (kN/m^2)	ϕ
90-175	35	22.0°
175-400	65	12.5°

2. C-U TESTS: In figures 18 to 22, stress-strain relationships obtained from C-U tests and pore pressures observed during shearing are given. Also the variation of pore pressure parameter, A, with strain is shown in the same figures.

Mohr envelope in terms of effective stresses is given in figure 23 . The shear strength parameters are found to be $c' = 5$ kN/m^2 , $\phi' = 31°$. Modified failure envelope in terms of effective stresses is given in figure 24. The parameters obtained from this envelope are $a' = 15$ kN/m^2 , $\alpha' = 26°$ corresponding to $c' = 5$ kN/m^2 and $\phi' = 31°$.

All above envelopes are based on maximum deviatoric stress failure criterion. The effective stress envelope that is based on the maximum principal stress ratio criterion is plotted in figure 25. and $c' = 0$ and $\phi' = 36°$ are obtained.

3. C-D TESTS: Stress-strain curves and the plot of change in volume during shearing versus axial strain

are presented in figures 26 to 29. From the Mohr envelope in figure 30 effective shear strength parameters $c' = 10\ kN/m^2$, $\varnothing' = 30^\circ$ are obtained. The modified failure envelope is plotted in figure 31 and $a' = 9\ kN/m^2$, $\alpha' = 25^\circ$ are found corresponding to $c' = 10\ kN/m^2$ and $\varnothing' = 30^\circ$.

4.4.2 Consolidation Test Results

The results of consolidation tests are expressed in terms of e-log p curves (figures 32-41) and summary of all the consolidation tests are given in table 7.

The test made on soaked sample (U2) was used to calculate the preconsolidation pressure and the coefficient of consolidation. Preconsolidation pressure was calculated by using two different methods, namely Rutledge-Schmertmann (Birand, 1968) and Casagrande (table 8). (Refer to appendix 3 for Rutledge-Schemertmann construction). c_v values calculated by the square root of time fitting method are given in table 9.

The coefficient of collapsibility, C, is estimated to be 0.438 by using equation 2 and results of tests U1 and U2 (appendix 4). Also from the result of test U6, C_p (section 2.2) was found to be 2.04. In figure 42, C_p values calculated for tests U3 to U10 were plotted against flooding pressure.

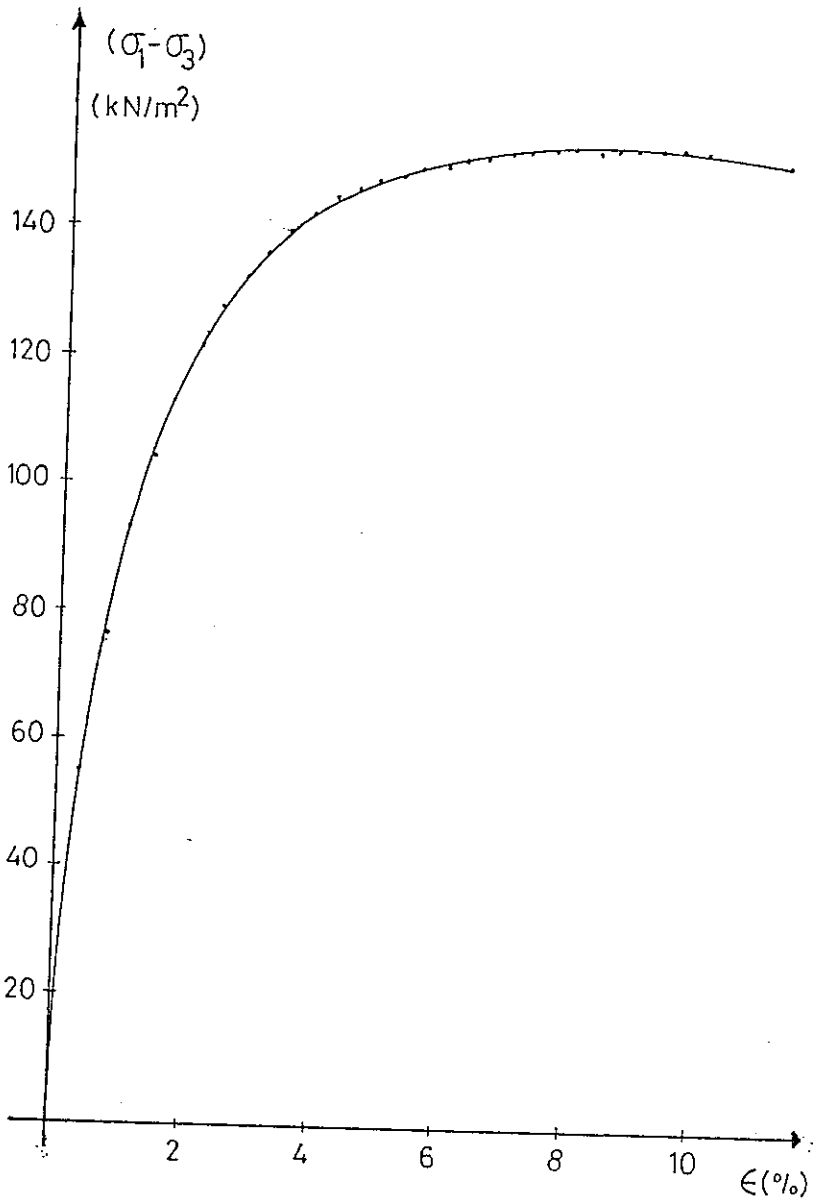

Figure 9. Stress-strain Curve for Test 1.

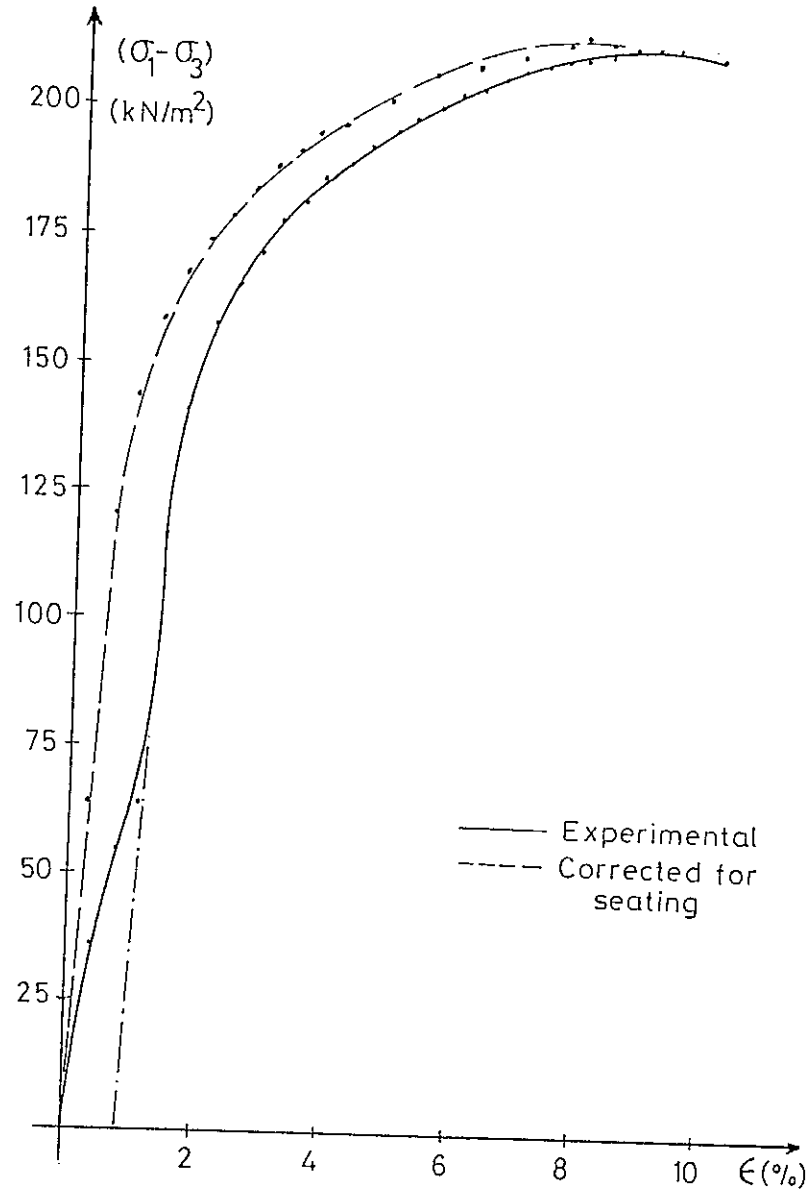

Figure 10. Stress-strain Curve for Test 2.

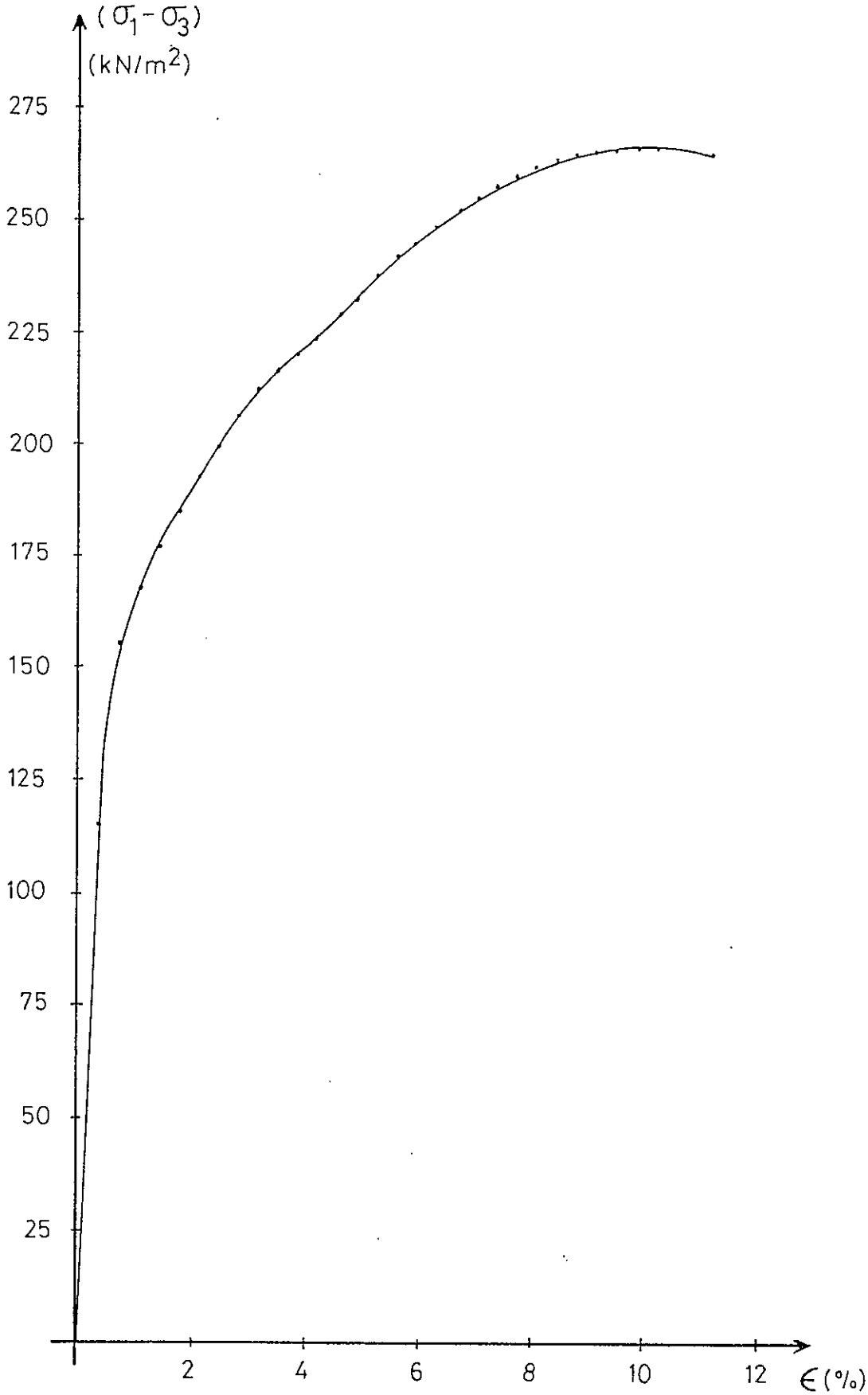

Figure 11. Stress-strain Curve for Test 3.

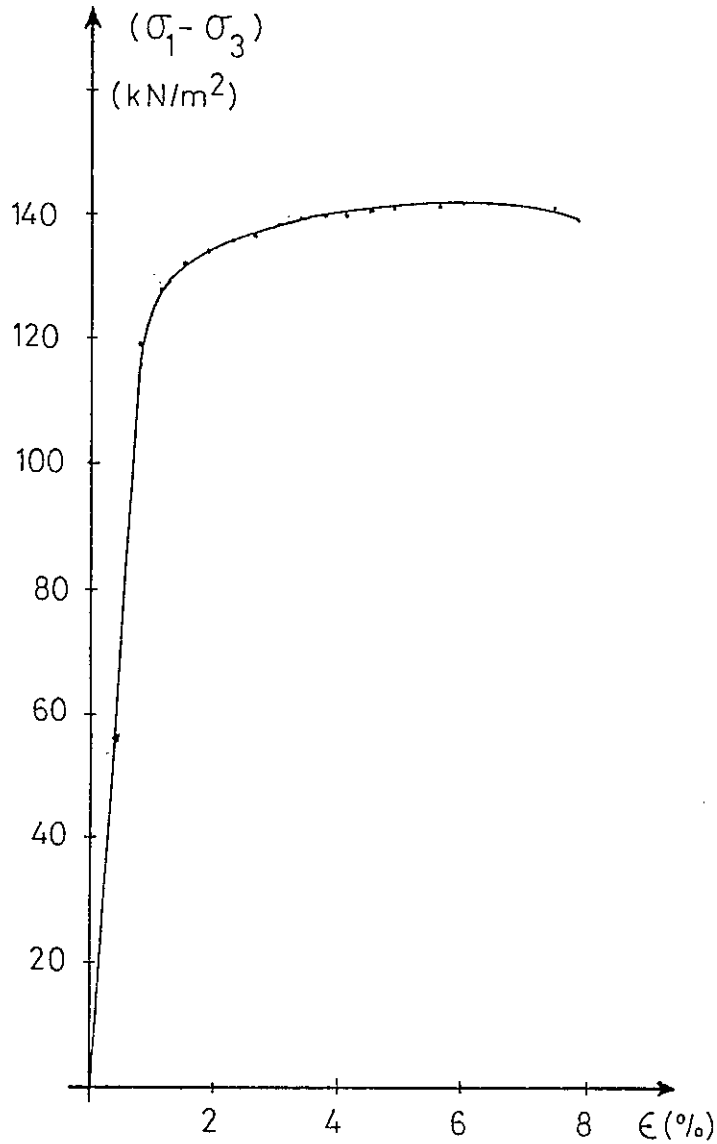

Figure 12. Stress-strain Curve for Test 4.

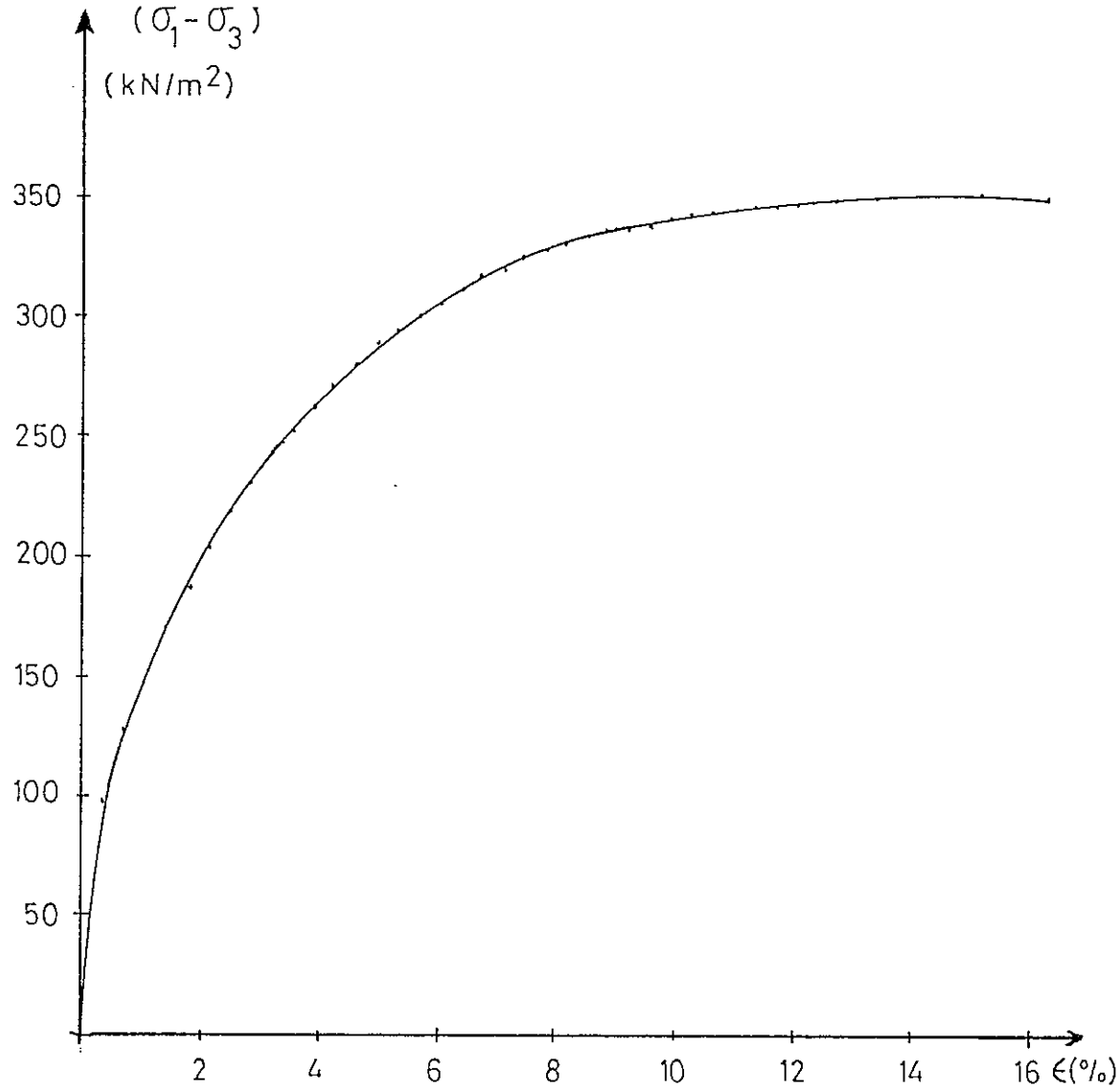

Figure 13. Stress-strain Curve for Test 5.

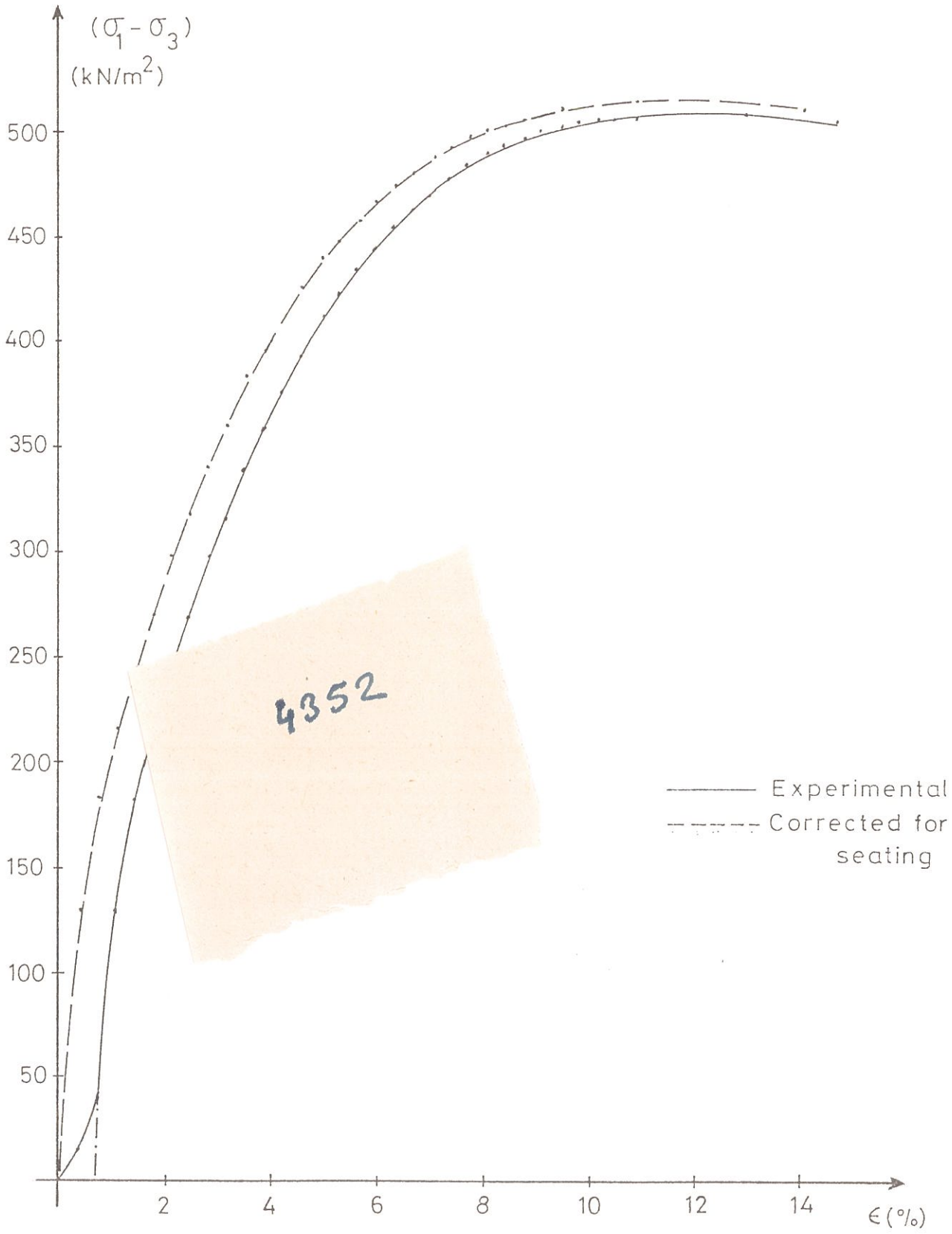

Figure 14. Stress-strain Curve for Test 6.

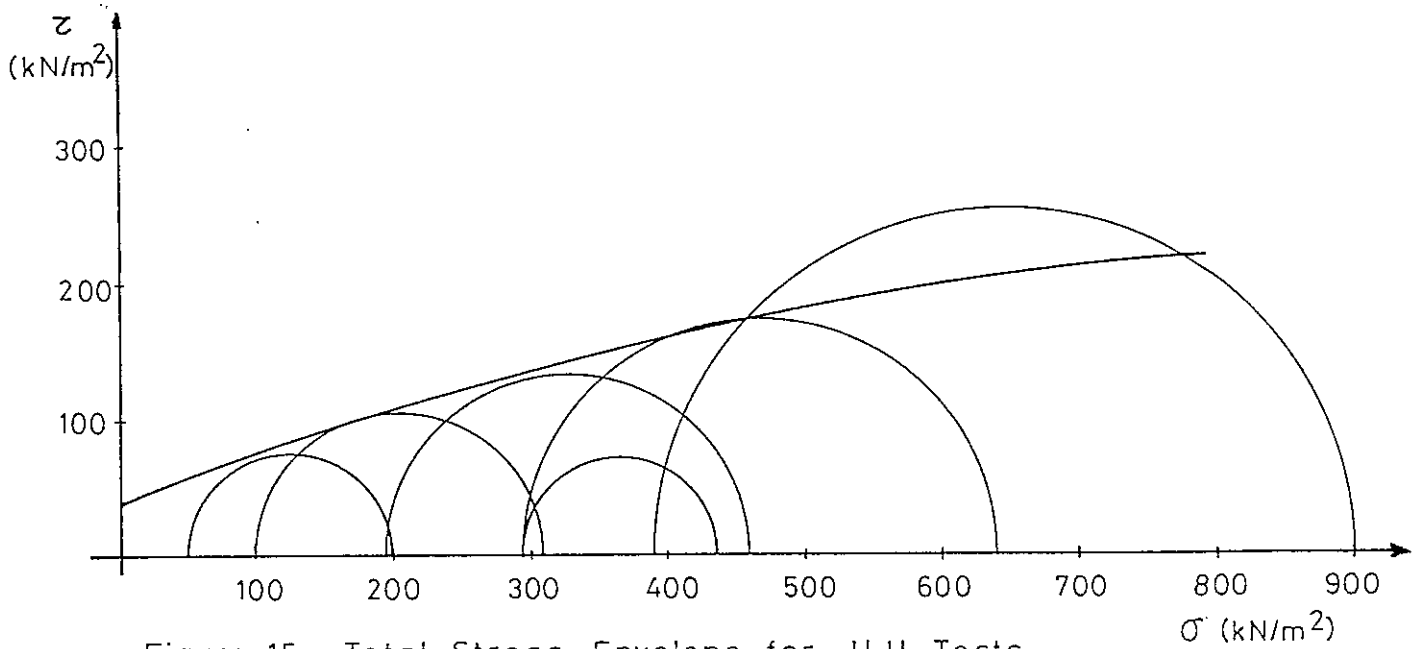

Figure 15. Total Stress Envelope for U-U Tests

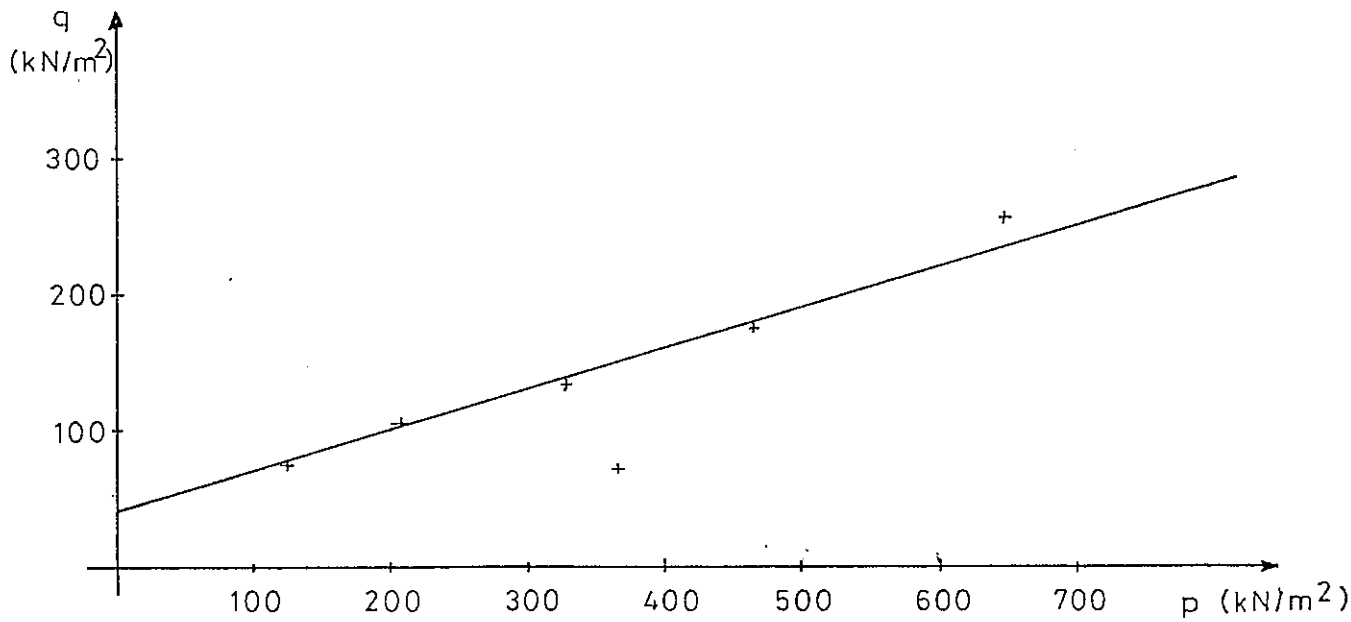

Figure 16. Modified Failure Envelope for U-U Tests

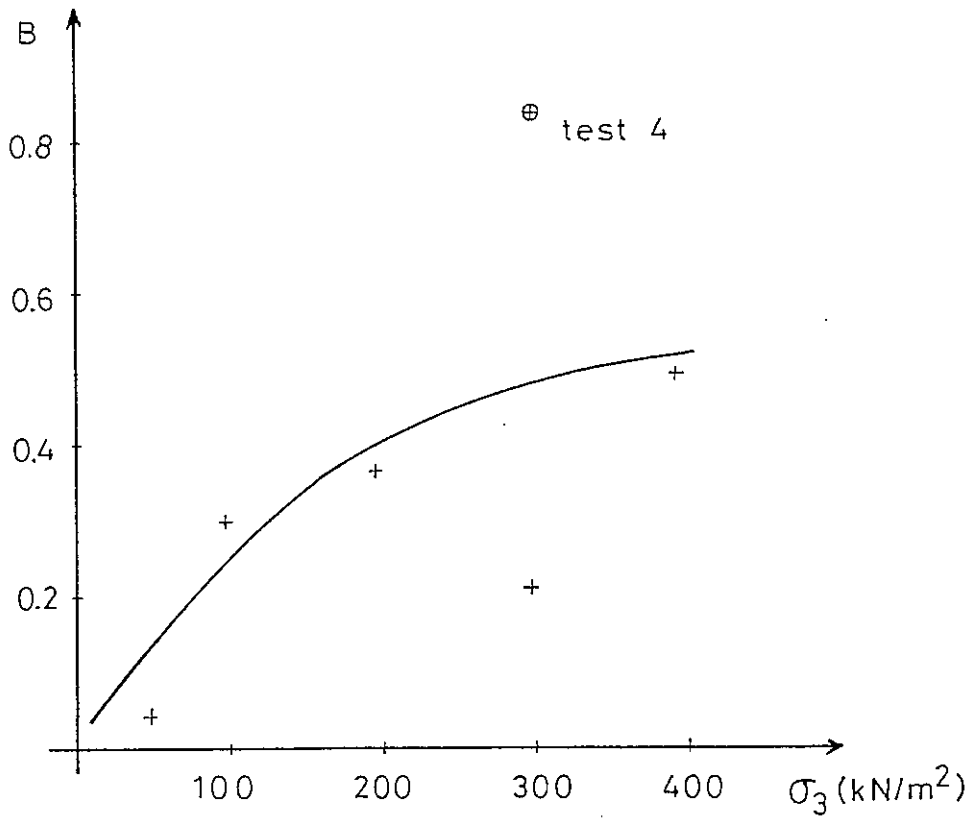

Figure 17. Variation of B with σ_3

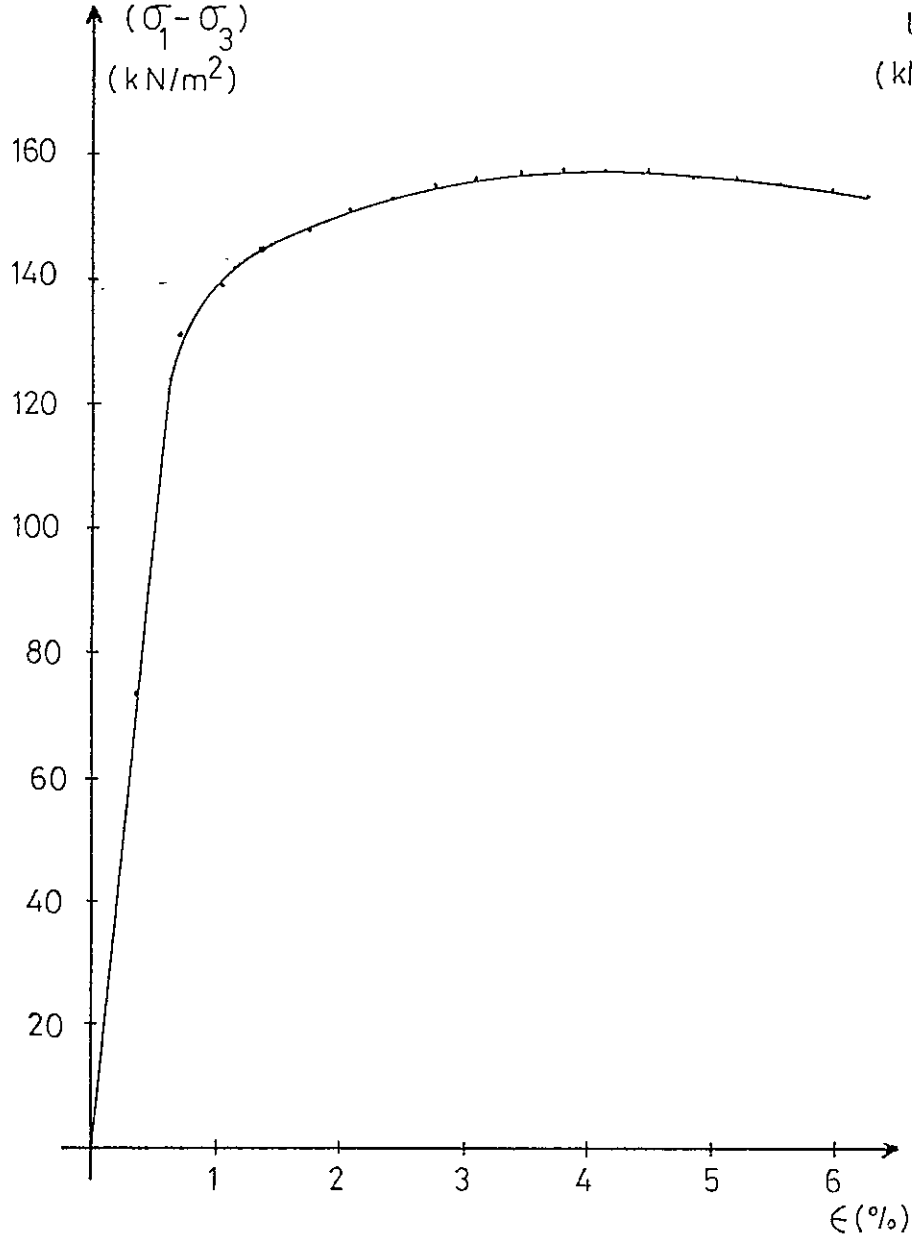

Figure 18. (a) Stress-strain Curve for Test 7.

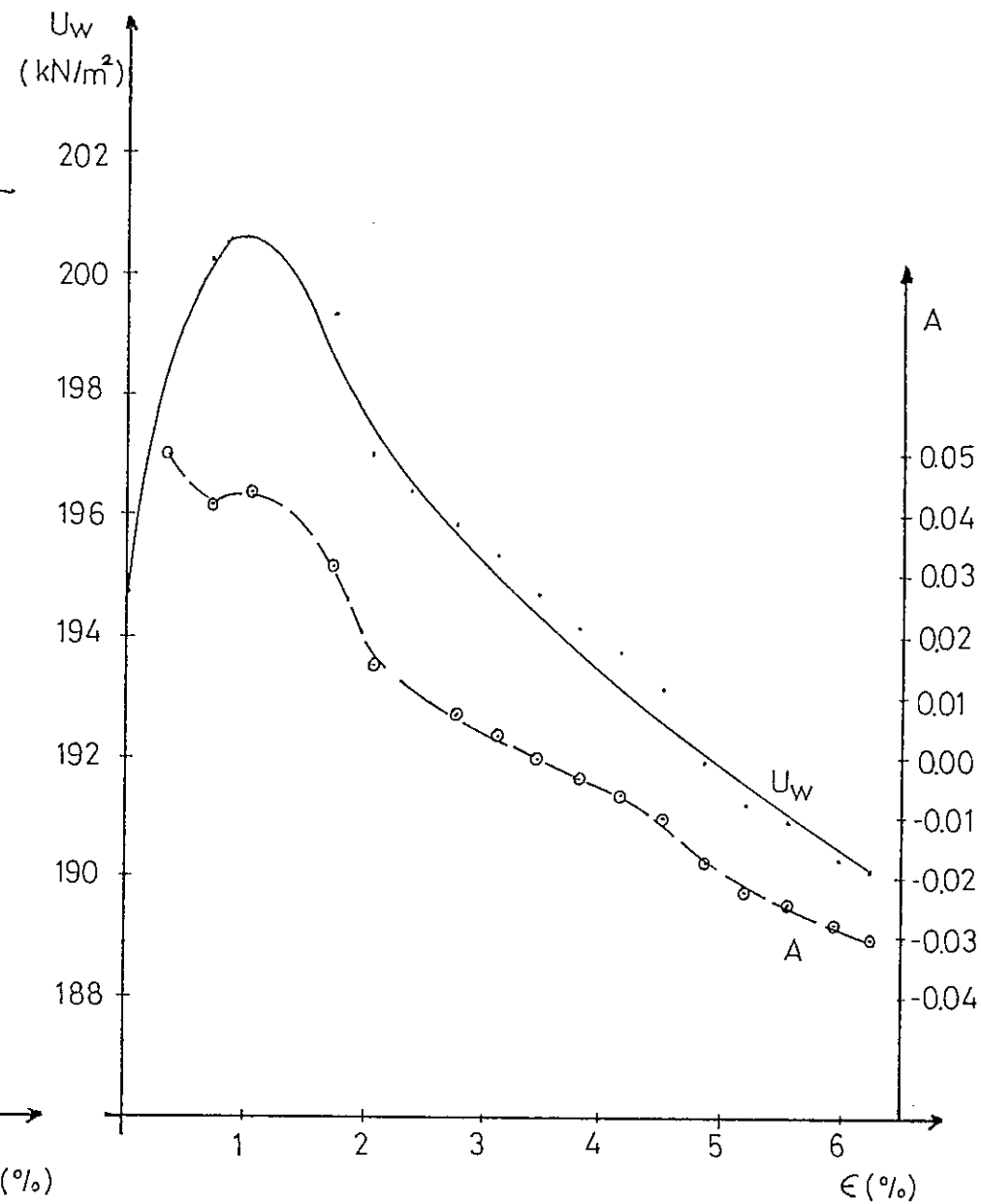

(b) Variation of U_w and A with Strain for Test 7.

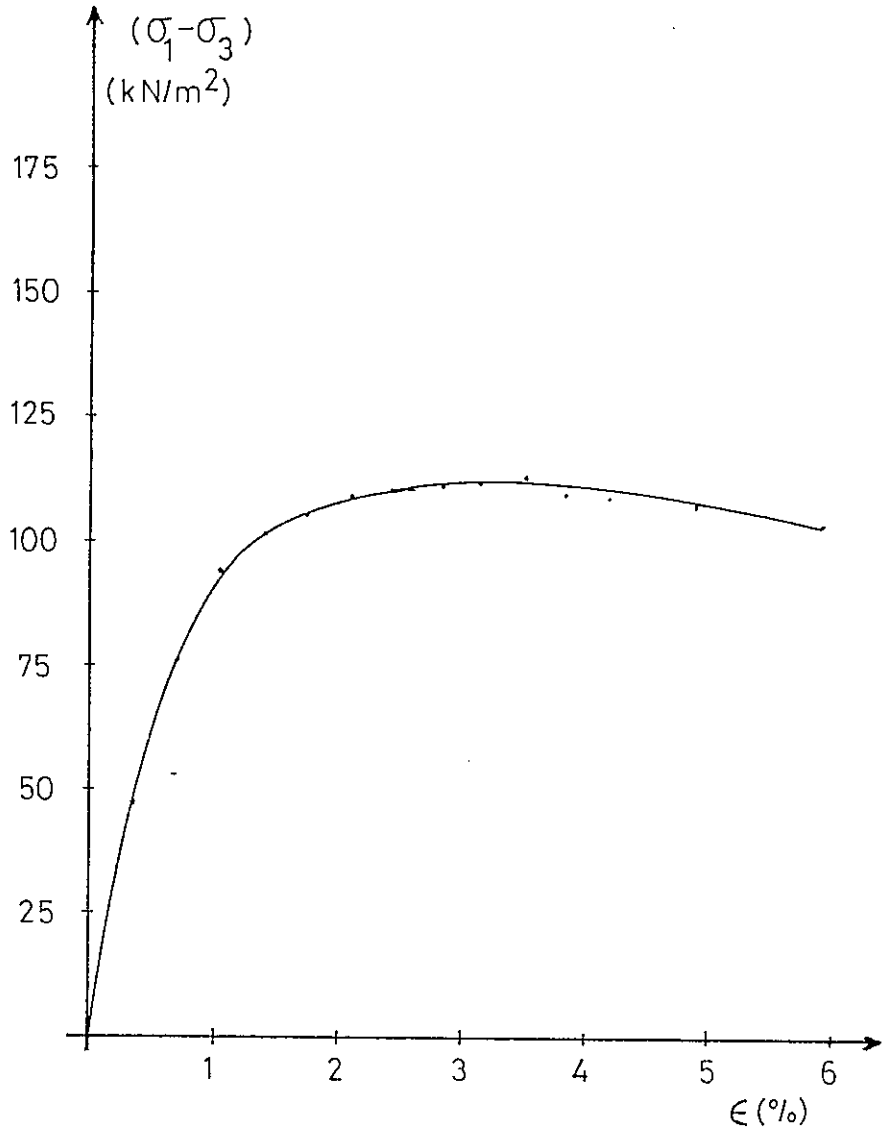

Figure 19. (a) Stress-strain Curve for Test 8.

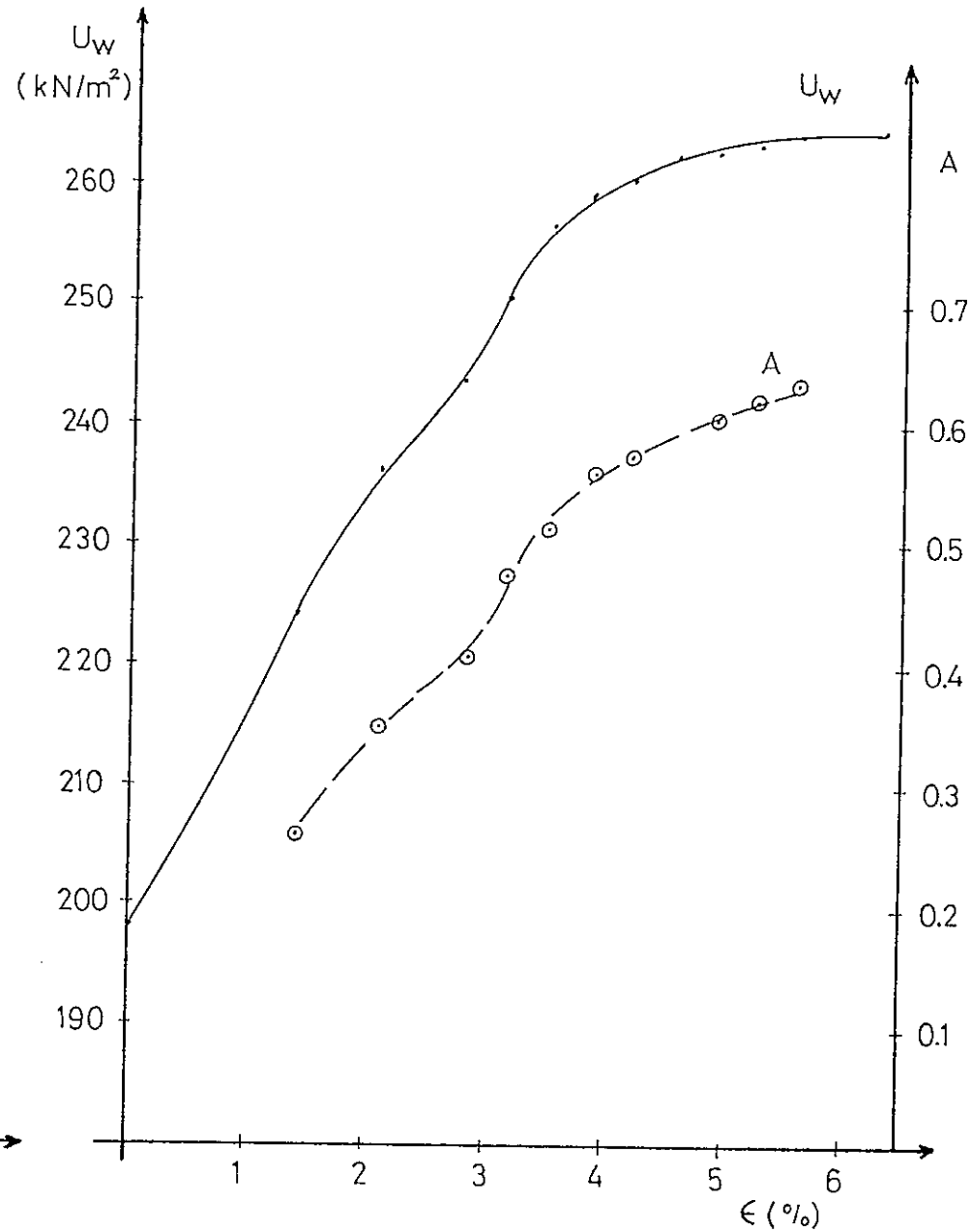

(b) Variation of U_w and A with Strain for Test 8.

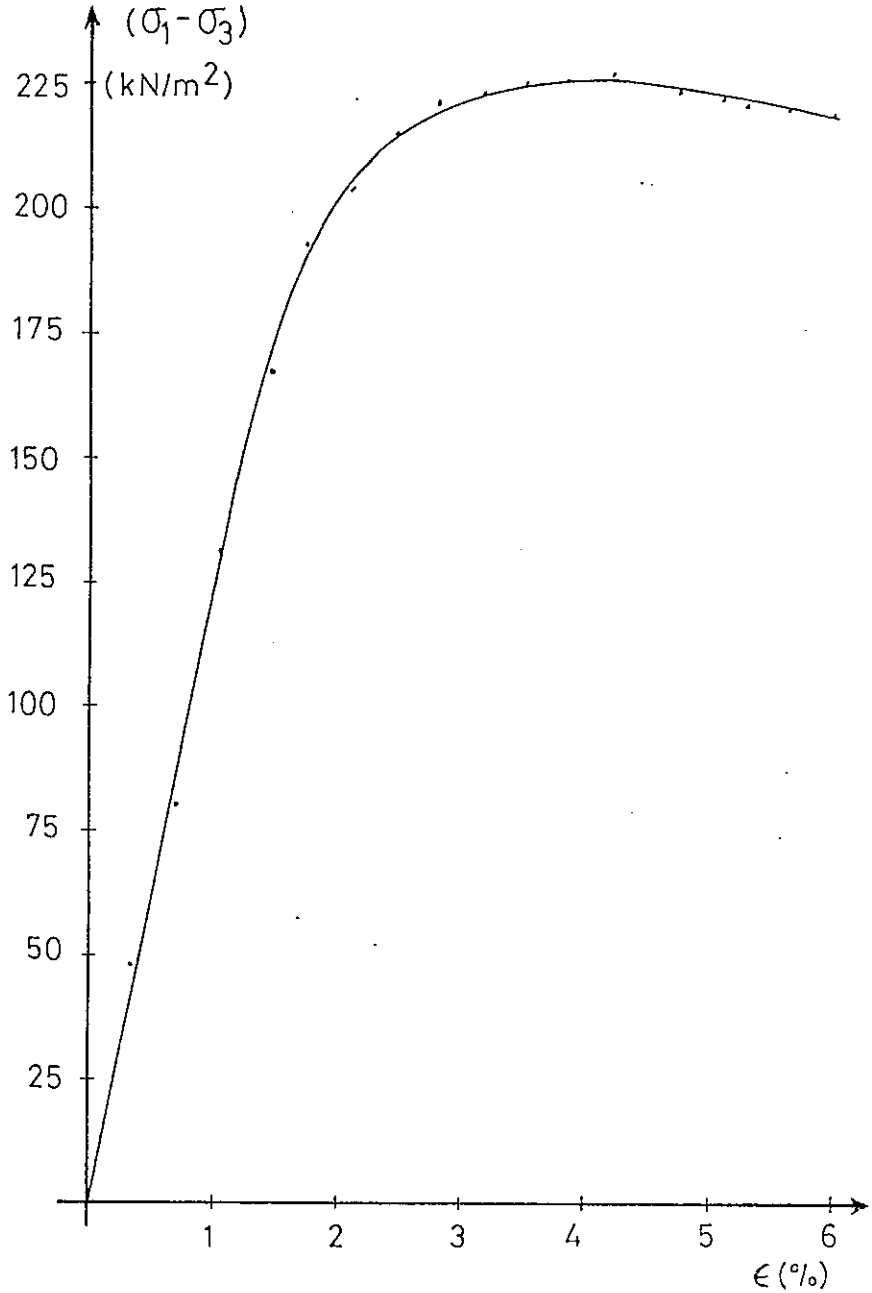

Figure 20. (a) Stress strain Curve for Test 9.

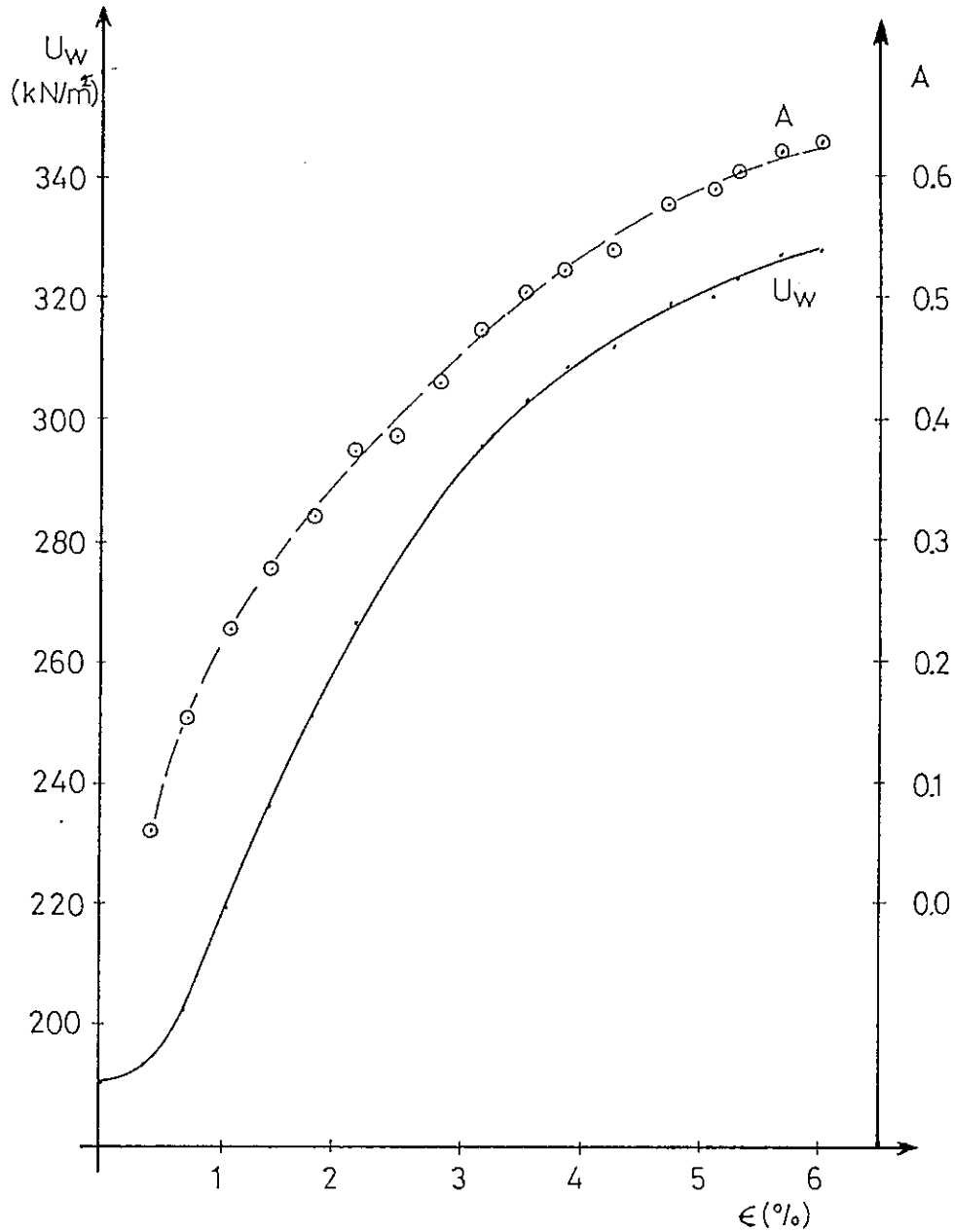

(b) Variation of U_w and A with Strain for Test 9.

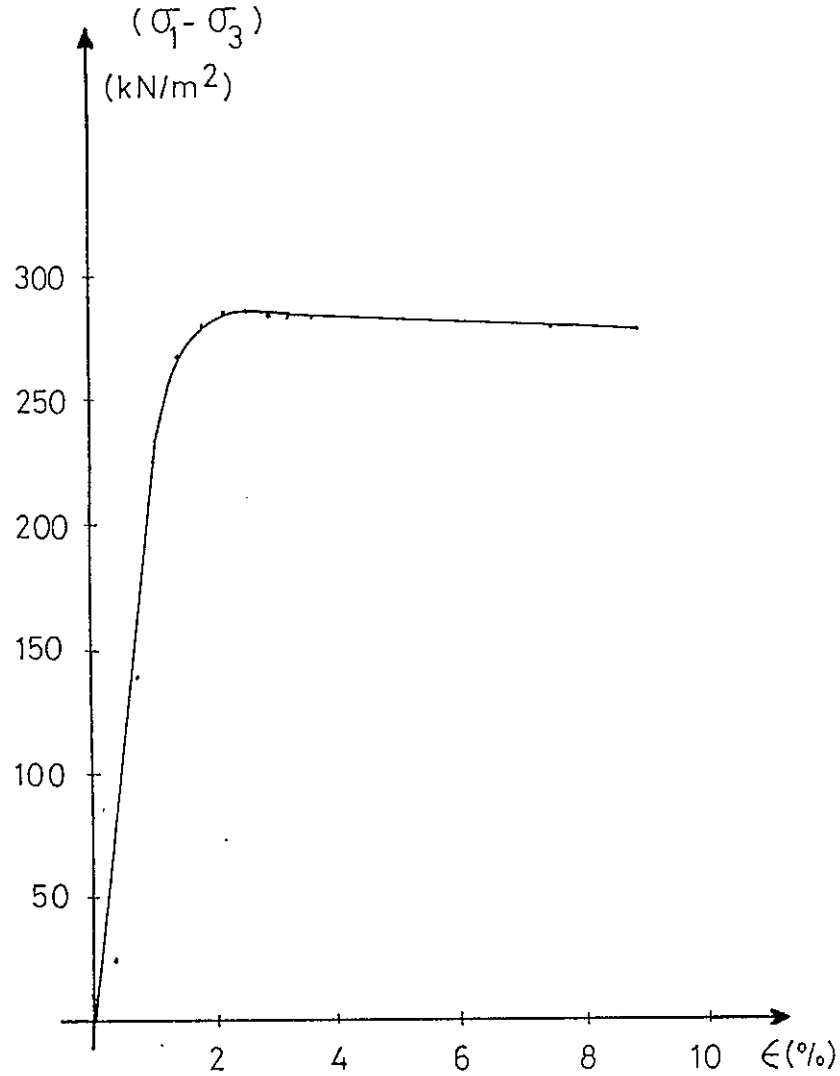

Figure 21. (a) Stress-strain Curve for Test 10.

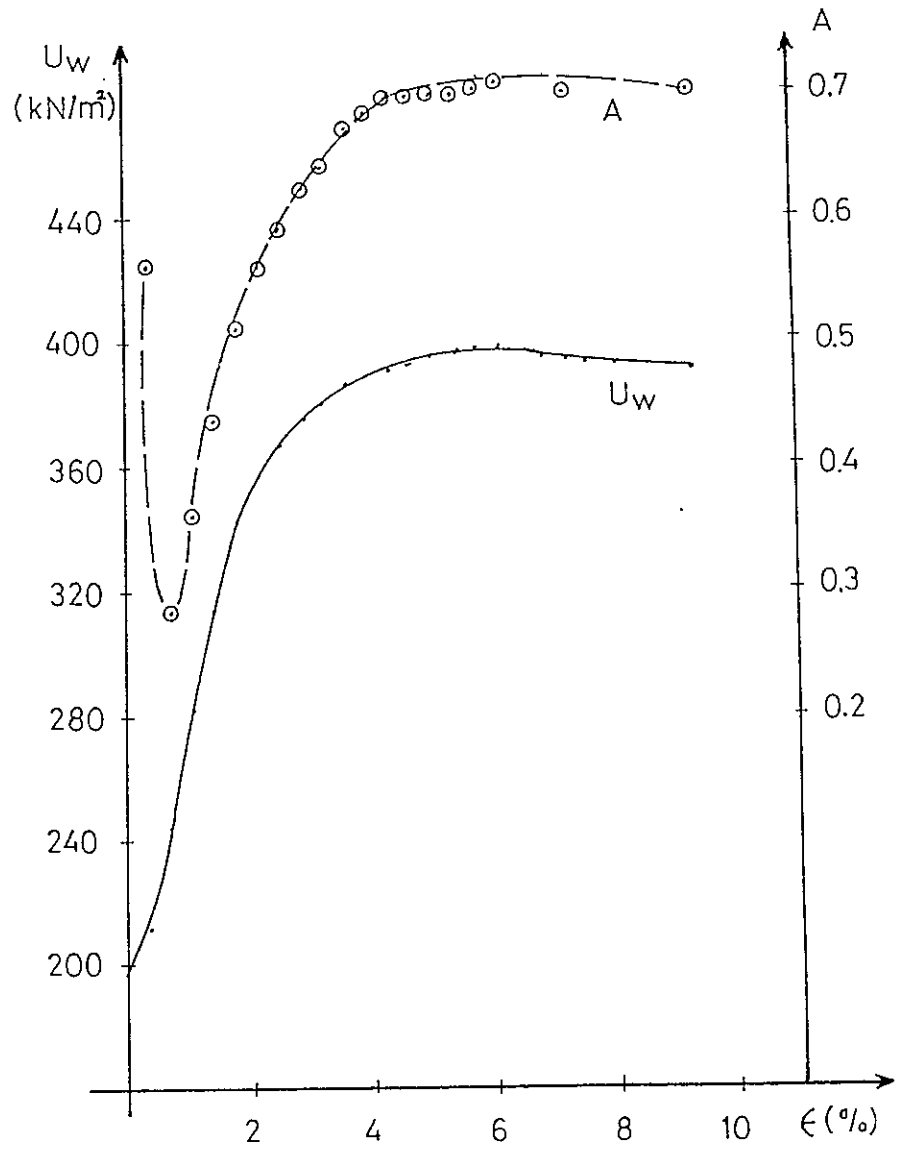

(b) Variation of U_w and A with Strain for Test 10.

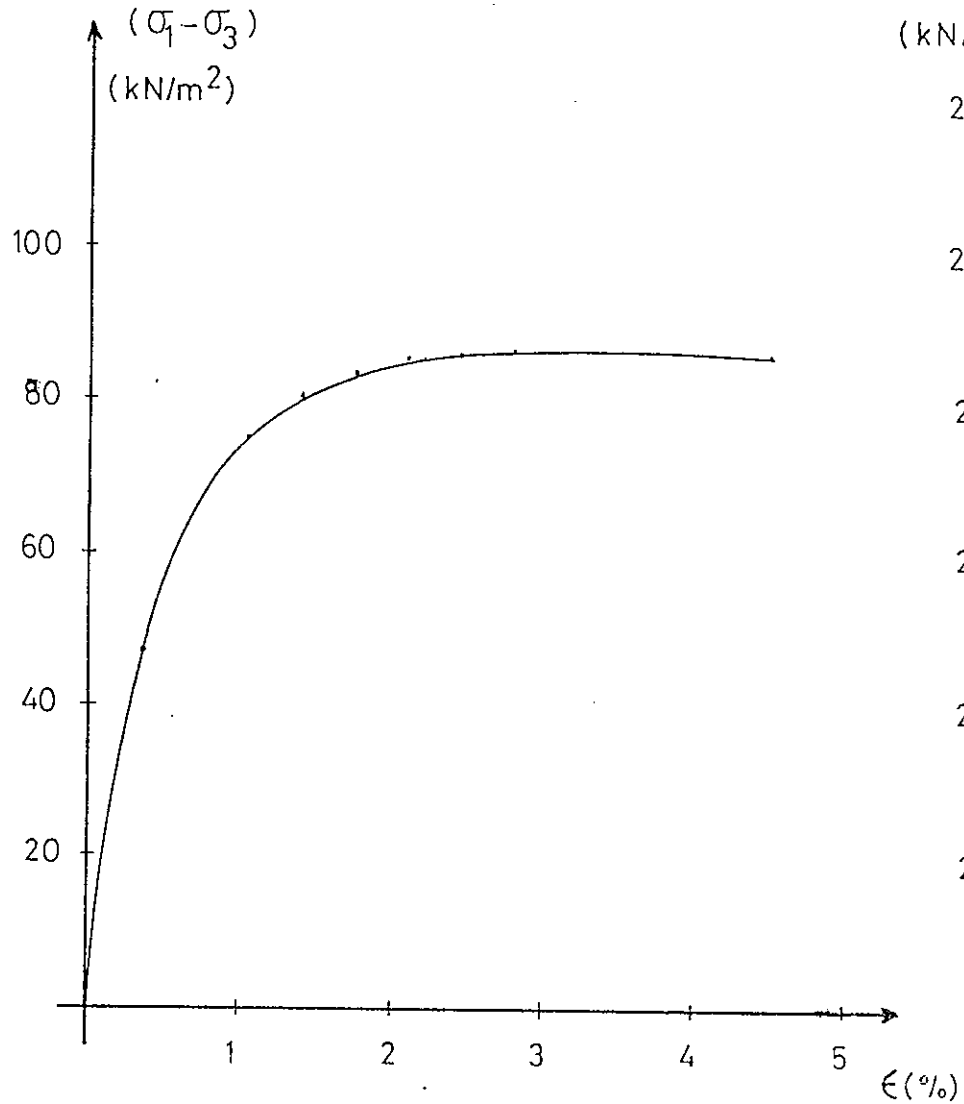

Figure 22. (a) Stress strain Curve for Test 11.

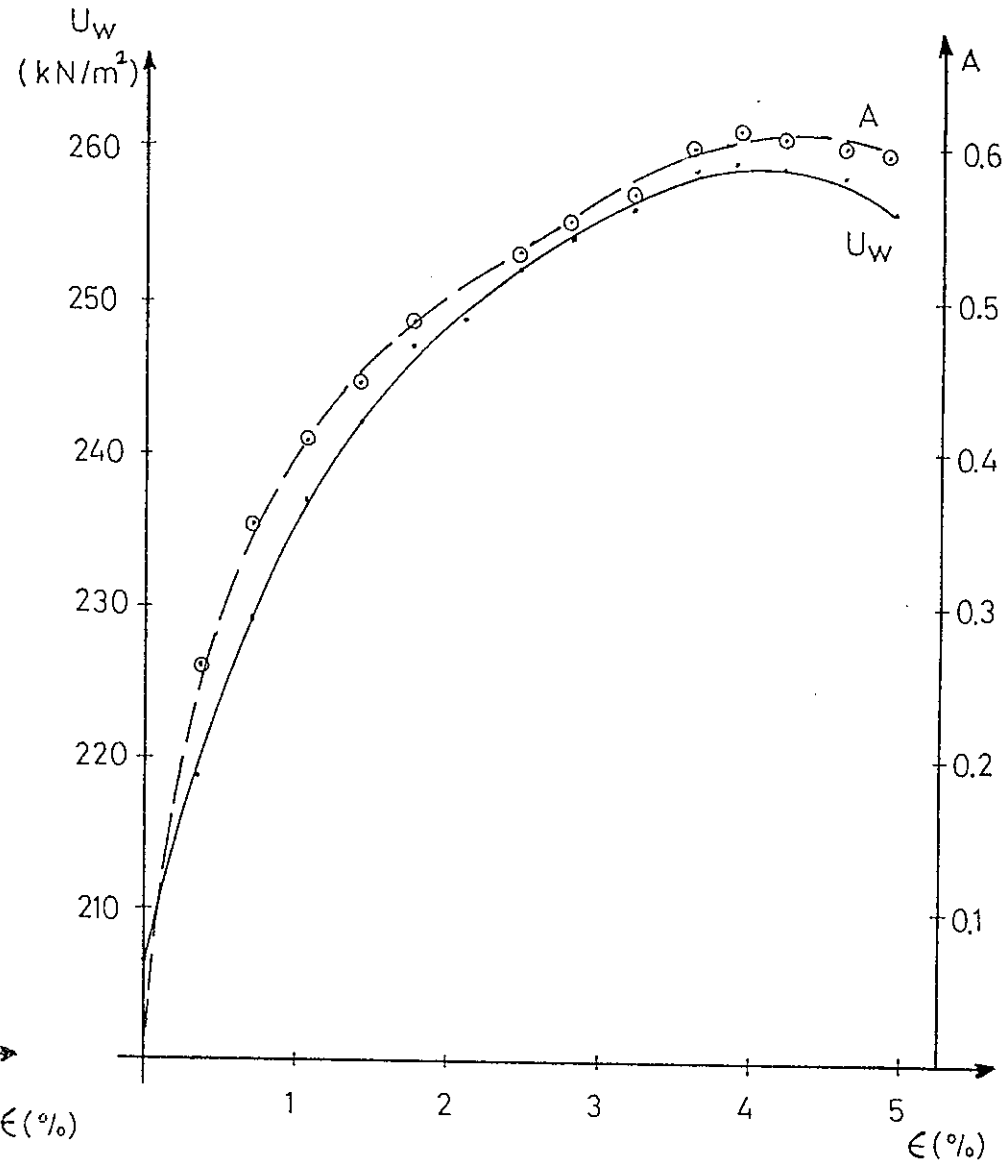

(b) Variation of U_w and .A with Strain for Test 11.

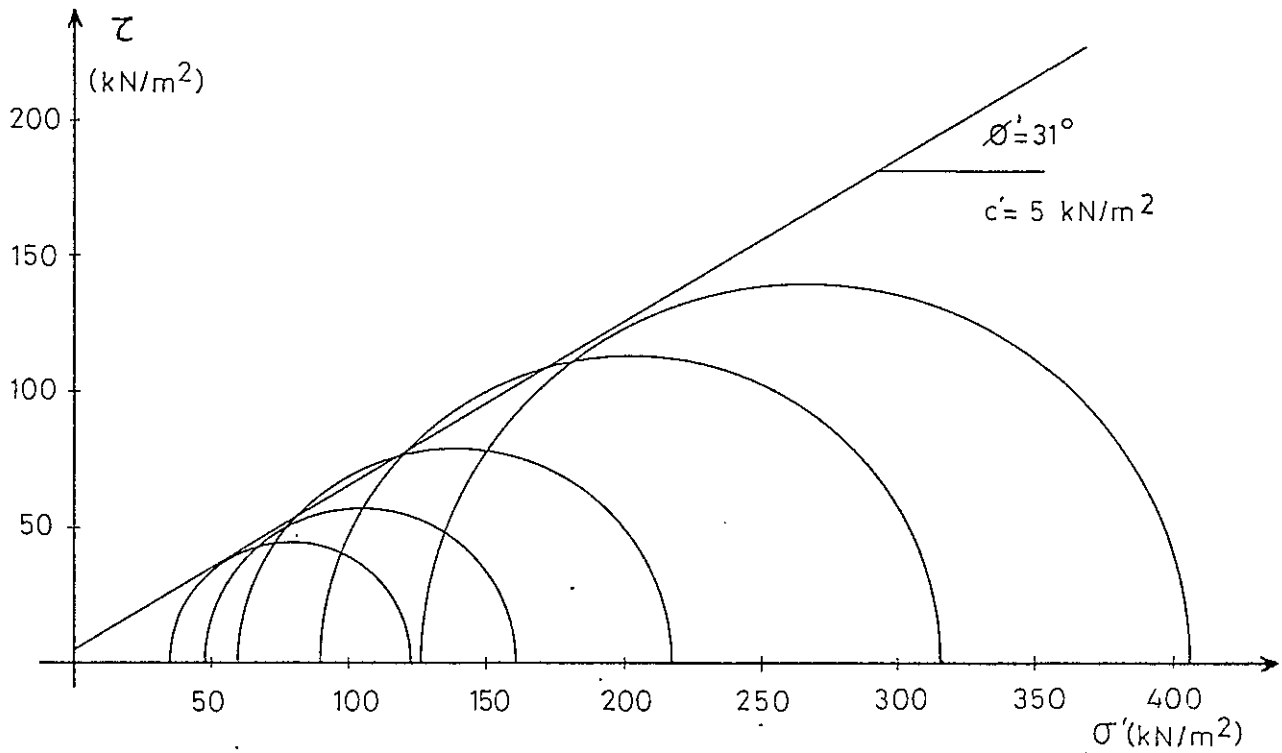

Figure 23. Effective Stress Envelope for C-U Tests $(\bar{\sigma}_1 - \bar{\sigma}_3)_{max.}$

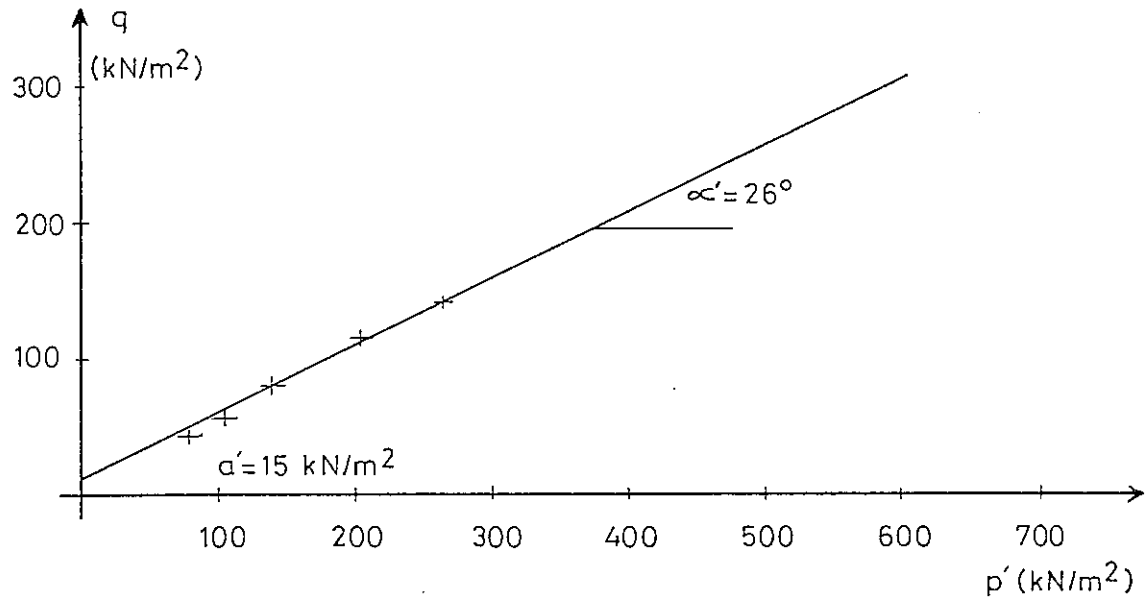

Figure 24. Modified Failure Envelope for C-U Tests (Effective Stress)

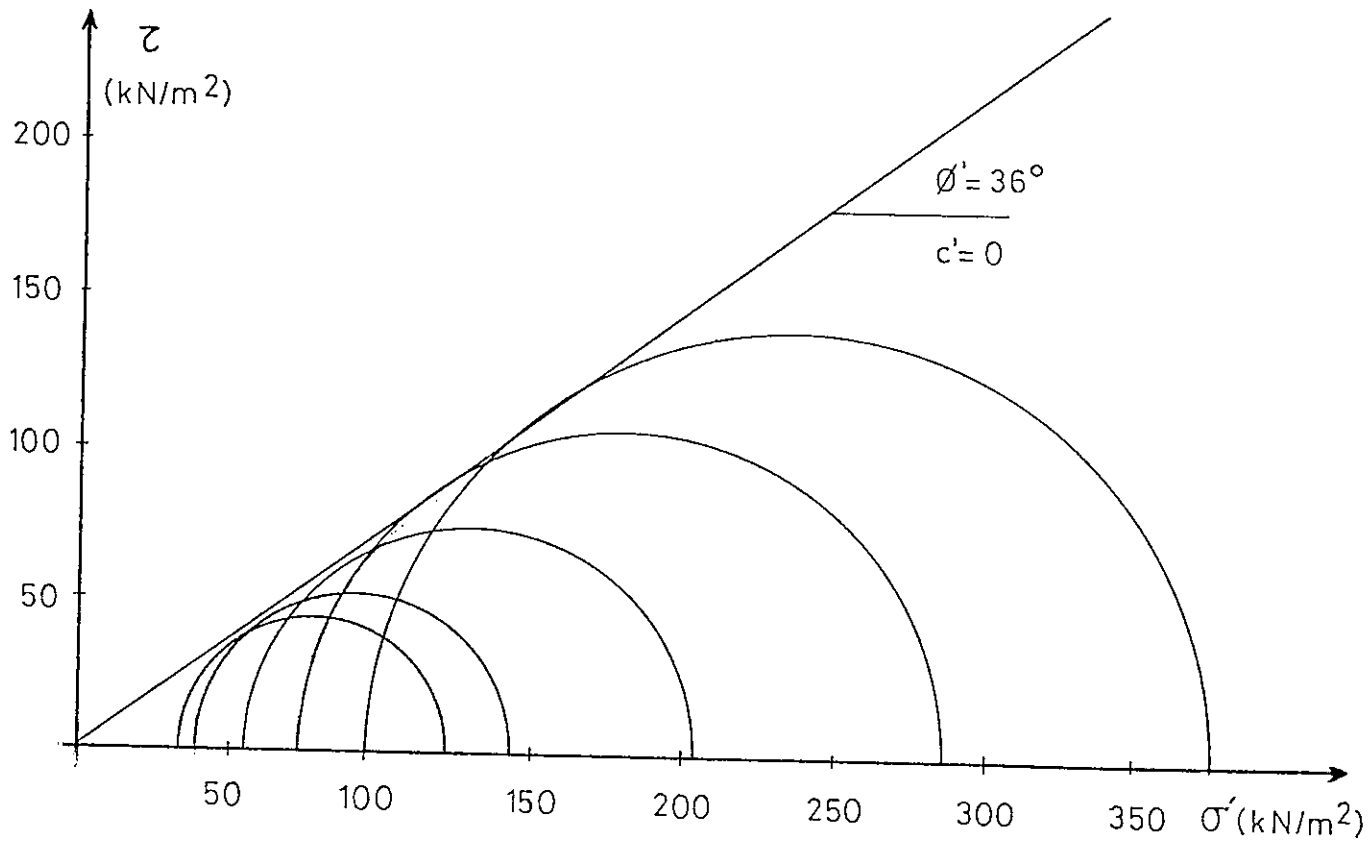

Figure 25. Effective Stress Envelope for C-U Tests. $(\frac{\sigma_1'}{\sigma_3'})_{max.}$

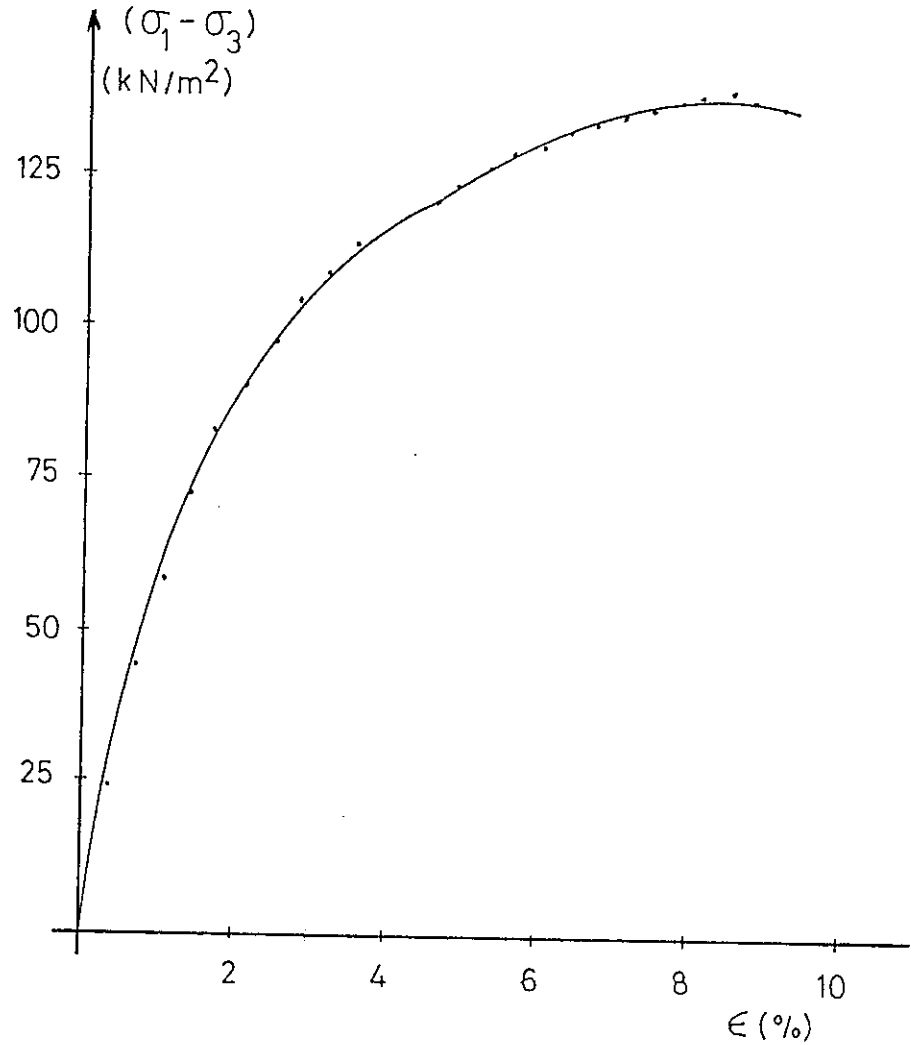

Figure 26. (a) Stress-strain Curve for Test 12

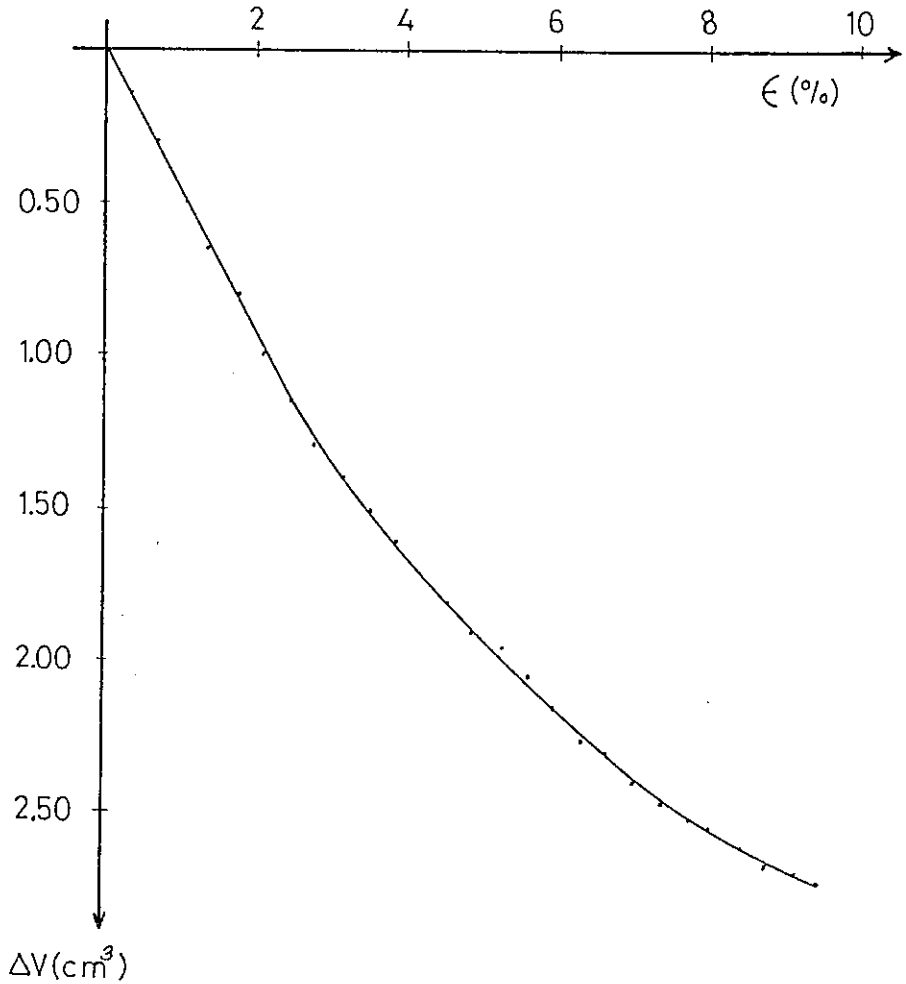

(b) Variation of Volume Change with Strain

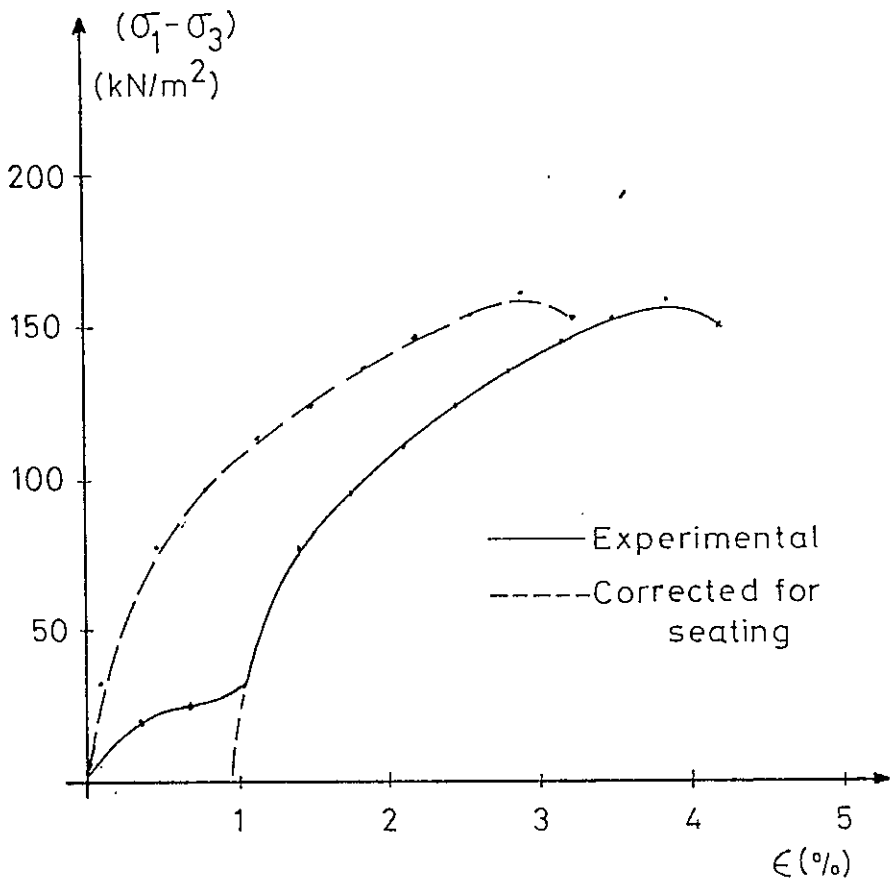

Figure 27:(a) Stress-strain Curve for Test 13.

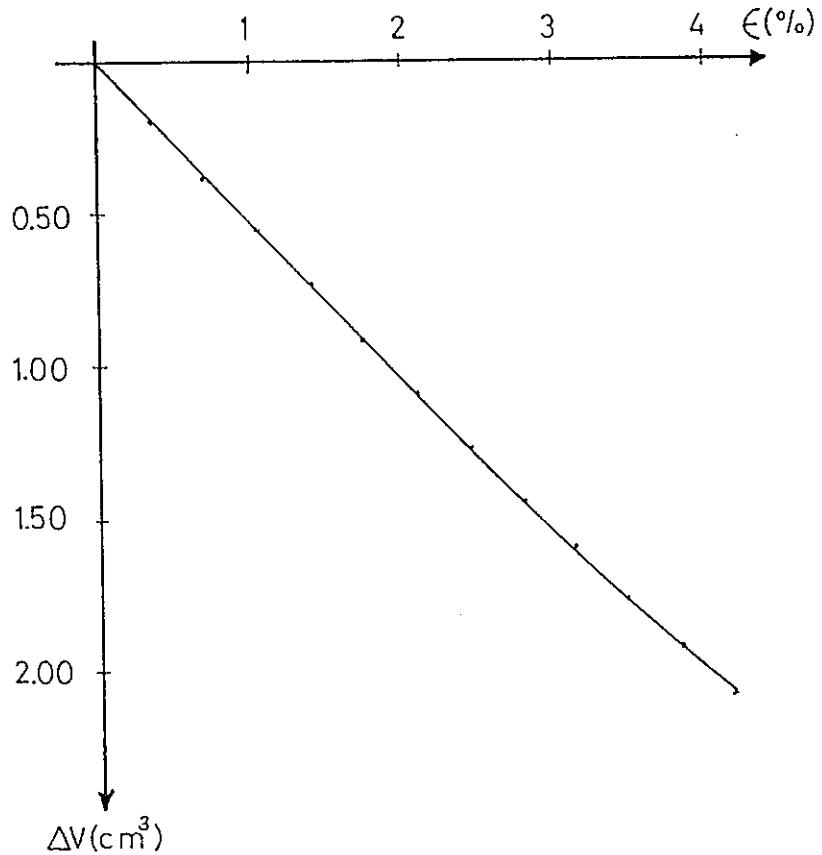

(b) Variation of Volume Change with Strain.

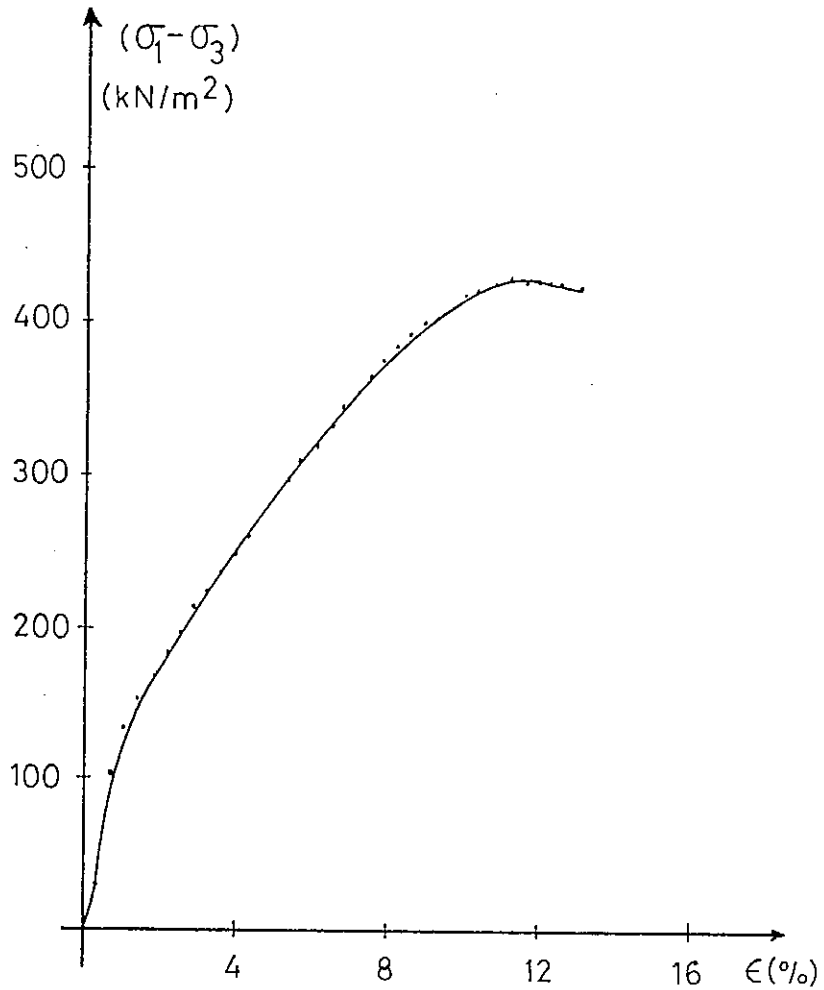

Figure 28. (a) Stress-strain Curve for Test 14.

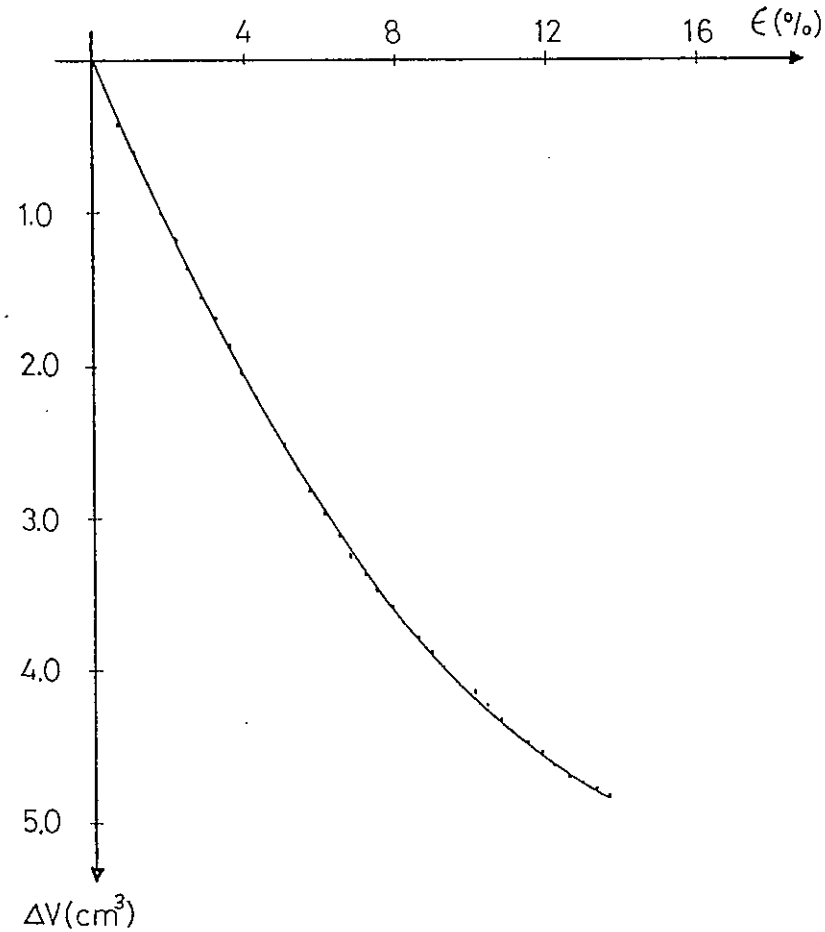

(b) Variation of Volume Change with Strain

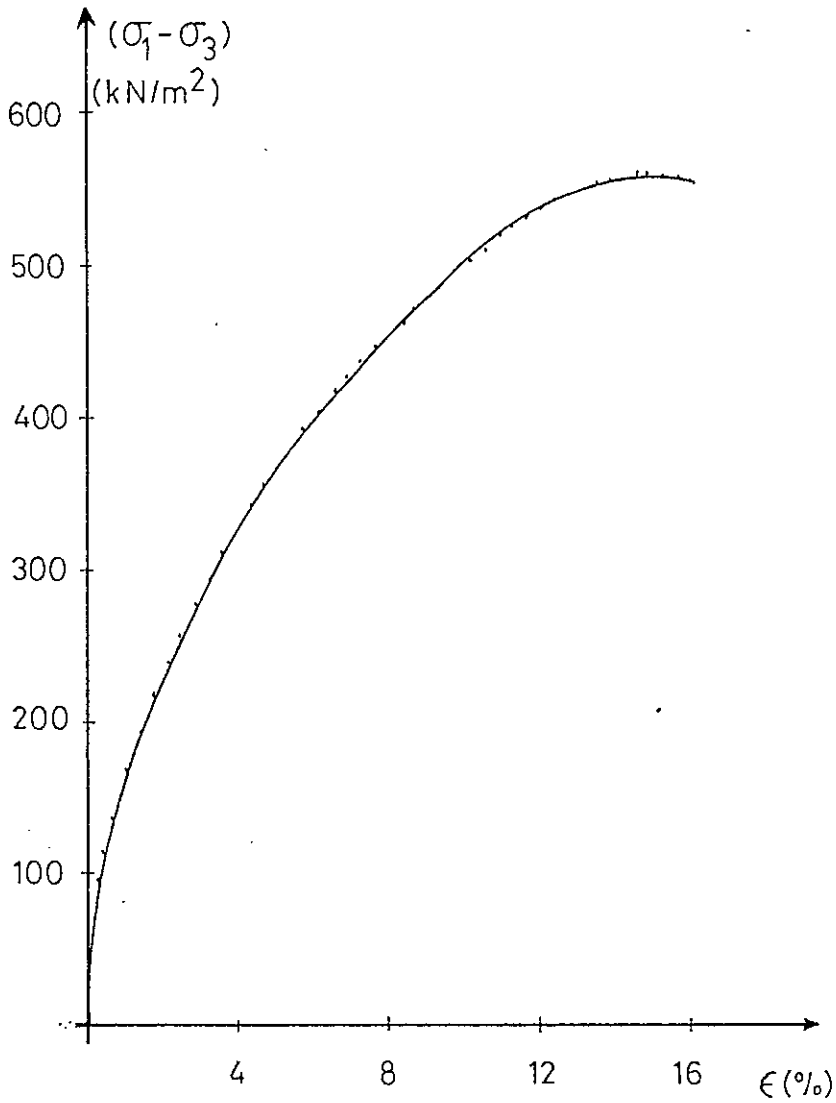

Figure 29. (a) Stress strain Curve for Test 15

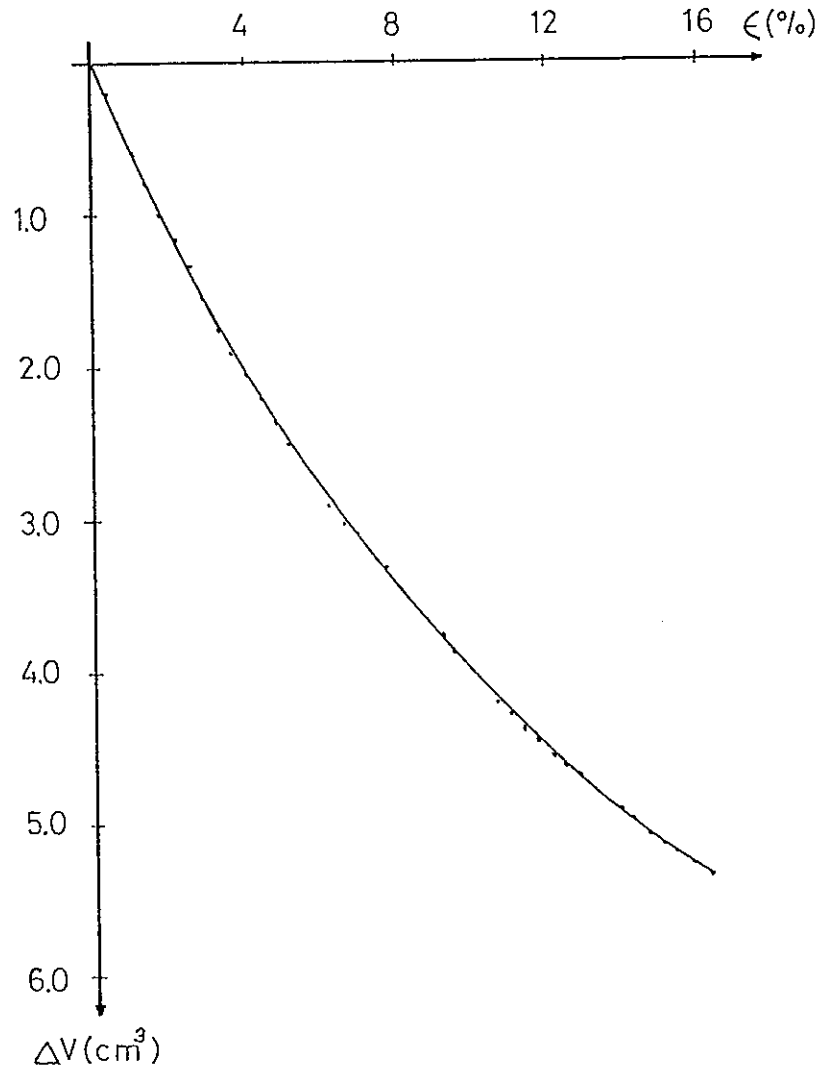

(b) Variation of Volume Change with Strain.

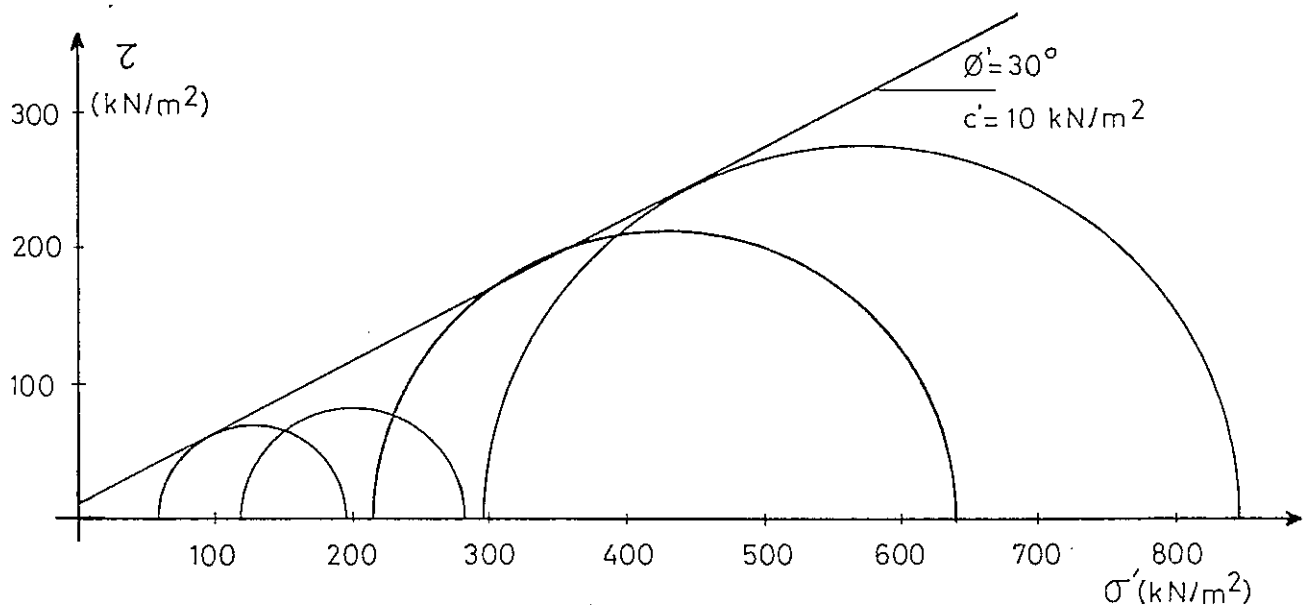

Figure 30. Effective Stress Envelope for C-D Tests

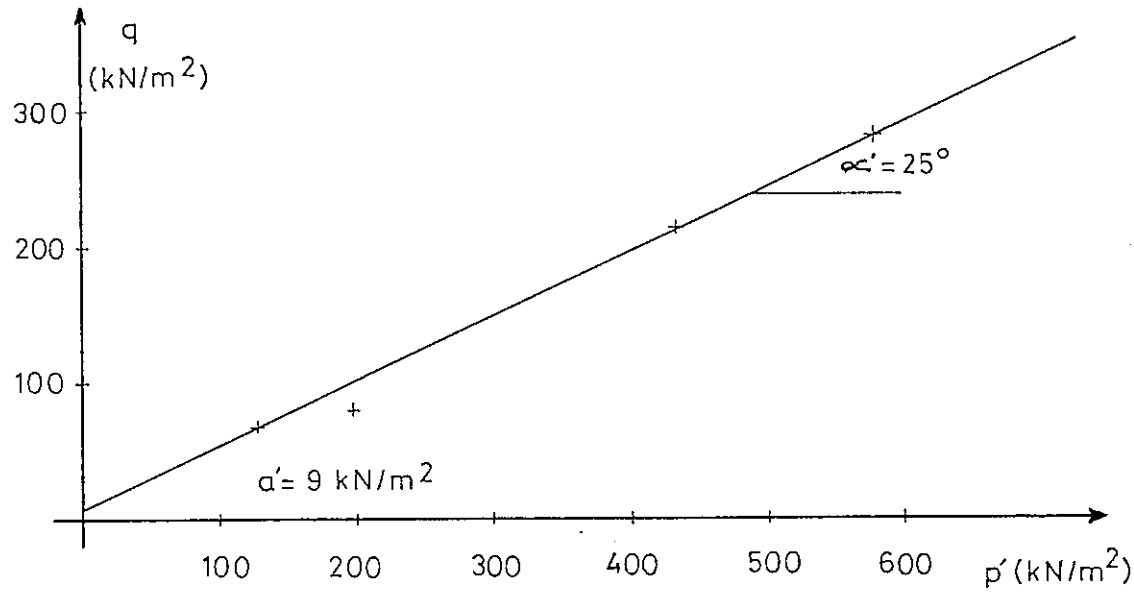

Figure 31. Modified Failure Envelope for C-D Tests.

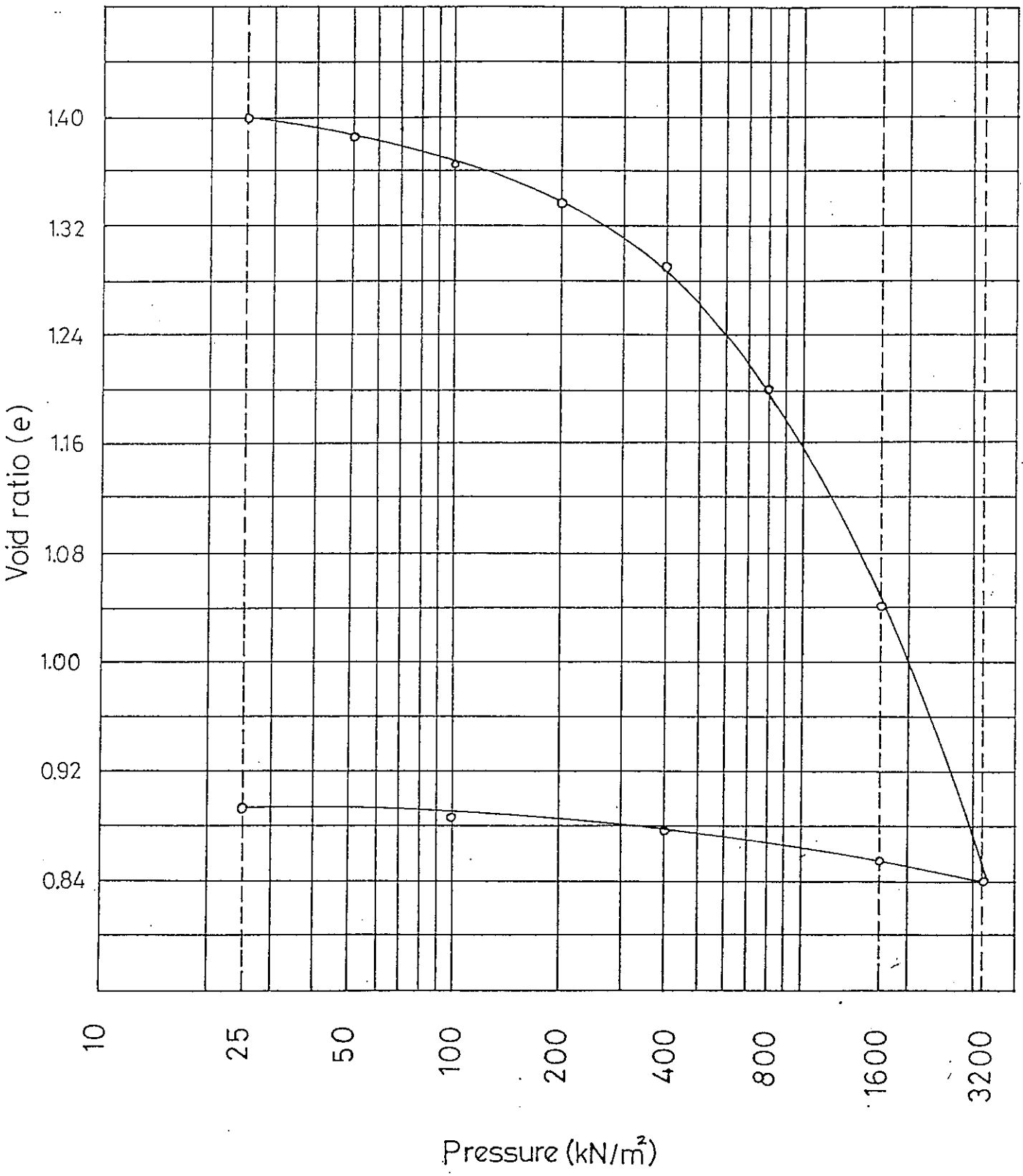

Figure 32. Void ratio-Pressure Curve

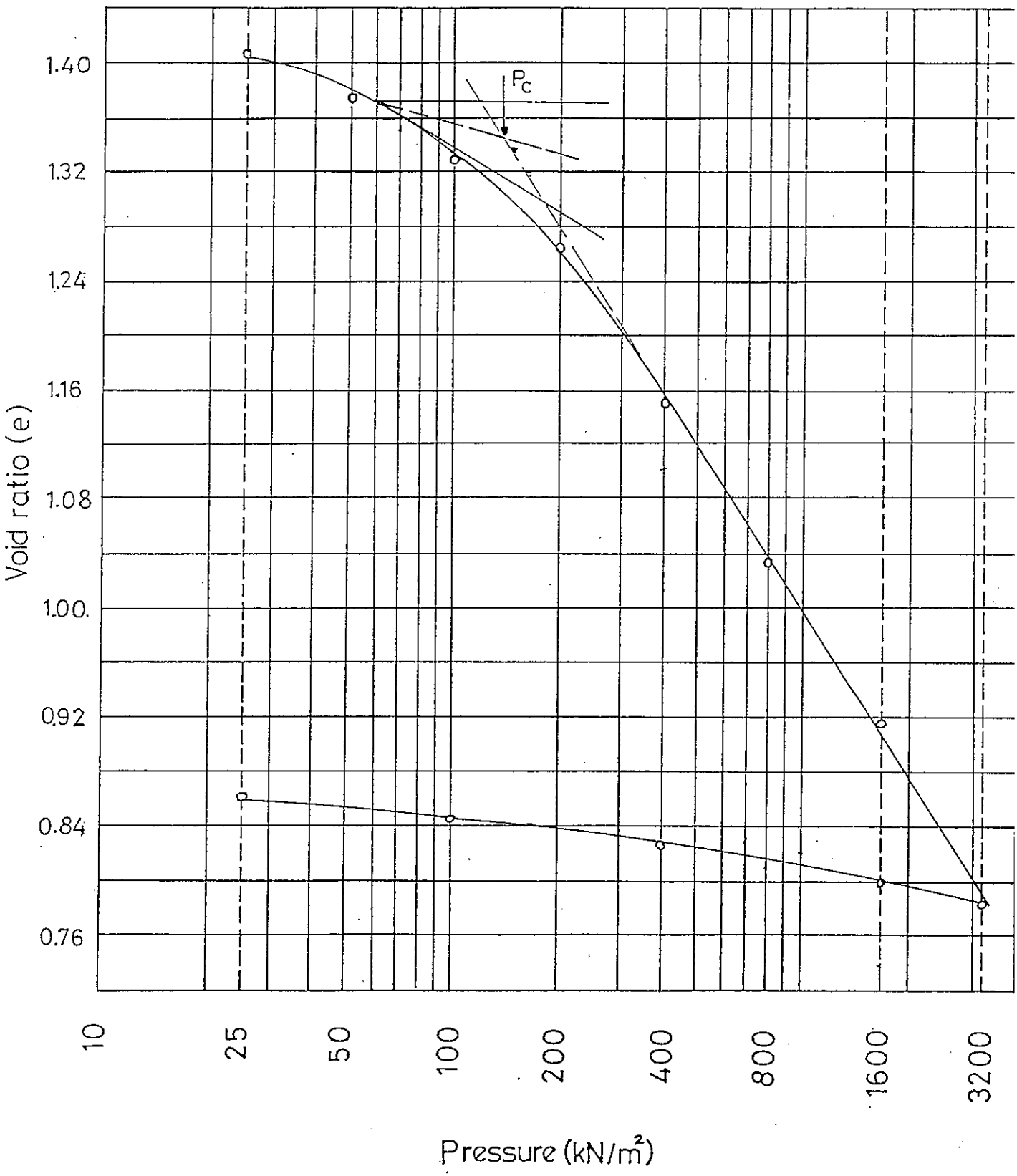

Figure 33. Void ratio-Pressure Curve

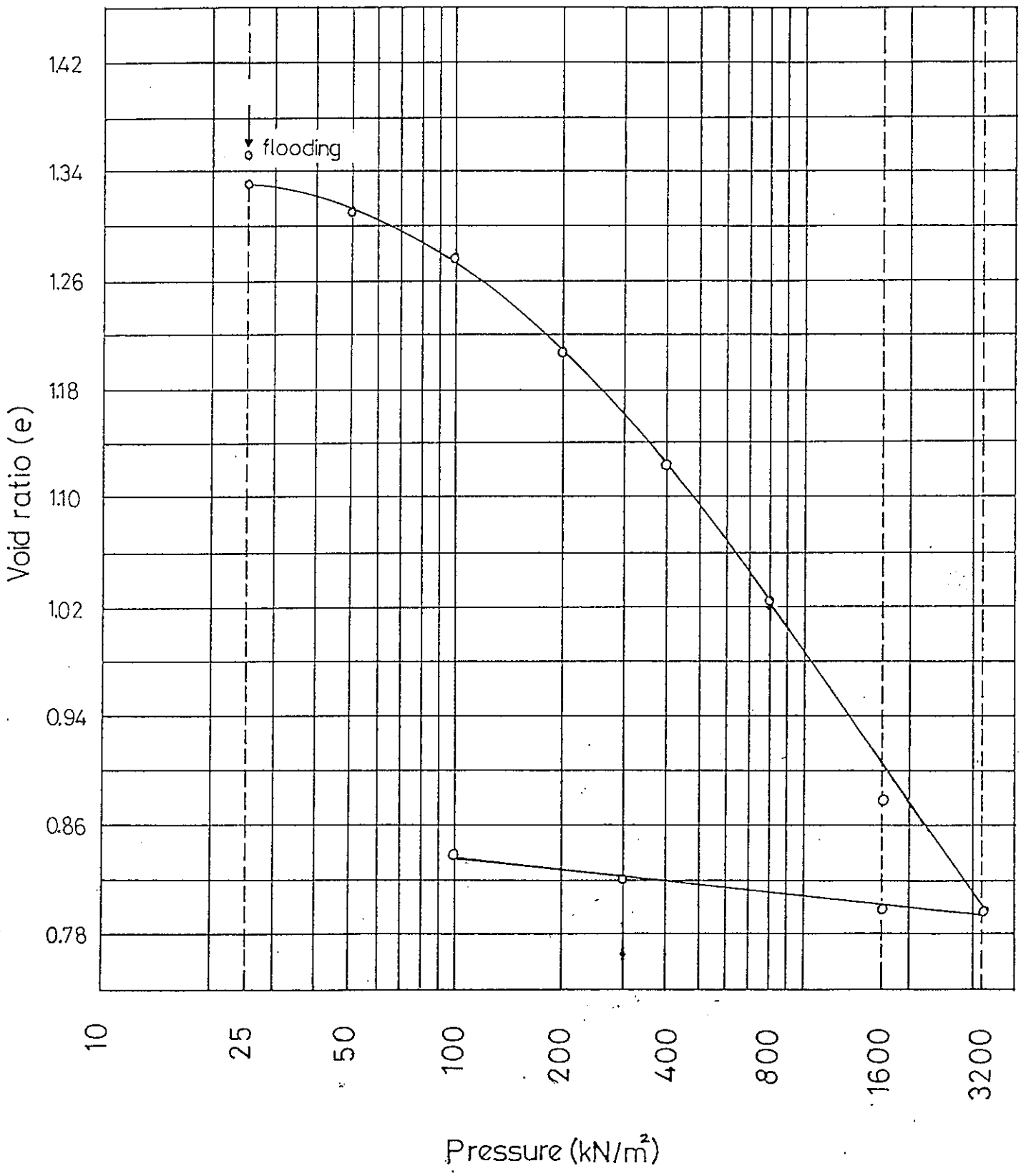

Figure 34 Void ratio-Pressure Curve

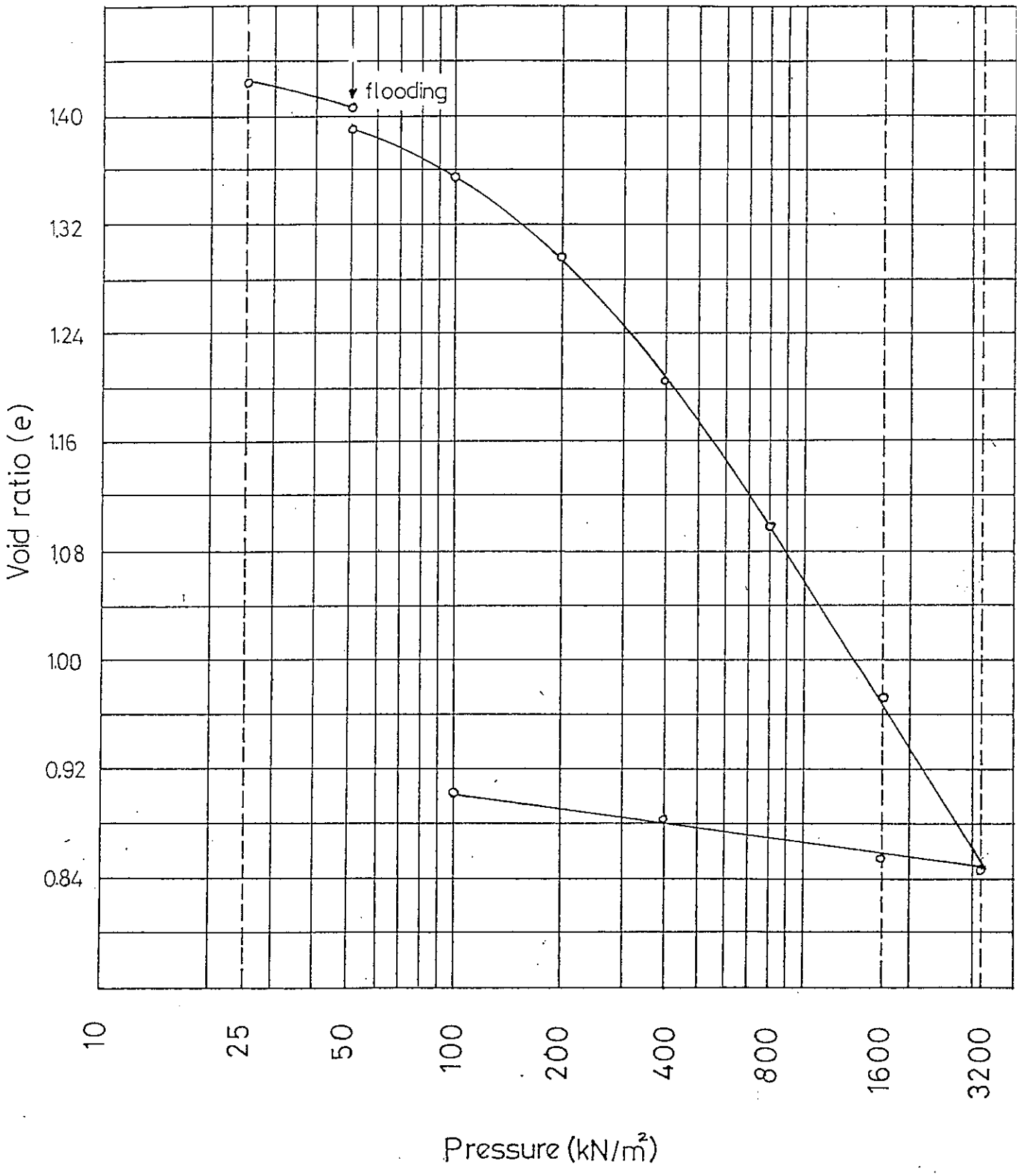

Figure 35. Void ratio - Pressure Curve

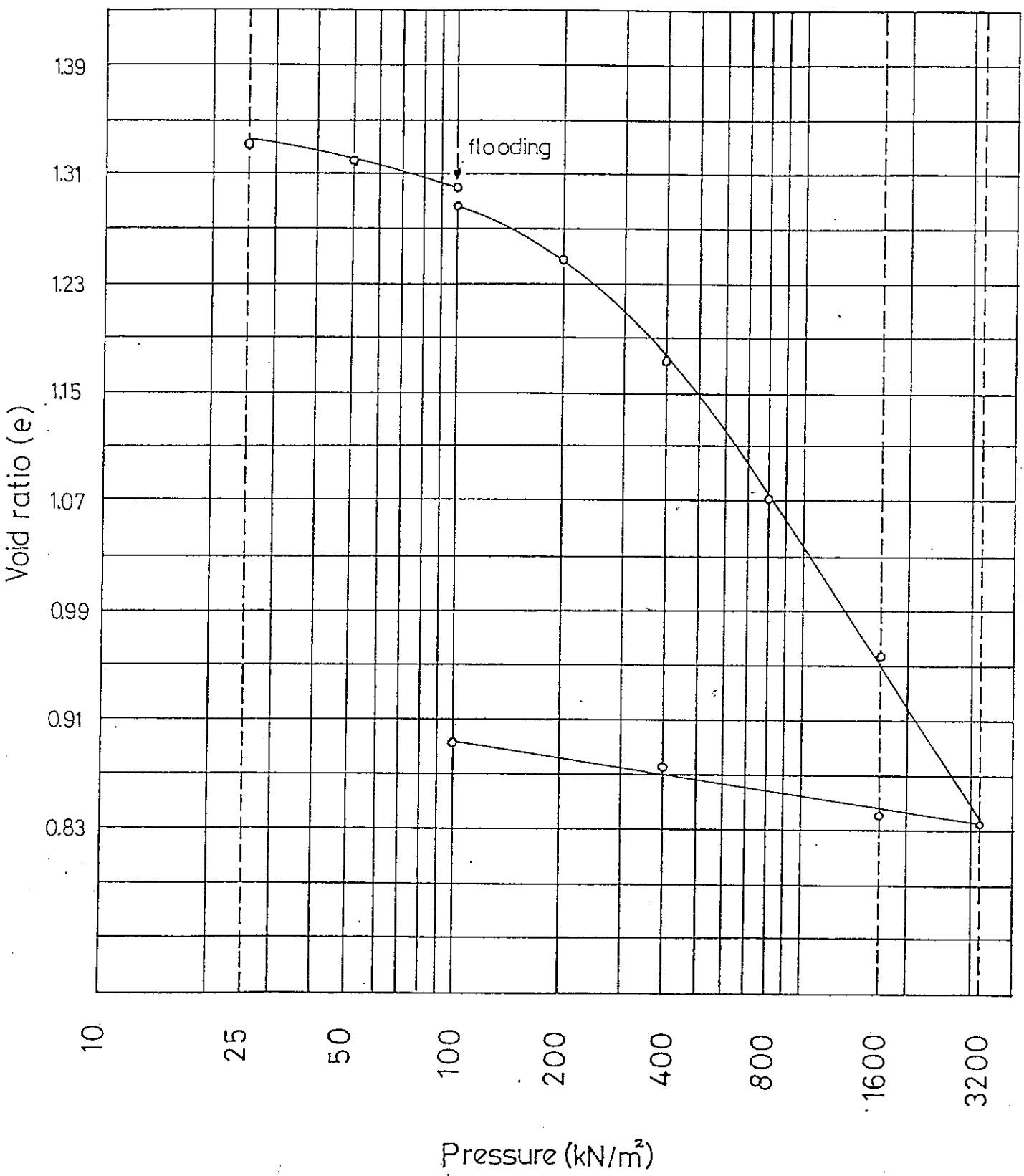

Figure 36. Void ratio-Pressure Curve

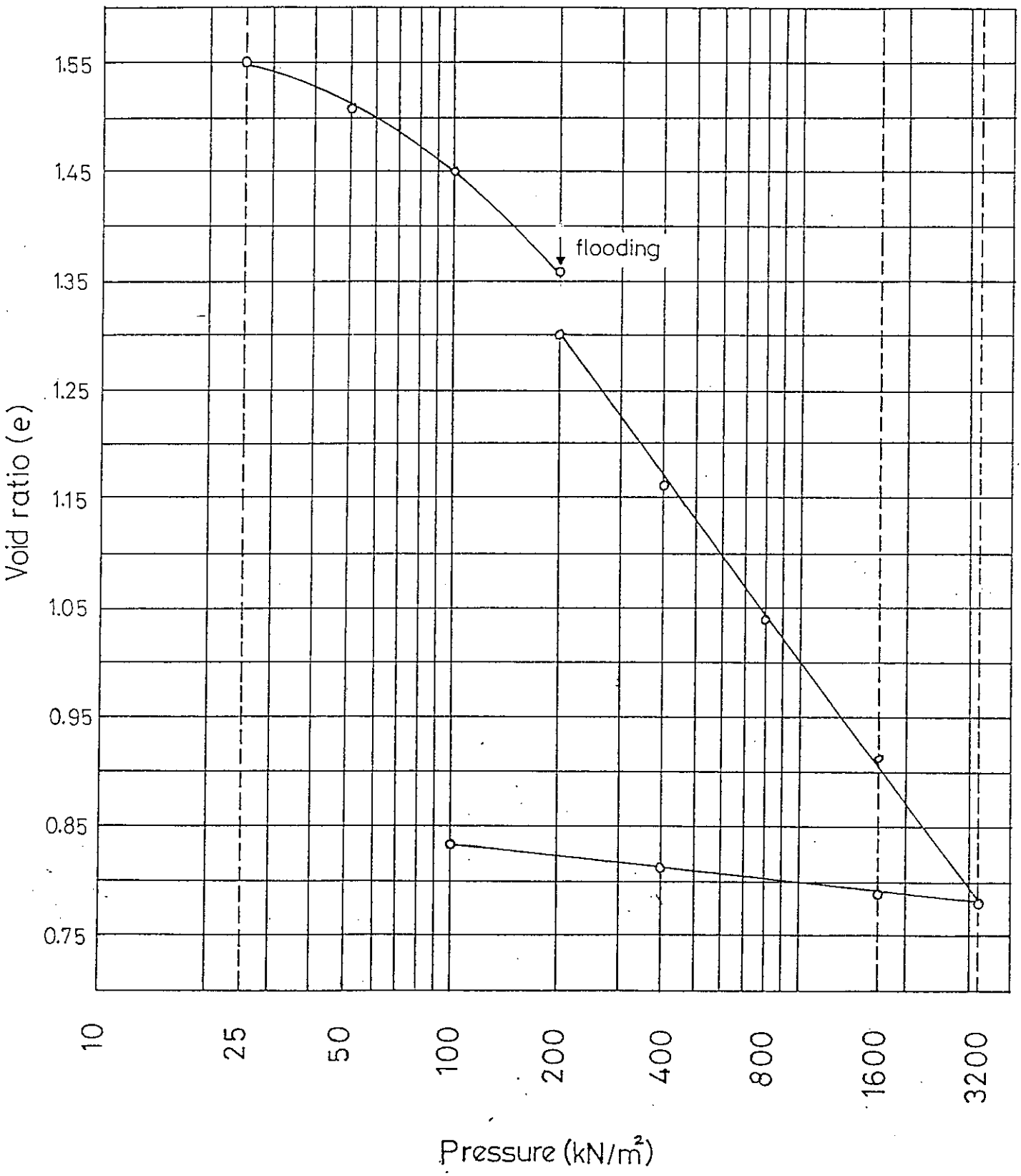

Figure 37. Void ratio-Pressure Curve

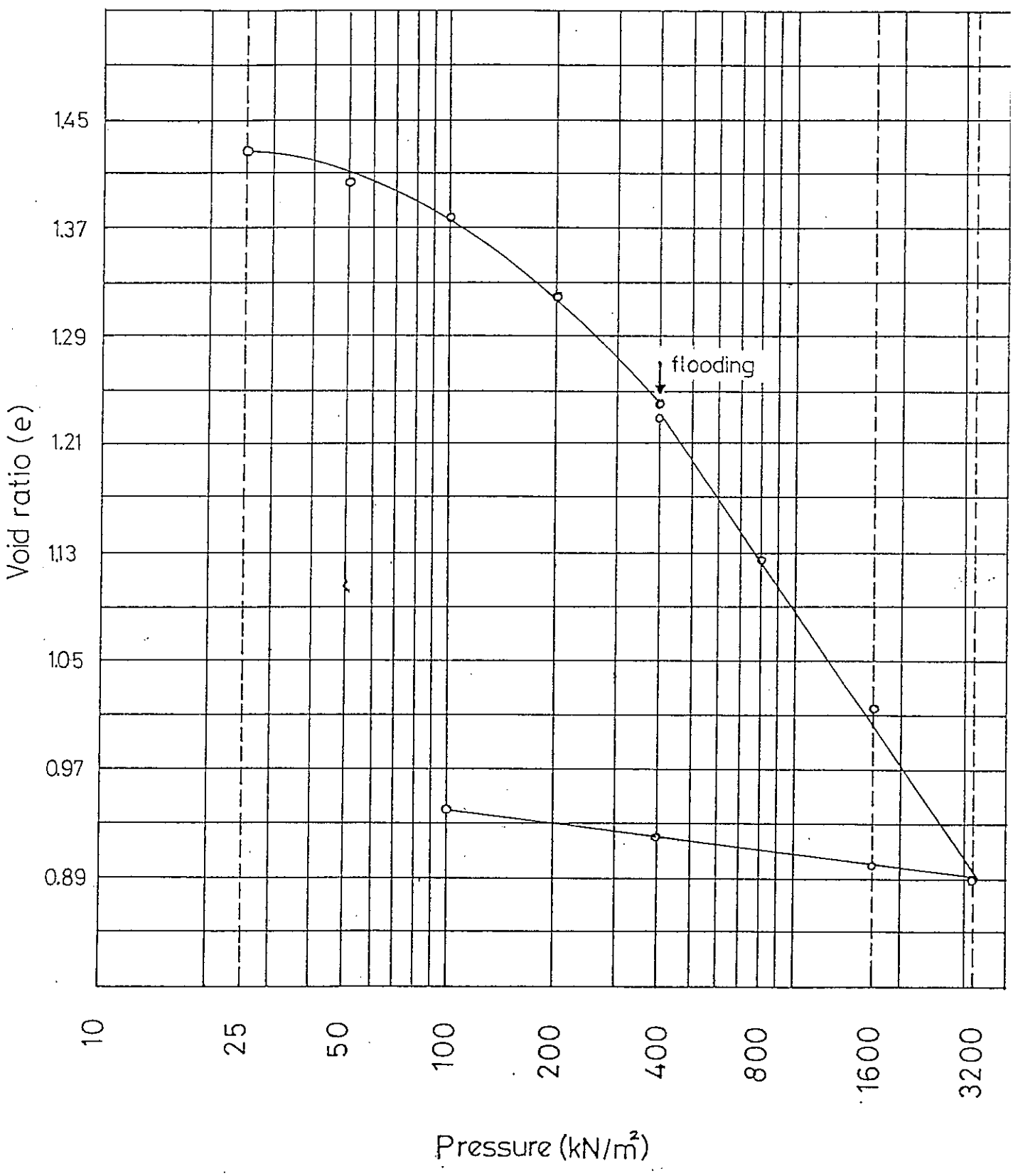

Figure 38. Void ratio-Pressure Curve

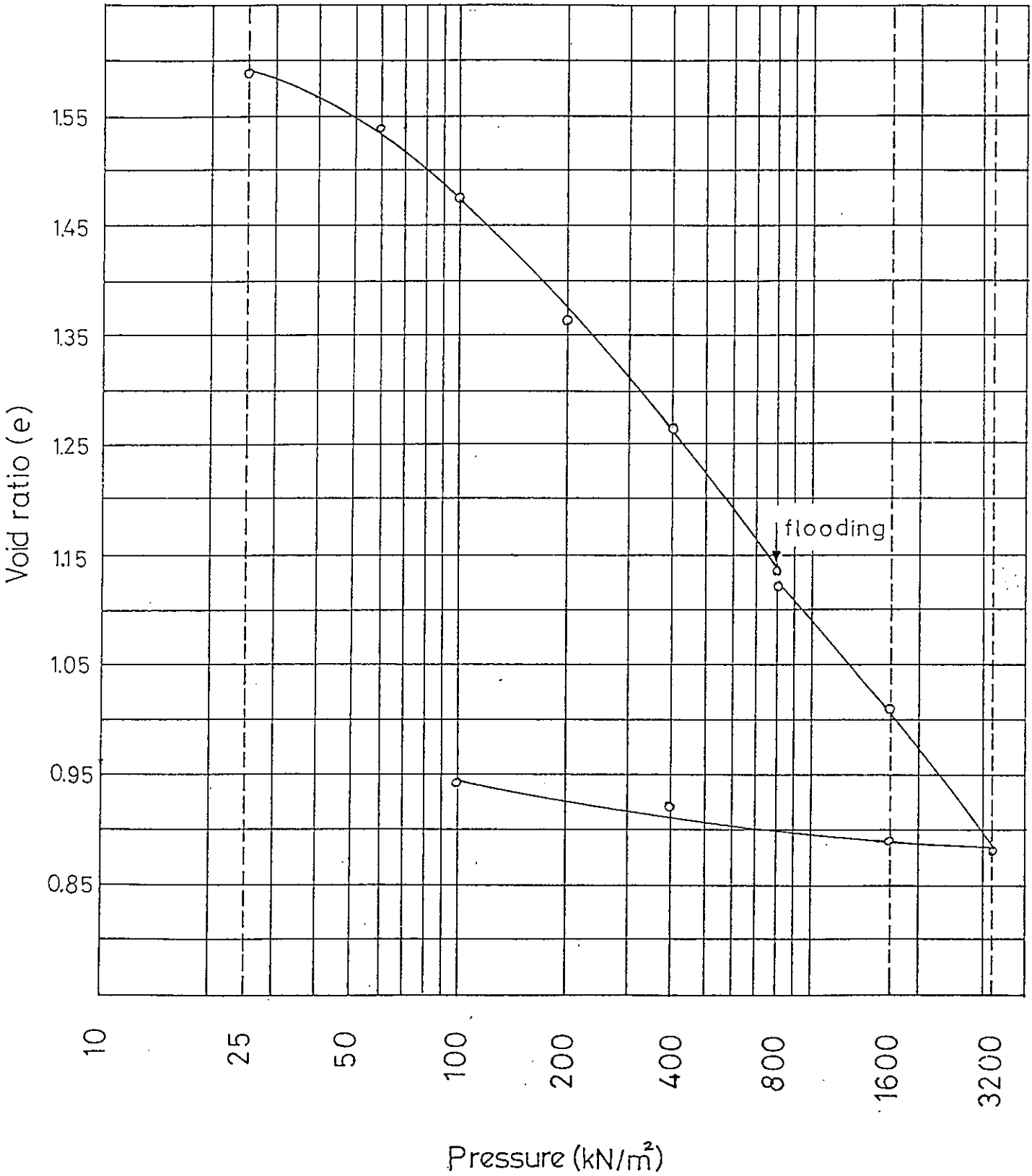

Figure 39. Void ratio- Pressure Curve

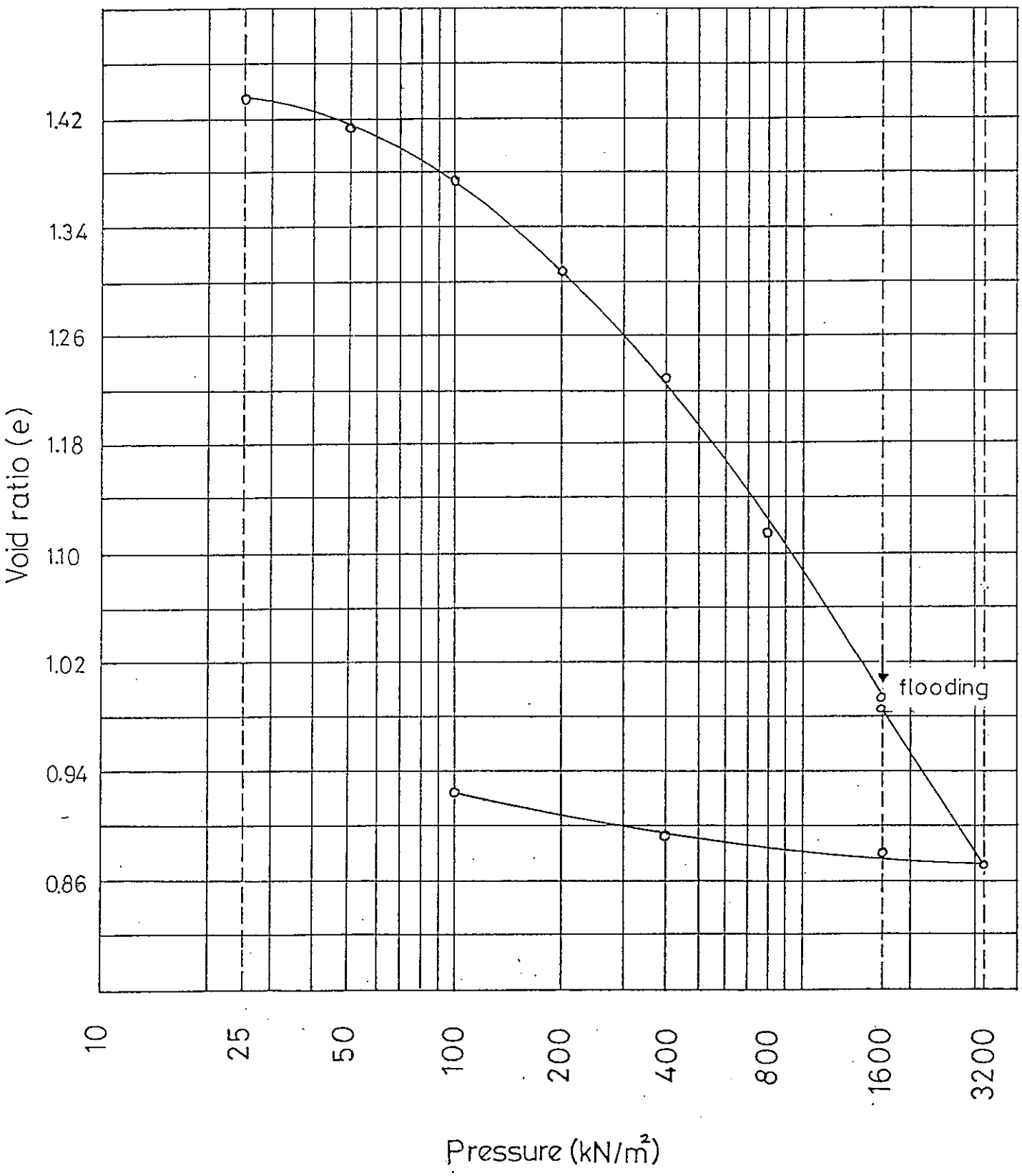

Figure 40. Void ratio-Pressure Curve

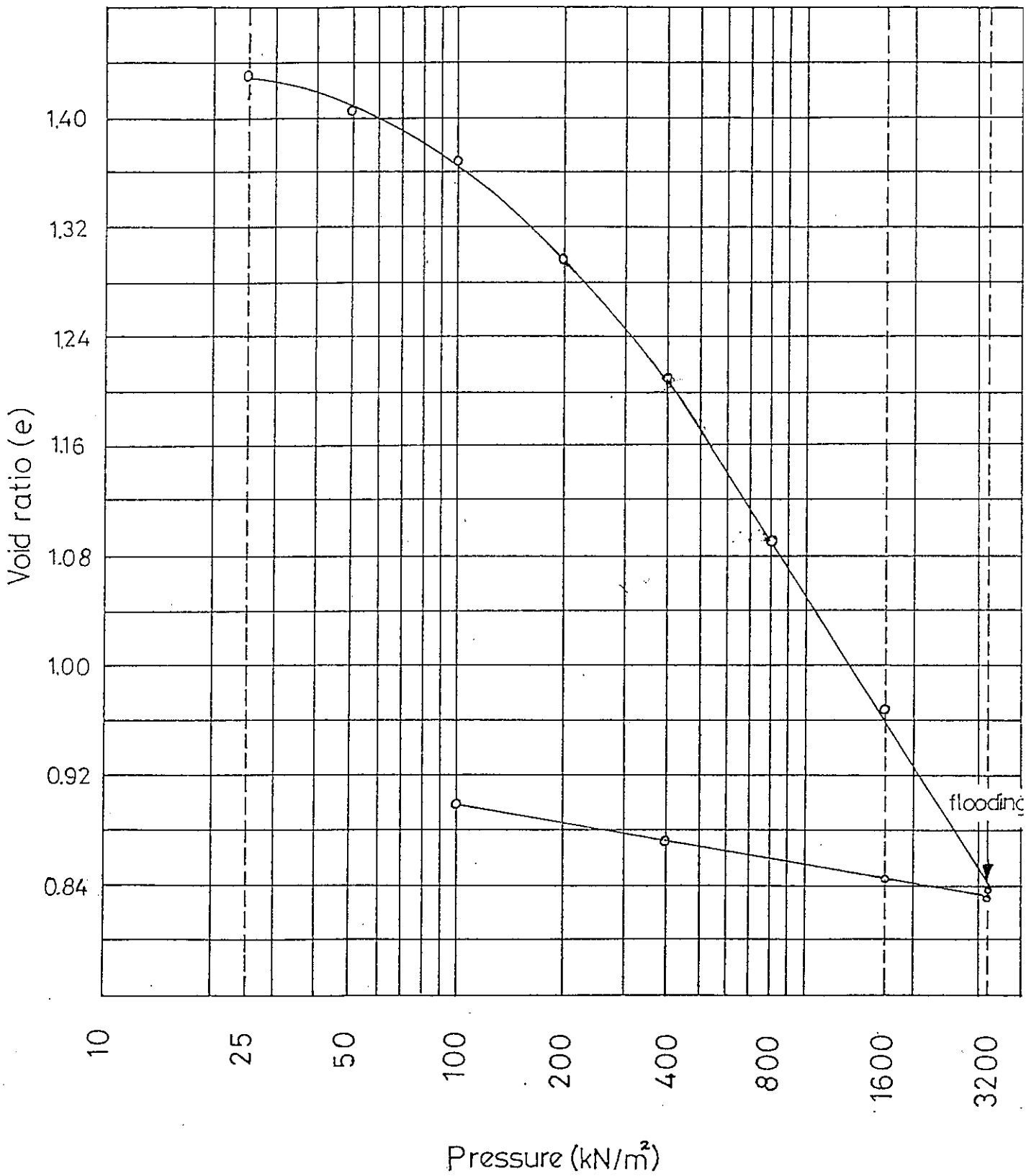

Figure 41 . Void ratio-Pressure Curve

TABLE 7. Summary of Consolidation Test Results

Test No	Bulk Weight of Soil (gr)	Dry weight of Soil (gr)	Area of Ring (cm^2)	Initial Height (cm)	Initial Volume (cm^3)	Bulk Unit Weight (kN/m^3)	Natural Water Content (%)	Initial Void Ratio (%)	Initial S (%)	Collapse Potential (%)	Flooding Pressure (kN/m^2)
U1	84.80	63.10	31.67	1.90	60.17	13.81	34.39	1.434	61.21	--	--
U2	84.00	62.80	31.67	1.90	60.17	13.68	33.76	1.446	59.59	--	0
U3	89.50	66.40	31.67	1.95	61.76	14.20	34.79	1.374	64.63	0.84	25
U4	88.30	63.90	31.67	1.95	61.76	14.01	38.18	1.467	66.44	0.61	49
U5	90.00	67.10	31.67	1.95	61.76	14.28	34.13	1.349	64.58	0.64	98
U6	77.00	59.10	31.67	1.90	60.17	12.54	30.29	1.599	48.35	2.04	196
U7	89.60	64.20	31.67	1.95	61.76	14.22	39.56	1.455	69.40	0.45	392
U8	82.80	59.70	31.67	1.95	61.76	13.14	38.69	1.640	60.22	0.27	785
U9	88.70	63.90	31.67	1.95	61.76	14.07	38.81	1.467	67.53	0.20	1569
U10	88.00	64.00	31.67	1.95	61.76	13.96	37.50	1.463	65.42	0.12	3138

Table 8. Preconsolidation Pressures

Method Used	Preconsolidation pressure (kN/m^2)
Casagrande	140
Rutledge-Schertmann	145

Table 9. Coefficient of Consolidation for Various Pressure Ranges

Pressure (kN/m^2)	Coefficient of Consolidation (cm^2/sec)
25 - 49	$4.75 * 10^{-3}$
49 - 98	$6.02 * 10^{-3}$
98 - 196	$1.80 * 10^{-3}$
196 - 392	$4.62 * 10^{-3}$
392 - 784	$1.93 * 10^{-3}$
784 - 1568	$3.70 * 10^{-3}$
1568 - 3137	$2.86 * 10^{-3}$

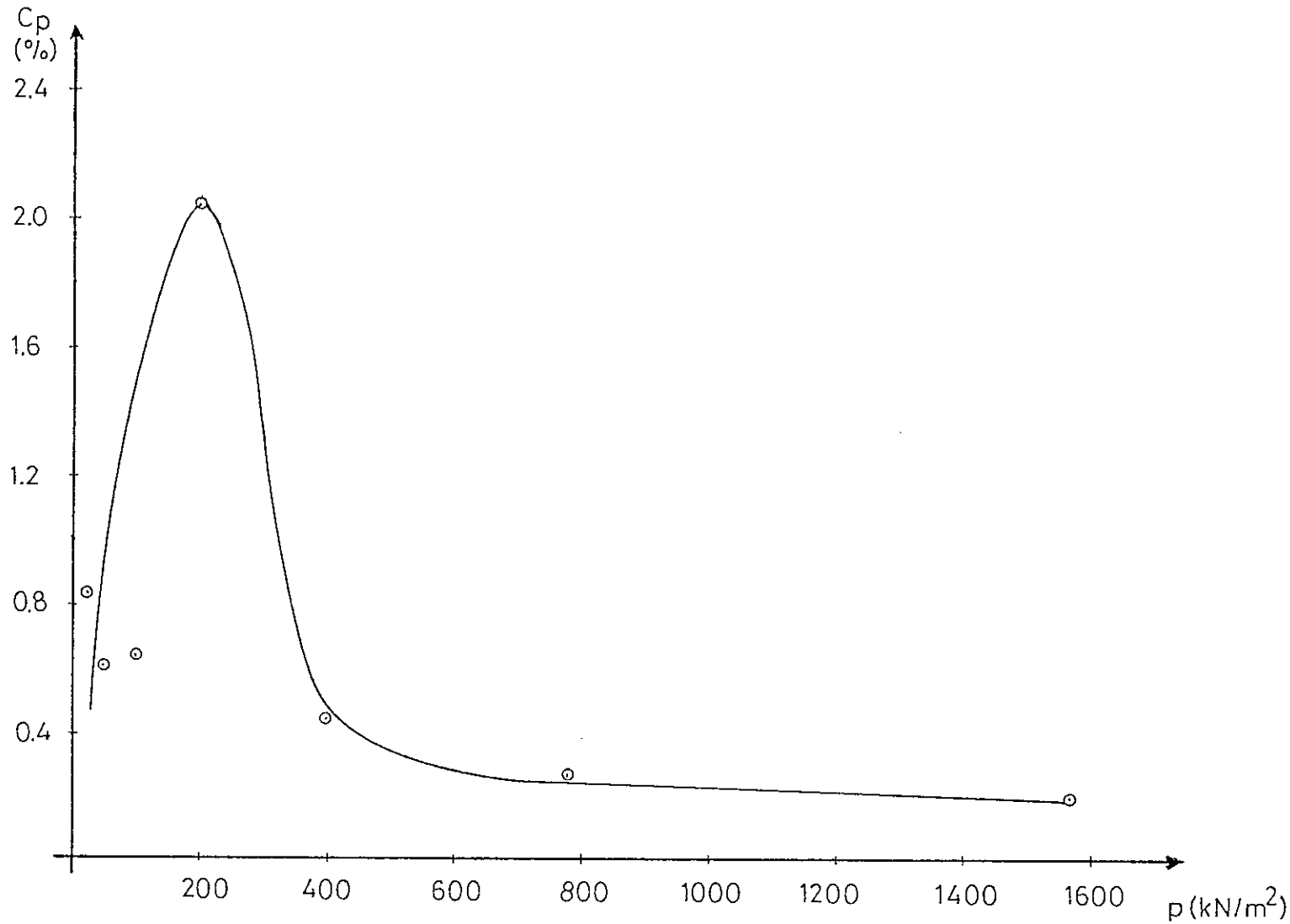

Figure 42. Collapse Potential versus Flooding Pressure.

5. DISCUSSION OF TEST RESULTS AND CONCLUSIONS

U-U TESTS

1. The shape of the mohr envelope obtained from U-U tests (figure 15) is a typical of partly saturated soils. As the mohr envelope was curved the shear strength parameters were determined for different ranges of total stresses (Table 6).

2. The specimen used in test 4 was accidentally wetted before testing. This caused the specimen to fail at a lower deviatoric stress as compared to the other samples. The high B value obtained was also due to this higher moisture content (i.e higher S), therefore this value was not taken into account while plotting figure 17. It is also observed that the failure strain for this test was lower than those for the other U-U tests.

3. In tests 1, 5 and 6 moisture contents were determined both at the beginning and after testing. Comparing these moisture contents, it is seen that there is an increase in moisture content during testing. This change is believed to be due to the leakage of water between the top cap and the rubber membrane.

4. The variation of pore pressure parameter B, as obtained from U-U tests, with cell pressure was plotted

in figure 17. An investigation of this figure shows that B values increase with increasing cell pressure as expected. The reason for this is that as the cell pressure increases, increasing amount of the air in the sample dissolves in the pore water leading to a higher degree of saturation.

C-U TESTS

5. The rate of shearing in C-U and C-D tests were estimated by using the c_v values as explained in sections 4.2.4.2 and 4.2.4.3. The c_v values and estimated shearing rates are summarized in table 10. These values of c_v are considerably high as compared to the ones obtained from consolidation tests, which are given in table 9. The high c_v values obtained in triaxial tests are believed to arise due to the increase in permeability due to the application of back pressure. The shearing rates were re-evaluated by using the maximum c_v value obtained from oedometer test and are presented in table 10.

6. In C-U and C-D tests, in order to have an idea about the degree of saturation after consolidation, the procedure described in section 4.2.4.1 was followed. B values are found to vary between 0.732 and 0.903. This shows that the samples could not reach full saturation

Table 10. Calculated and Applied Shearing Rates

TEST	TEST TYPE	2.h' (cm)	c_v (cm^2/sec)	(1) Rate calc. (mm/min)	(2) Rate calc. (mm/min)	Rate app. (mm/min)
7	C-U	7.329	$1.162*10^{-1}$	1.429	0.0739	0.020
8	C-U	7.267	$3.707*10^{-1}$	4.594	0.0746	0.020
9	C-U	7.202	$2.514*10^{-1}$	3.140	0.0752	0.020
10	C-U	7.092	$3.223*10^{-1}$	4.091	0.0764	0.020
11	C-U	7.205	$2.402*10^{-2}$	0.300	0.0752	0.020
12	C-D	7.202	----	---	0.0056	0.004
13	C-D	7.263	$5.045*10^{-1}$	0.373	0.0056	0.004
14	C-D	7.079	----	---	0.0057	0.004
15	C-D	6.960	$1.648*10^{-1}$	0.127	0.0054	0.004

1. calculated by using c_v values of triaxial test
2. calculated by using max. c_v of oedometer test

after consolidation under the applied back pressures. However the value of back pressure to achieve the full saturation should be somewhat lower than the one determined by equation 5, because in equation 5 the effect of confining pressure is not taken into account in addition to the factors explained in section 2.4.

7. The undrained shear strength is plotted against the consolidation pressure, as shown in figure 43. This relationship can be represented by a straight line.

8. The values of A obtained were between 0.515 and 0.615 except for test 7. The value of A in test 7 appeared to be negative.

In the calculation of A values B = 1 was used instead of the B values obtained before shearing, since the degree of saturation increases during the shearing and B values approach to unity.

9. The values of strength parameters corresponding to two different failure criteria namely, maximum deviatoric stress criterion and maximum principal stress ratio criterion, were given in section 4.4.1. A comparison of ∅' value for two different failure criteria shows that ∅' determined by maximum principal stress ratio criterion is higher. It is also clear that the strains at failure are greater when failure is

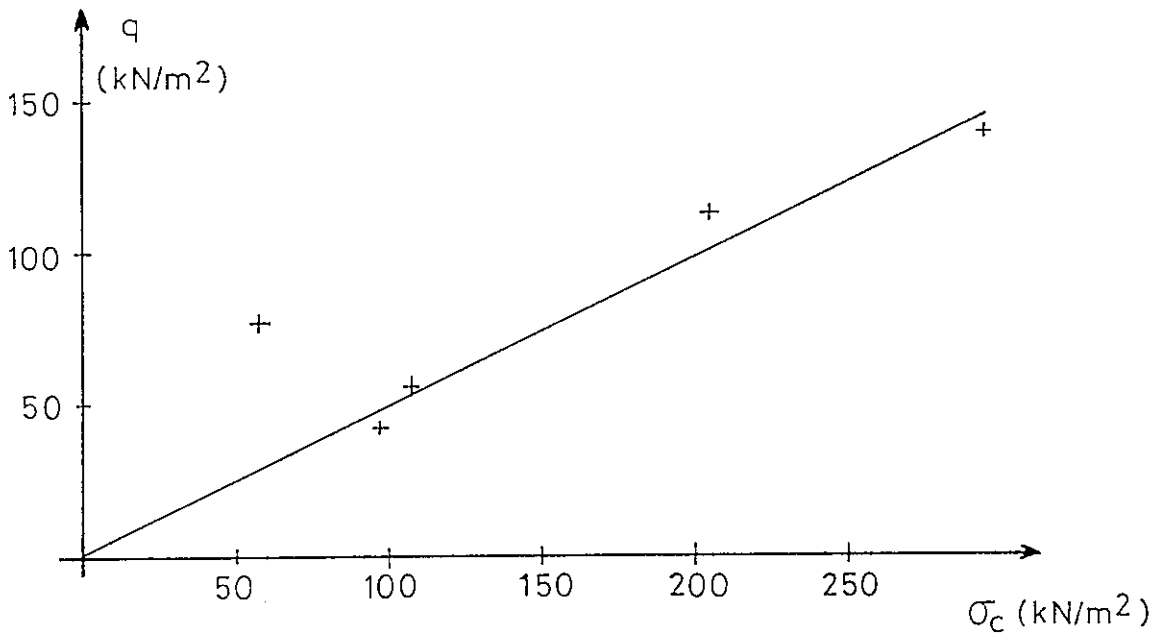

Figure 43. Undrained Shear Strength versus Consolidation Pressure

defined by this criterion (Table 5). The results are in accordance with the ones determined by Simons (1960) who stated that for normally consolidated soils, the maximum deviatoric stress failure criterion gives a flatter failure envelope than the one obtained by using the maximum principal stress ratio failure criterion.

C-D TESTS :

10. The shearing rates for C-D tests were determined by the same procedure followed during C-U tests. Failure strain was taken to be 15% in rate calculations, being larger than the one suggested to define the failure in C-U tests (12%). The calculated and applied rates of shear are given in table 10.

11. For all of the C-D tests, volume change during shearing was plotted against axial strain (figure 20b - 23b). An investigation of these figures shows that in all of the tests the volume of the specimen decreases due to the drainage of the pore water out of the specimen (assuming full saturation after consolidation). Also it is observed from table 3 that the moisture content after shearing is greater than the initial one. It is suggested that during the consolidation stage there is a decrease in volume of the specimen due to the compression of air. However at

the same time there is a flow of water into the sample due to the applied back pressure. Therefore the moisture content at the end of consolidation is greater than the initial one. This increased moisture content decreases, to some extend by the drainage of water out of the sample during shearing. However at the end of shearing stage the moisture content is still greater than its initial value.

During the shearing stage of C-U tests a change in moisture content is not expected, but the moisture content after shearing in C-D tests decrease (as explained above) as compared to the ones before shearing. This can be observed by comparing the final moisture content of C-U and C-D tests (Table 3).

CONSOLIDATION TESTS AND COLLAPSIBILITY OF THE SOIL

12. The avarage bulk unit weight of the soil tested was around 13.79 kN/m^3. The avarage dry unit weight of the soil was determined to be 10.14 kN/m^3 by using an avarage moisture content of 36.01 % . Dry density versus liquid limit of the soil was plotted in figure 44 as described in section 2.2. The soil with a liquid limit of 47% and dry density 10.14 kN/m^3 is classified as collapsible by using figure 44.

13. Another qualitative evaluation of collapse potential was made according to the method described in section 2.2 part 1. The collapse potential, C_p, was estimated to be 2.04% from test U6. According to table 1, the soil is in the range of "moderate trouble" (after Das, 1984)

14. In figure 42 the variation of collapse potential is plotted against flooding pressure. It is seen that up to 196 kN/m^2 the collapse potential increases by increasing flooding pressure. However beyond this value there is a marked decrease in the collapse potential. Mazen (1986) also found for two different soils that the collapse potential increases with increasing flooding pressure up to a certain pressure level and after this pressure, further increase in flooding pressure results in a decrease of collapse potential.

15. The value of C_p found for 196 kN/m^2 seems to be significantly higher than those obtained from other tests. C_p value is expected to be lower if the initial degree of saturation was higher which was the case in other tests.

16. The consolidation tests were carried on samples with 6.35 cm diameter. As the effect of side

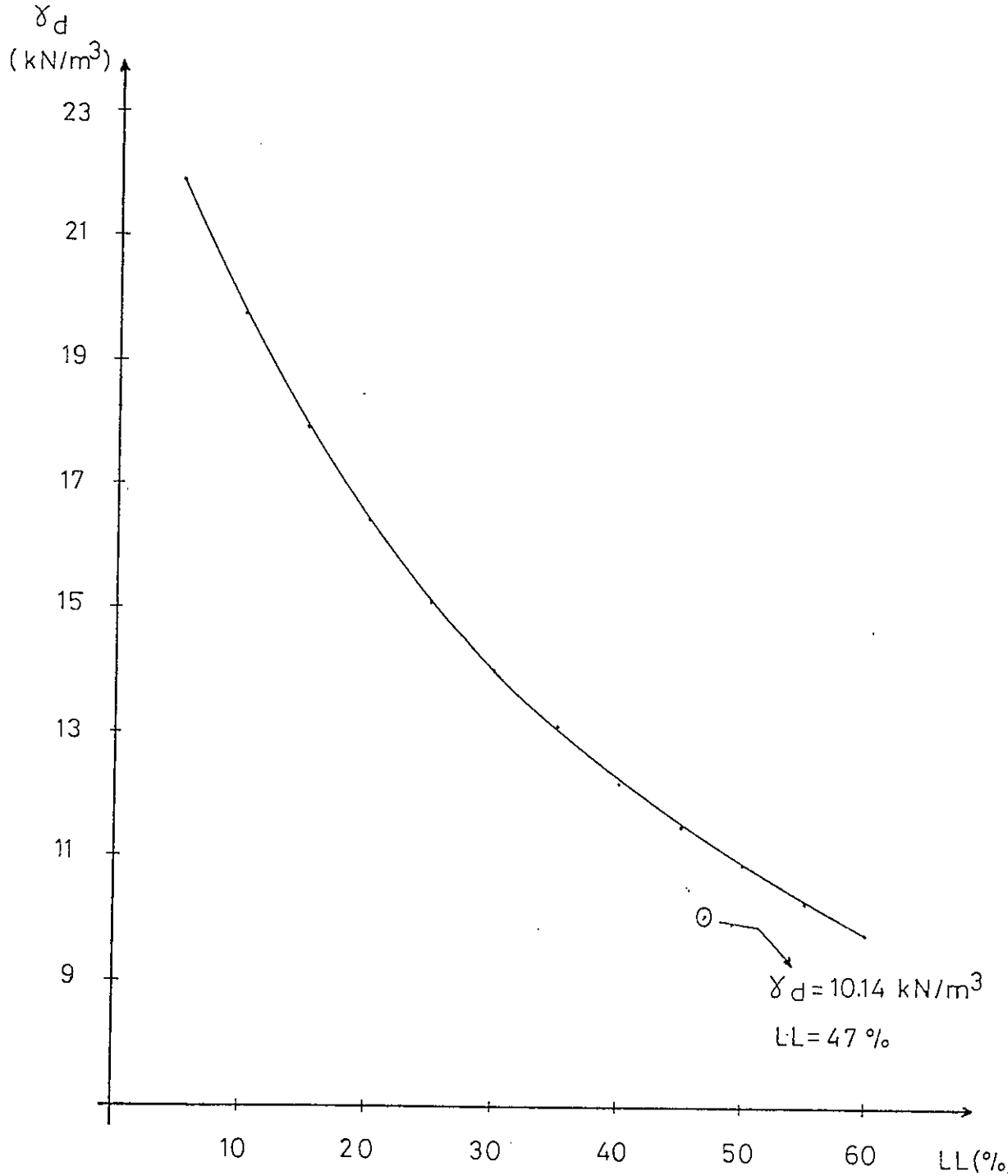

Figure 44. Variation of Dry Density with Liquid Limit

friction is significant in small samples, the use of samples with larger diameters would probably result in higher C_p values.

For further study it is suggested that a more detailed investigation of collapsibility should be made by using larger diameter samples. Also it is suggested that the shear strength of the soil should be investigated by making different types of tests . It is believed that this study will provide some initial data for further studies.

REFERENCES

1. Atalay, İ. (1978), "The Geology and Geomorphology of The Erzurum Plain and Its Surroundings", Atatürk Üniversitesi Yayınları, No.543.
2. Bakişkan, İ. (1978), "Shear Strength of Two Clays in The Ankara Region", Master Thesis, M.E.T.U., Ankara, Turkey, 1978.
3. Birand, A. (1968), "A Method of Computing Ultimate Settlements for Preconsolidated Ankara Clay", M.E.T.U., Journal of Pure and Applied Sciences, Vol.1., No.1., pp. 49-59.
4. Bishop, A.W. and Henkel, D.J. (1974), "The Measurement of Soil Properties in The Triaxial Test", William Clowes and Sons, Limited, London, Great Britain.
5. Blight, G.E. (1963), "The Effect of Nonuniform Pore Pressure on Laboratory Measurement of The Shear Strength of Soils", Laboratory Shearing of Soils, pp. 173-191.
6. Craig, R.F. (1984), "Soil Mechanics", Van Nostrand Reinhold (UK) Co. Ltd, Hong Kong, 1984.
7. Das, B.M. (1984), "Principles of Foundation Engineering", Brooks Cole Engineering Division,

California, 1984.

8. Ergun, U. (1986), Private communication.
9. Henkel, D.J. and Gilbert, G.D. (1952), "The Effect of The Rubber Membrane on The Measured Triaxial Compression Strength of Clay Samples", Geotechnique, Vol.3, pp.20-29.
10. Kimura, T. and Saitoh, K. (1983), "The Influence of Strain Rate on Pore Pressures in Consolidated Undrained Triaxial Tests on Cohesive Soils", Soils and Foundations, Vol.23, No.1., pp.80-90.
11. Koçyiğit, A., Öztürk, A., İnan, S. ve Gürsoy, H. (1985), "Karasu Havzasının (Erzurum) Tektonomorfolojisi ve Mekanik Yorumu", Cumhuriyet Üniversitesi Yer Bilimleri Dergisi, C-2, S-1, sayfa 1-15.
12. Lambe, T.W. and Whitman, R.V. (1979), "Soil Mechanics", John Wiley and Sons, Delhi, India.
13. Lowe, J. and Johnson, T.C. (1960), "Use of Back Pressure to Increase Degree of Saturation of Triaxial Test Specimens", ASCE, Research Conference on Shear Strength of Cohesive Soils, pp.819-836.
14. Mirata, T. (1976), "Short-Term Stability of Slopes in Ankara Clay", Ph.D Thesis, M.E.T.U., Ankara, Turkey, 1976.

15. Mirata, T. (1980), "Laboratory Instructions for Soil Mechanics Students", Department of Civil Engineering, M.E.T.U., Ankara, 1980

16. Mirata, T. (1984), "Earth Structures Lecture Notes", unpublished, M.E.T.U., Ankara.

17. Mirata, T. (1986), Private communications.

18. Reginatto, A.R. and Ferraro, J.C. (1973), "Collapse Potential of Soils and Soil-Water Chemistry", Proceedings of the 8 I.C.S.M.F.E., Moscow, 1973, Vol.3, pp.177-183.

19. Simons, N.E. (1960), "The Effect of Overconsolidation on the Shear Strength Characteristics of an Undisturbed Oslo Clay", ASCE, Research Conference on Shear Strength of Cohesive Soils, Colorado, pp.747-763.

20. Smith, G.N. (1968), "Elements of Soil Mechanics for Civil and Mining Engineers", Fletcher and Son Ltd, Norwich, Great Britain,(1977).

21. Zada, M.C.I. (1986), "An Investigation on Collapsible Soils", Master Thesis, M.E.T.U., Ankara, Turkey, 1986.

APPENDICES

APPENDIX 1

Calibration Curves for Transducers

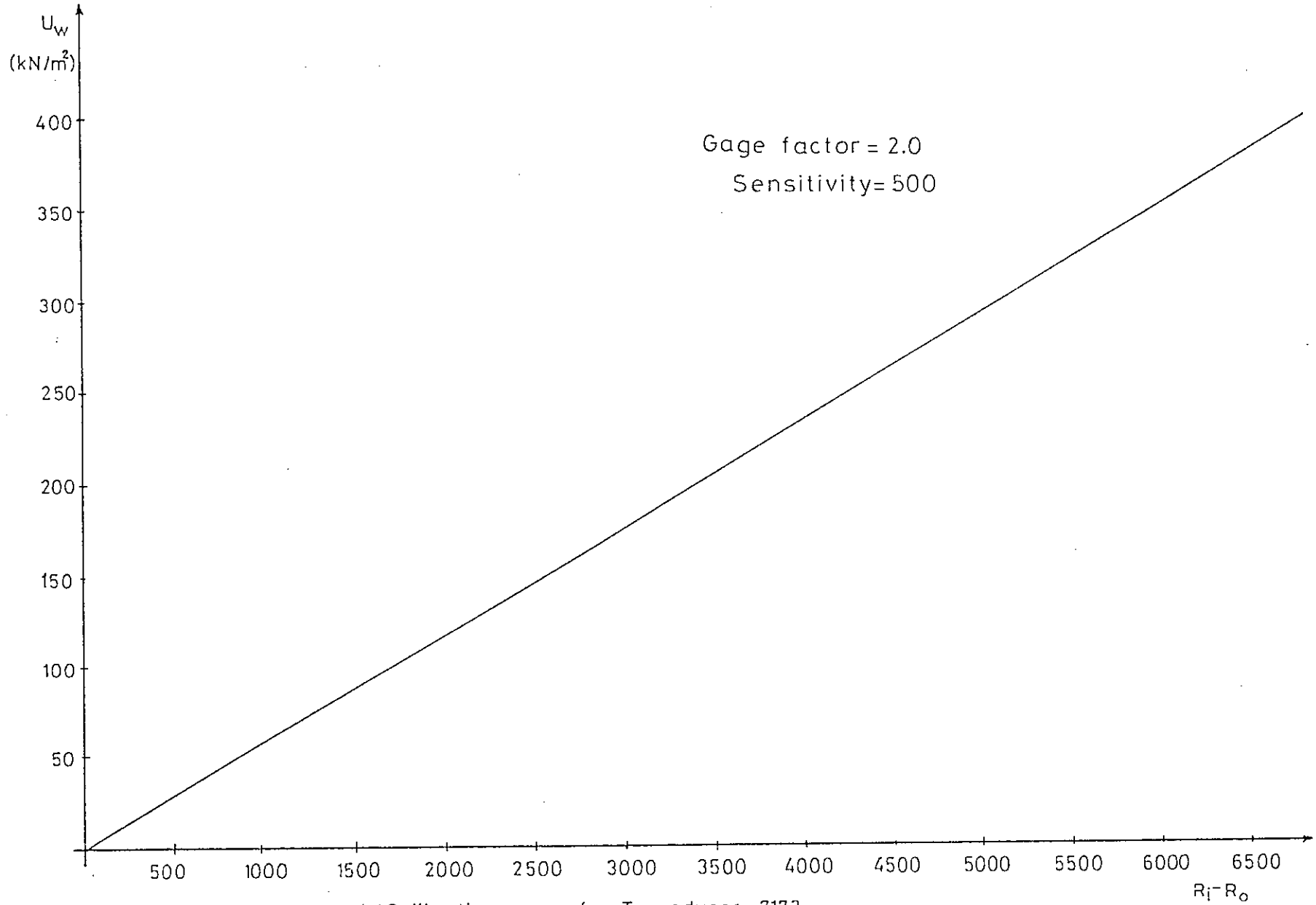

A1.1 Calibration curve for Transducer 7173

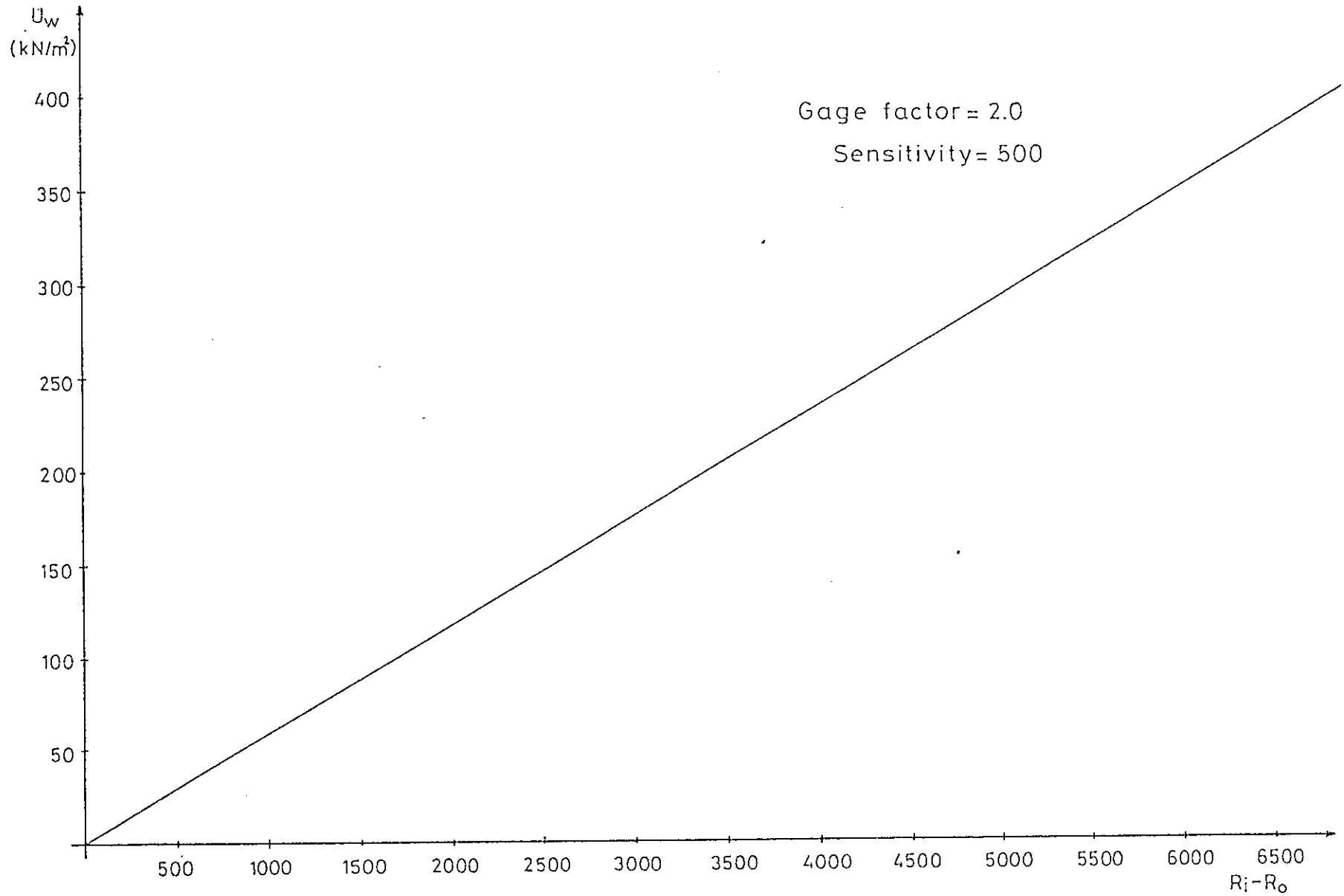

A1.2 Calibration curve for Transducer 7223

APPENDIX 2

Calibration Curves for Triaxial Cells

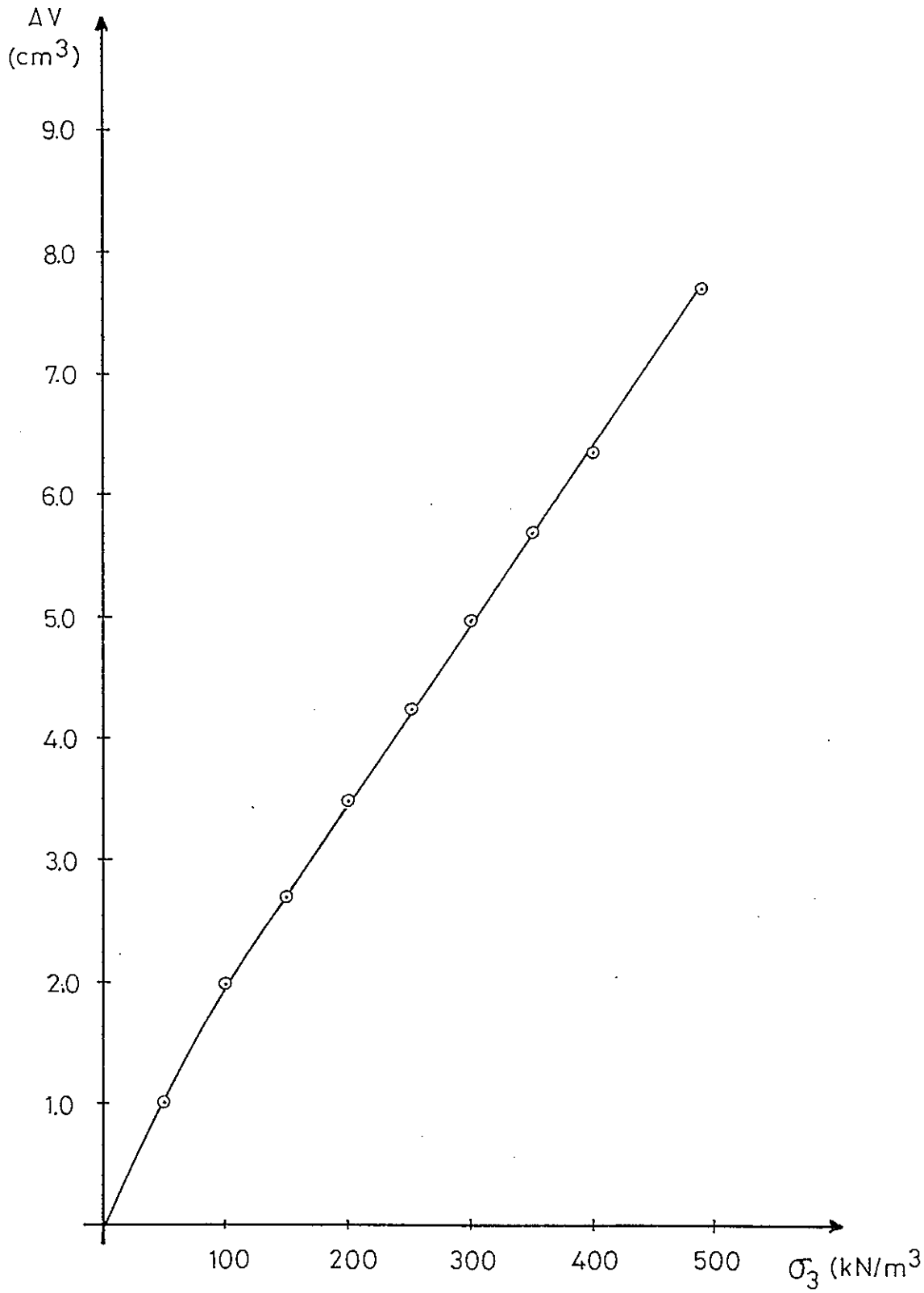

Fig. A 2.1 Calibration Curve for Triaxial Cell 2.

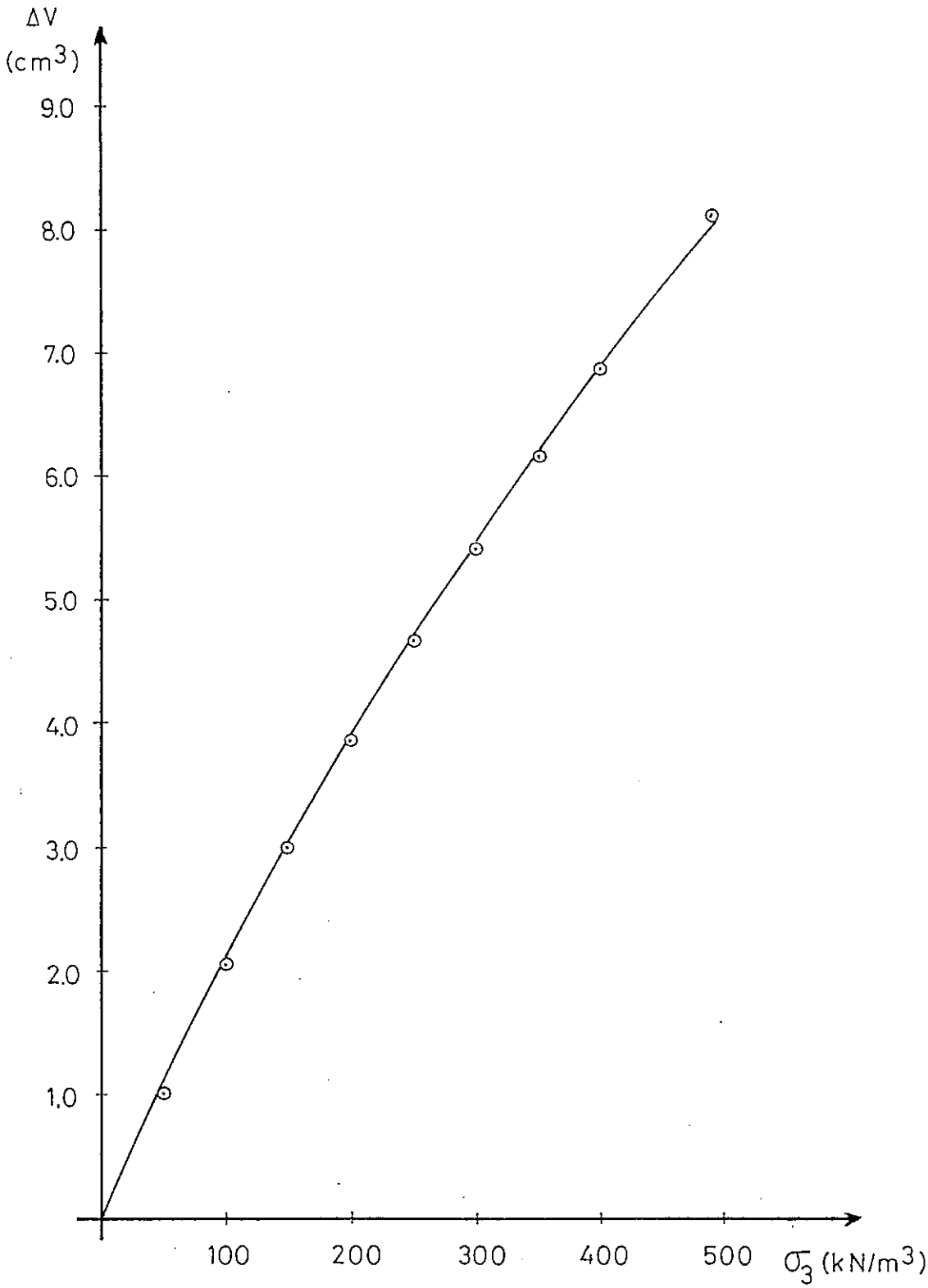

A 2.2 Calibration Curve for Triaxial Cell 3.

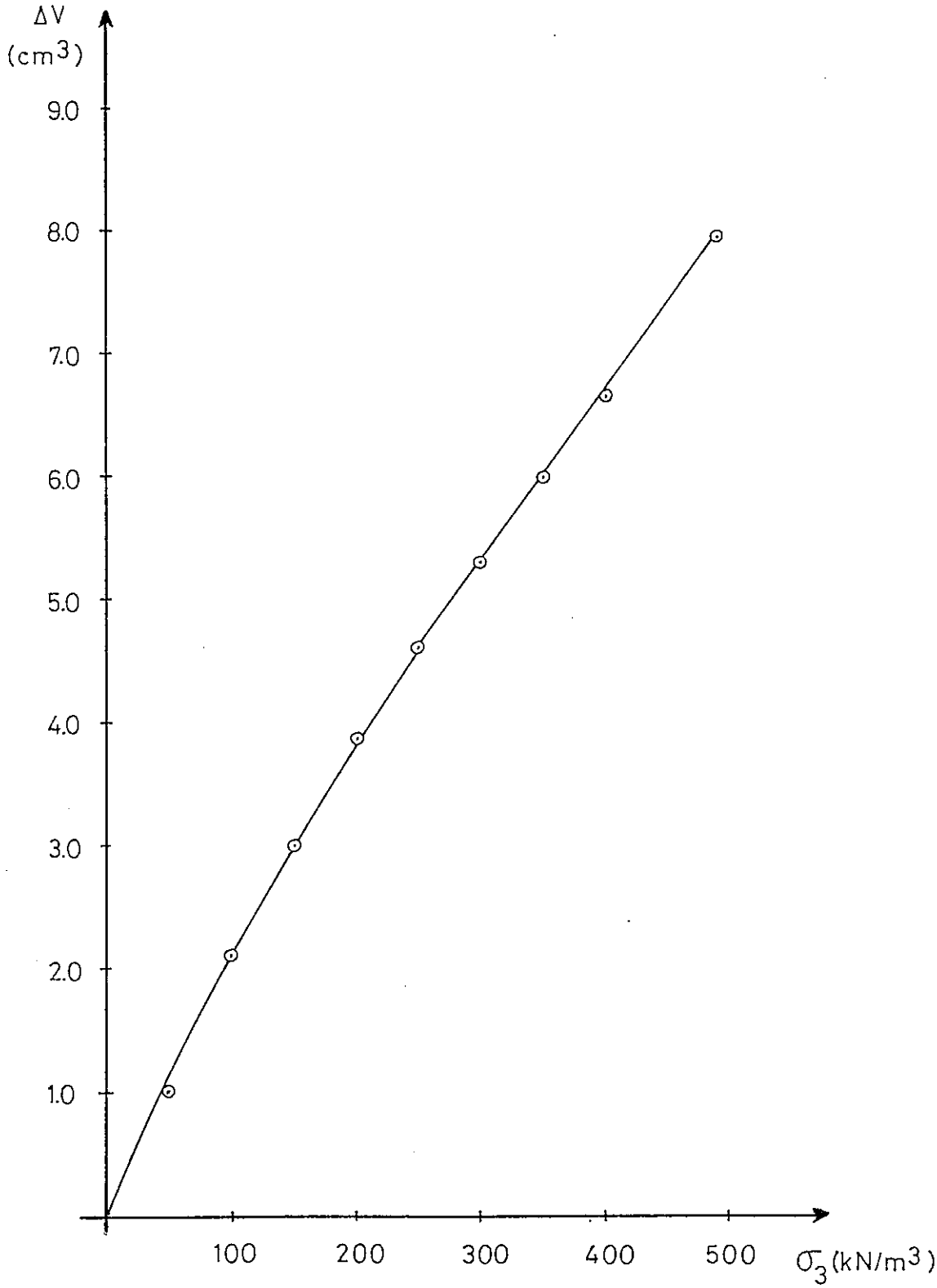

:A2.3 . : :Calibration Curve for Triaxial Cell 4.

APPENDIX 3

Rutledge-Schertmann Construction

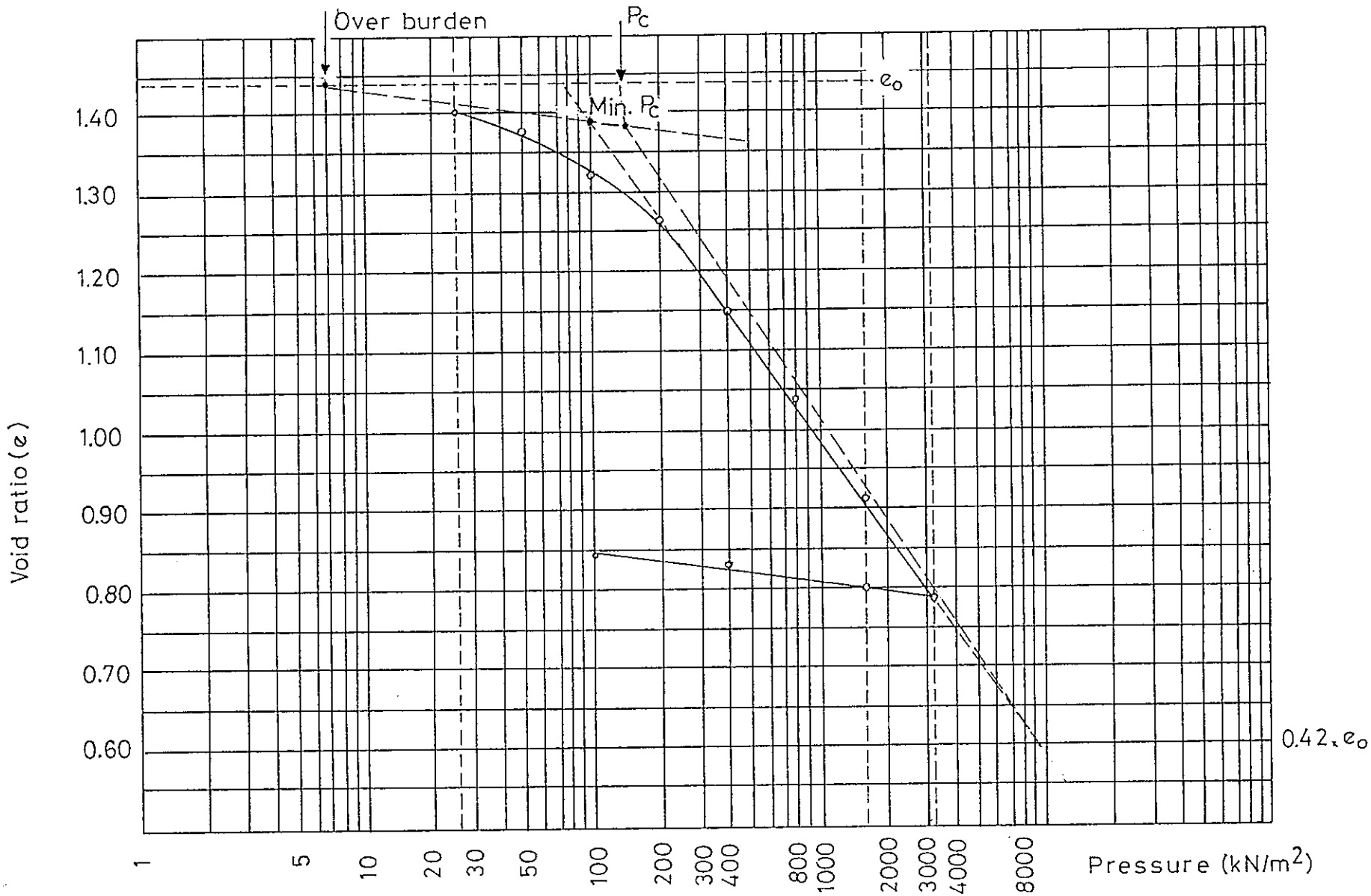

A3.1 Rutledge-Schmertmann Construction.

APPENDIX 4

Void ratio-Pressure Curves for

Double Oedometer Test